

**Proteomics analysis of brain AVM endothelium post irradiation in
pursuit of targets for AVM molecular therapy**

Margaret Simonian, BSc, MPhil

A thesis presented for the degree of Doctor of Philosophy

Australian School of Advanced Medicine

Faculty of Medicine and Health Sciences

Macquarie University

Table of Contents

LIST OF FIGURES AND TABLES	6
DECLARATION.....	11
ACKNOWLEDGMENT	12
Summary.....	13
Chapter1. General Introduction	14
1.1. Arteriovenous malformations and goals of project.....	15
1.1.1. <i>Treatment options</i>	16
1.1.2. <i>Development of new treatments for brain AVMs</i>	20
1.2. Vascular endothelium	24
1.2.1. <i>Function of vascular endothelium</i>	25
1.2.2. <i>Thrombogenesis</i>	25
1.2.3. <i>Thromboresistant properties of vascular endothelium</i>	25
- <i>Plasminogen activators</i>	26
- <i>Heparin-like molecules</i>	26
- <i>Antithrombin III</i>	26
- <i>Annexin V</i>	26
1.2.4. <i>Endothelial response to irradiation</i>	27
1.2.5. <i>Selected endothelial vascular molecules and their response to irradiation</i>	28
- <i>PECAM-1</i>	28
- <i>Cadherin-5</i>	29
- <i>Integrins</i>	30
1.3. Membrane proteins	31
1.4.1. <i>Biotinylation</i>	35
1.5. Proteomics	36
1.5.1. <i>Proteomics in medicine</i>	38
1.5.2. <i>Quantitative proteomic techniques</i>	38
- <i>Isobaric Tag for Relative and Absolute Quantitation (iTRAQ)</i>	39
- <i>Mass spectrometry expression (MS^E)</i>	40
Chapter 2: <i>In vitro</i> biotinylation protocol optimizations of murine endothelial cell cultures (bEnd3)	41
2.1 Introduction.....	42
2.2. In vitro biotinylation of bEnd.3 cultures - first trial	42

2.2.1. Materials and methods	42
2.2.1.1. Mouse endothelial cell cultures (bEnd.3)	42
2.2.1.2. Cell density and total protein concentrations	42
2.2.1.3. In vitro biotinylation	43
2.2.1.4. Digestion of eluted proteins and LC-MS/MS analysis	44
2.2.1.5. Data processing	44
2.3.1. Materials and methods	46
2.3.1.1. In vitro biotinylation	46
2.3.1.2. One dimensional electrophoreses	46
2.3.1.3. MALDI-TOF mass spectrometry	46
2.3.1.4. Data processing	47
2.3.2. Results	47
2.4. In vitro biotinylation of BSA and <i>E.coli</i> - First trial	51
2.4.1.1. Total protein concentration of <i>E.coli</i>	51
2.4.1.2. In vitro biotinylation of BSA	52
2.4.1.3. Capture of biotinylated BSA	52
2.4.1.4. Protein digestion, purification and LC-MS/MS analysis	52
2.4.2. Results	53
2.5. In vitro biotinylation of BSA and <i>E.coli</i> - Second trial	58
2.5.1. Materials and methods	58
2.5.1.1. In vitro biotinylation of BSA	58
2.5.1.2. Capture of biotinylated BSA	58
2.5.1.3. Protein digestion, purification and LC-MS/MS analysis	59
2.5.1. Results	59
2.6. In vitro biotinylation of BSA with different biotin concentrations - Third trial	66
2.6.1. Materials and methods	66
2.6.1.1. In vitro biotinylation	66
2.6.2. Results	67
2.7. In vitro biotinylation of BSA using different biotin concentrations with <i>E.coli</i>	77
2.7.1. Materials and methods	77
2.7.1.1. In vitro biotinylation	77
2.7.1.2 Results	78
2.8. In vitro biotinylation of bEnd3 cell cultures - new trials	83
2.8.1. Materials and methods	83
2.8.1.1. In vitro biotinylation	83

2.8.1.2. Tryptic digestion of biotinylated proteins and LC-MS/MS analysis	84
2.8.1.3. Data processing	85
2.8.2. Results.....	85
2.9 Western blot analysis of bEnd.3 cells	88
Chapter3. <i>In vitro</i> biotinylation and iTRAQ-mass spectrometry of bEnd.3 cells	90
3.1 Introduction.....	91
3.2 Materials and Methods.....	91
3.2.1 Mouse endothelial cell cultures (bEnd.3)	91
3.2.2 Cell density and total protein concentration	91
3.2.3 Irradiation of bEnd.3 cells	92
3.2.4 <i>In vitro</i> biotinylation of bEnd.3 cells	92
3.2.5 Capture of biotinylated proteins	92
3.2.8 Immunocytochemistry	94
3.3 Data analysis	94
3.4.1. iTRAQ-MS analysis.....	97
3.4.2. Immunocytochemistry	102
3.4.2.1. Cadherin 5	102
3.4.2.3. CD109.....	104
3.4.2.4. Protein disulfide isomerise (PDI)	105
3.5 Discussion.....	106
Chapter 4. <i>In vitro</i> biotinylation and mass spectrometry expression (MS ^E) of bEnd.3 cell cultures post irradiation	109
4.1 Introduction.....	110
4.2 Materials and Methods of MS ^E optimization on bEnd.3	111
4.2.1 Cell culture irradiation	111
4.2.2. <i>In vitro</i> biotinylation and MS ^E analysis	111
4.2.3 Data analysis	112
4.2.4 Results.....	112
4. 3. Optimization of the <i>in vitro</i> biotinylation protocol for MS ^E analysis.....	115
4.3.1 Results.....	115
4.3.2. Results.....	118
4.4. <i>In vitro</i> biotinylation and mass spectrometry expression MS ^E of bEnd.3 cell cultures post irradiation	119
4.4.1.1 Mouse endothelial cell cultures (bEnd.3)	119
4.4.1.2 Cell density and total protein concentration	120
4.4.1.3 Irradiation of bEnd.3 cells	120

4.4.1.4 <i>In vitro</i> biotinylation of bEnd.3 cells	120
4.4.1.5 Capture of biotinylated proteins	120
4.4.1.6 Tryptic digestion of biotinylated proteins and MS ^E analysis	121
4.4.2 Data analysis	121
4.4.3 Results	122
4.4.4 Discussion	127
Chapter 5. <i>In vivo</i> biotinylation optimization of the rat model of AVM	132
5.1. Introduction	133
5.2. First <i>in vivo</i> biotinylation perfusion trial	133
5.2.1. Material and Methods	133
5.2.1.1 Rat model	133
5.2.1.2 <i>In vivo</i> biotinylation perfusion	133
5.2.1.3 Membrane protein extraction	134
5.2.1.4 Capture of biotinylated proteins	135
5.2.1.5 Tryptic digestion of biotinylated proteins and Nano-LC-MS/MS	135
5.2.2. Data analysis	135
5.3. Second <i>in vivo</i> biotinylation perfusion trial	141
5.3.1. Materials and methods	141
5.3.1.1 Rats	141
5.3.1.2 <i>In vivo</i> biotinylation perfusion	141
5.3.1.3 Membrane protein extraction	142
5.3.1.4 Capture of biotinylated proteins	143
5.3.1.5 Tryptic digestion of biotinylated proteins and MS ^E analysis	143
5.3.2. Data analysis	144
5.3.3. Results	144
Chapter 6. <i>In vivo</i> biotinylation and response of endothelial cells to irradiation in the rat model of AVM	146
6.1. Introduction	147
6.2. Material and Methods	147
6.2.1 Rats	147
6.2.2 Gamma knife surgery	148
6.2.3 <i>In vivo</i> biotinylation perfusion	148
6.2.4 Membrane protein extraction	150
6.2.5 Capture of biotinylated proteins	151
6.2.6 Tryptic digestion of biotinylated proteins and MS ^E analysis	151

6.3. Data analysis	151
6.4. Results.....	152
6.5. Discussion.....	156
Chapter 7. General Discussion.....	159
7. General discussion	160
References.....	168
Appendix 1. Publication	180
Appendix 2. Publication	182
Appendix 3. Publication	184
Supplementary Tables.....	185
Appendix 4. Conference presentations, Awards and Research Article Reviews	190
Appendix 5. Final ethics approval.....	192

LIST OF FIGURES AND TABLES

Figure 1. Angiogram demonstrating an AVM in the brain. A compact collection of vessels (the ‘nidus’), connects the feeding arteries directly to the draining veins (http://www.aneurysm-stroke.com/av-malformation.php)	15
Figure 2. Embolization of brain AVM is performed under X-ray guidance. A small catheter is inserted through the femoral artery in the groin and navigated to the brain arteries (http://www.aneurysm-stroke.com/av-malformation.php)	17
Figure 3. Cerebral angiograms demonstrating an AVM, before embolization (left) and post embolization (right). (http://www.aneurysm-stroke.com/av-malformation.php)	17
Figure 4. Elekta linear accelerator (left) [Elekta Synergy]. Gamma knife RZ (right) [Macquarie University Hospital]	18
Figure 5. Patient wearing a metal frame for radiosurgery by Gamma Knife. 192 radioactive beams are focused on the target in the brain (right) [Journal of the American Academy of Physicians, 2008]	19
Figure 6. T1-weighted coronal and sagittal MRIs demonstrating a large untreatable AVM that involves the midbrain and thalamus in a young male patient (courtesy of Prof. Marcus Stoodley, Macquarie University)	20
Figure 7. A: Schematic showing the rat model of AVM. A carotid-jugular anastomosis (1) creates an arterial feeder, an arterIALIZED vein (2), a nidus (3), and a draining vein (4). B: trans-femoral carotid arteriogram demonstrating the model AVM (Tu, J et al 2010)	21
Figure 8. Histological comparison between the arteriovenous fistula (AVF) nidus and a human AVM nidus. A: AVF nidus 21 days after creating the fistula showing arterIALIZED vessels (A) and venous vessels (V). B: Human AVM nidus showing the lumen (L)	21
Figure 9. Radiosurgery of the rat AVM model. A: frame attached to stereotactic ring used for human LINAC-based radiosurgery. B & C: AVM model nidus located using CT scan. D: Axial image of CT scan of rat with the AVM targeted for radiosurgery (Storer, K et al 2007)	22
Figure 10. A: Section of irradiated fistula tissue in a rat model of AVM after treatment with saline only, showing no evidence of thrombosis. B: Sections of irradiated fistula tissue in a rat model of AVM after combined treatment with TF and LPS, which induced thrombosis (indicated by arrows) (Storer, K et al 2007)	22
Figure 11. The endothelium and smooth muscle in human artery (Tapp Medical)	24
Figure 12. Structure of PECAM-1 in human	28
Figure 13. Structure of cadherin-5	29
Figure 14. CDH5 gene location on the long arm of chromosome 16, six cadherin cluster	29
Figure 15. Structure of integrin	30
Figure 16. Integral membrane proteins. (www.sparknotes.com)	31

Figure 17. Cell membrane and classes of membrane proteins. The cell membrane is covered by carbohydrate chains on its outer surface, called the glycocalyx.....	32
Figure 18: A. Scinomix ultrasonic probe sonicator (Scinomix); B. Probe sonication of a sample.....	34
Figure 19. Sulfo-NHS-biotin reacts with the primary amine of lysine residue of the target protein to form a stable product. Sulfo-NHS is released as byproduct.....	36
Figure 20. Schematic of the basic components of a mass spectrometer.....	37
Figure 21. Q-TOF mass spectrometer.....	37
Figure 22. Overview of proteomic analysis using iTRAQ reagents.....	39
Figure 23. Mascot search results of bEnd.3 cells, first trial. Sixteen proteins only were identified.....	45
Figure 24. A: Mascot search results for BSA, matched peptides are in bold red. B: Matched peptide spectrum with ion score of 109.....	49
Figure 25. A: Mascot search results for protein alpha casein, matched peptides are in bold red. B: Matched peptide spectrum with ion score of 131.....	51
Figure 26. A: Mascot search results identified BSA (the fourth on the list). B: Protein view of BSA matched peptides in bold red. C: Peptide spectrum with ion scores of 118.....	57
Figure 27. A: Mascot search results identified BSA. B: Protein view showing matched peptides in bold red. C: matched peptide spectrum with ion score of 120.....	61
Figure 28. A: Mascot search results identified fewer serum albumins. B: Protein view showing matched peptides in bold red. C: matched peptide spectrum with ion score of 129.....	66
Figure 29. A: Matched peptides of BSA in sample 1, with score of 1102. B: Peptide spectra with ion score of 110.....	69
Figure 30. A: Matched peptides of BSA in sample 2 with score of 989. B: Peptide spectra with ion score of 107.....	72
Figure 31. A: Matched peptides of BSA in sample 3 with score of 1266. B: Peptide spectra with ion score of 109.....	75
Figure 32. No serum albumin was detected in the control sample, because BSA was not biotinylated, therefore was not captured.....	82
Figure 33. Mascot search results of bEnd3 control sample. No membrane proteins were identified.....	87
Figure 34. Confirmation of the presence of MAdCAM-1 in bEnd.3 cells at passages 29, 31 and 32.....	89
Figure 35. Confirmation of the presence of VCAM-1 in bEnd.3 cells at passages 29, 31 and 32.	89

Figure 36. Screen shot of Protein Pilot showing the analysis parameters used. Detected protein threshold (unused ProtScore) set > 1.3 with confidence > 95%.....	95
Figure 37. Screen shot of Protein Pilot showing the identified proteins and their peptide information.....	96
Figure 38. Expression level of PECAM-1 in radiated cells is higher than in controls at 24 h. (R:C) = 1.45 with 99% confidence.....	101
Figure 39. Expression level of Cadh-5 in radiated is higher than controls at 24h. (R:C) = 1.60 with 99% confidence.....	101
Figure 40. Fluorescent staining of cadherin 5 at 24 h and 48 h post irradiation. Expression levels of this protein were higher in irradiated cell compared to the controls.....	102
Figure 41. Fluorescent staining of PECAM-1 at 24 h, 48 h and 72 h post irradiation. Expression levels of this protein were higher in irradiated cells compared to the controls at these time points.....	103
Figure 42. Fluorescent staining of CD109 at 6 h and 48 h post irradiation. Expression levels of this protein increased at 6 h in irradiated cells compared to the controls and decreased at 48 h in irradiated cells.....	104
Figure 43. Fluorescent staining of PDI at 6 h and 24 h post irradiation. Expression levels of this protein increased at 6 h and 24 h in irradiated cells compared to the controls. An image of PDI stained with cy5 at 6 h in irradiated cells is also shown.....	105
Figure 44. Base peak ion (BPI) chromatograms of bEnd.3 showing heavy contamination at A, B and C compared to standard protein digest (D).....	113
Figure 45. MALDI chromatograms of bEnd3, showing many SDS detergent peaks (44kDa)	114
Figure 46. LCMS chromatogram for sample A. No detergents peaks were observed.....	116
Figure 47. LCMS chromatogram for sample B. Clear from detergents.....	116
Figure 48. LCMS chromatogram for sample C. No detergents peaks were observed.....	117
Figure 49. MALDI analysis on samples A, B and C, all were clear from detergents.....	117
Figure 50. LCMS chromatogram of bEnd3, clear from detergents and sodium ions.....	119
Figure 51. Membrane protein expression in irradiated (R) and control (C) in bEnd3 cells at 24 h post irradiation.....	126
Figure 52. Membrane proteins expression in irradiated (R) and (C) in bEnd3 cells at 48h post irradiation.....	127
Figure 53. <i>In vivo</i> biotinylation perfusion steps in the rat model of AVM.....	137
Figure 54. Screen shot of Mascot search results of the rat model of AVM showing identified serum albumins and haemoglobins.....	140
Figure 55. Anastomosis was performed by connecting the Jugular vein to the common carotid artery (Left) to create the arteriovenous fistula (AVF) (Right).....	148

Tables

Table 1. Selected common detergents and their properties	34
Table 2. Peptide sequences that matched BSA, their query numbers and ion scores, $p < 0.05$	49
Table 3. Peptide sequences matched alpha casein, their query and ion scores, $p < 0.05$	50
Table 4. Peptide sequences that matched BSA, their numbers and ion score	54
Table 5. Peptide sequences matched BSA, their query and ion scores, $p < 0.05$	62
Table 6. Peptide sequences matched BSA, their query numbers and ion scores $p < 0.05$	66
Table 7. Different BSA biotinylation conditions.....	70
Table 8. Peptide sequences matched BSA in S1, their query and ion scores with $p < 0.05$	70
Table 9. Peptide sequences matched BSA in S2, their query and ion scores with $p < 0.05$	73
Table 10. Peptide sequences matched BSA in S3, their query and ion scores with $p < 0.05$..	76
Table 11. Four BSA samples reactions.....	77
Table 12. Summary of the two halves of the four BSA samples.....	78
Table 13. Peptide sequences matched BSA in S1B sample, their query numbers and ion scores with $p < 0.05$	79
Table 14. Peptide sequences that matched BSA in S1A sample, their query numbers and ion scores with $p < 0.05$	80
Table 15. Peptide sequences that matched BSA in S2A sample, their query numbers and ion scores with $p < 0.05$	80
Table 16. Peptide sequences that matched BSA in S3A sample, their query numbers and ion scores with $p < 0.05$	81
Table 17. Peptide sequences that matched BSA in S4A sample, their query numbers and ion scores with $p < 0.05$	81
Table 18. The five bEnd3 biotinylation conditions	84
Table 19. Membrane proteins of bEnd.3 cell cultures identified using 4.2nM of biotin.....	85
Table 20. Membrane proteins of bEnd.3 cell cultures identified using 67 μ M of biotin	86
Table 21. Membrane proteins of bEnd.3 cell cultures identified by three iTRAQ -MS	98
Table 22. Average protein expression ratios (control: irradiated), in at least two out of three iTRAQ experiments and the time point at which they showed significant up or down regulation or (fold change) with $p < 0.05$	98
Table 23. Up-regulated membrane proteins of bEnd.3 cells at various time points and their average (irradiated: control) ratios, $p < 0.05$	99
Table 24. Optimization of the <i>in vitro</i> biotinylation protocol for MS ^E analysis using <i>E.coli</i> 115	
Table 25. Total number of proteins identified by two MS ^E analyses in irradiated and control cell cultures (bEnd3).....	122

Table 26. Numbers of membrane proteins of bEnd3 detected by two independent MS ^E analyses in both irradiated	122
Table 27. Membrane proteins identified in irradiated (R) and control (C) samples at 6 h after irradiation, their average masses, average concentration on column (fmol) and number of replication in the MS runs; n= 6 (R); n= 6 (C)	124
Table 28. Membrane proteins identified in irradiated (R) and control (C) samples at 24 h after irradiation, their average masses, average concentration on column (fmol) and number of replication in the MS runs; n=6 (R); n=6 (C)	124
Table 29. Membrane proteins identified in irradiated (R) and control (C) samples at 48 h after irradiation, their average masses, average concentration on column (fmol) and number of replication in the MS runs; n=6 (R); n=6 (C)	125
Table 30. Membrane protein upregulation in irradiated (R) vs control (C) cells at 24 h post irradiation, their accession number, molecular weight, average concentration on column (fmol) and average concentration ratios (irradiated : control); n= 6 (R); n= 6 (C).	125
Table 31. Membrane protein upregulations in irradiated (R) vs control (C) cells at 48 h post irradiation, their accession number, molecular weight, average concentration on column (fmol) and average concentration ratios (irradiated : control); n= 6 (R); n= 6 (C)	126
Table 32. Selected membrane proteins for the AVM rat model identified by LC-MS analysis using the Mascot search engine, their scores and number of matched peptides.....	138
Table 33. All membrane proteins in the rat model of AVM identified by LC-MS	139
Table 34. The four modifications used for the second <i>in vivo</i> biotinylation trial in the rat model of AVM.....	142
Table 35. All membrane proteins identified by MS ^E analysis in the rat model of AVM.....	144
Table 36. Membrane proteins shared between irradiated (R) and control (C) rats, their sequence accession number, molecular weight, average concentration on column (fmol) and average concentration ratios (irradiated : control); n=9.	153
Table 37. Membrane proteins present in irradiated rats (R) and not in control rats (C), their accession number, molecular weight and average concentration on column (fmol) in irradiated and control rats	153
Table 38. Membrane proteins identified by LC-MS/MS in irradiated rats.	154
Table 39. Membrane proteins identified by LCMS/MS in control rats.....	155
Table 40. Membrane proteins shared their presence between murine endothelial cell cultures and the rat model of AVM.....	167

DECLARATION

I certify that the work in this thesis entitled “Proteomics analysis of brain AVM endothelium post irradiation in pursuit of targets for AVM molecular therapy” has not previously been submitted for a degree nor has it been submitted as part of requirements for a degree to any other university or institution other than Macquarie University.

I also certify that the thesis is an original piece of research and it has been written by me. Any help and assistance that I have received in my research work and the preparation of the thesis itself have been appropriately acknowledged.

In addition, I certify that all information sources and literature used are indicated in the thesis.

The research presented in this thesis was approved by Macquarie University Ethics Review Committee; reference number 2010/037, from 2010-2013



Margaret Simonian

ID: 40715830

July 2016

ACKNOWLEDGMENT

I would like to express my gratitude to my supervisor Professor Marcus Stoodley for his help and support throughout my candidature.

My sincere thanks go to my co-supervisor Professor Mark Molloy for his tremendous help and advice during my project. His consistent, support and advice in every aspect of my candidature is greatly appreciated.

I would like to acknowledge the valuable assistance provided by my research collaborator Professor Joseph Loo at the University of California Los Angeles (UCLA).

I would like to acknowledge the assistance provided by lab members, staff and neurosurgery team at the Australian School of Advanced Medicine (Macquarie University). The staff at the Australian Proteome Analysis Facility (APAF, Macquarie University). The lab members and staff at the University of California Los Angeles (UCLA), David Geffen School of Medicine Dept of Biological Chemistry. The assistant of Professor Roger Chung, and the faculty of medicine & health sciences HDR (Macquarie University).

Thanks to the Radiation Oncology Department at Macquarie University Hospital and UCLA Hospital for allowing the use of their facilities.

Finally and most importantly my deepest gratitude goes to my family, my parents Zvart and karekin Simonian, for their love of science and constant encouragement for me to pursue higher and higher degree in my chosen field of science, and to my brothers Sarkis and Antranik. Your love and constant support made my journey possible.

Summary

Brain arteriovenous malformations (AVMs) are congenital abnormalities that consist of direct connections between arteries and veins. Ruptured AVMs are the major cause of haemorrhagic stroke in children and young adults. Treatment of AVM depends on their size and location. Radiosurgery is the treatment recommended for lesions < 3 cm; however vascular occlusion after radiosurgery can take up to 3 years to complete, while patients remain at risk of haemorrhage. Approximately one third of AVMs are unsuitable for current treatment methods of surgery and radiosurgery, such as large and deep AVMs, therefore there is a need for a new treatment that is safer and more effective than current treatment methods. This thesis research will be focused on identifying proteins on the surface of AVM vessels in response to radiosurgery that can be used as targets for AVM molecular therapies, as a new treatment method.

- *Project aims*

Specifically, this project aimed to identify proteins in irradiated AVM endothelium that are different from those expressed in normal vessels. Protein candidates could then be investigated for a ligand-directed treatment to promote rapid thrombosis in AVM vessels post radiosurgery. *In vitro* and *in vivo* biotinylation methods to label membrane proteins were first optimized then employed in murine cerebral endothelial cell cultures (bEnd.3) and the rat model of AVM. Membrane protein changes in response to irradiation were assessed using proteomics analysis. This is the first time that proteomics has been employed in the study of AVM endothelium.

- *Hypothesis*

The central hypothesis is that radiosurgery induces changes in AVM endothelial membrane proteins that allow discrimination from normal endothelial cells, providing protein targets that can be used for a ligand-based vascular targeting therapy.

- *Results*

Cell surface protein biotinylation and quantitative proteomics analyses successfully identified membrane proteins from endothelial cell cultures and the animal model of AVM in response to irradiation. The most significant in the cell cultures were, PECAM, cadherin 5, PDI, integrin alpha5, integrin alpha6, integrin beta1, CD109, EPCR and multimerin2, and in the rat model were, profilin1, potassium voltage gated channel protein, chloride intracellular channel protein 2 and ESAM-1. Most up-regulations were observed at 24h post irradiation.

The upregulated membrane proteins identified from this thesis novel research are currently being investigated as potential targets for the ligand-directed molecular targeting trials in the rat model of AVM.

Chapter1. General Introduction

1.1. Arteriovenous malformations and goals of project

Brain arteriovenous malformations (AVMs) consist of a tangle of abnormal arteries and veins linked by one or more fistulae (Friedlander, RM 2007) (Figure 1). The cause of brain AVMs is not well known; some theories suggest that they may be caused by a clot or a rupture of blood vessels during foetal development (McCormick, F 1966) and others suggest that they develop postnatally, undergoing a period of growth in childhood or early adulthood (Jeffree, R and Stoodley, M 2009). The growth may be caused by venous hypertension or by shear stress that stimulates growth factor expression by endothelial cells lining the arteriovenous fistula (Jeffree, R and Stoodley, M 2009).

Arteriovenous malformations in the brain can occur in any region, and range in size from small (< 3 cm) to large (> 6 cm). Patients with AVMs present with headaches (often migraines), seizures and most commonly, haemorrhage. The first haemorrhage is most likely to occur between the ages of 20 – 40 years (Crawford, P *et al.* 1986; Brown, R *et al.* 1996). The risk of haemorrhage is 4% per year for unruptured AVMs and is higher for ruptured AVMs (Halim, A *et al.* 2004). Each haemorrhage carries a 20% risk of death and 30% risk of morbidity (Brown, R *et al.* 1988; Ondra, S *et al.* 1990).

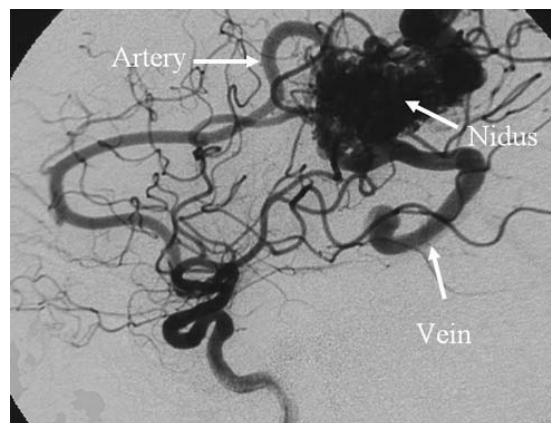


Figure 1. Angiogram demonstrating an AVM in the brain. A compact collection of vessels (the 'nidus'), connects the feeding arteries directly to the draining veins (<http://www.aneurysm-stroke.com/av-malformation.php>)

AVMs are not inherited, with the exception of hereditary hemorrhagic telangiectasia (HHT) condition. Genetic studies suggested that HHT are caused by mutations in either endoglin (ENG) gene or activin receptor-like kinase 1 (ACVRL1) gene, both are associated with TGF β /BMP signalling. Mutation in the co-receptor ENG is associated with HHT1, while HHT2 is associated with mutations in the signalling receptor ACVRL1 (Hashimoto T, et al 2001).

1.1.1. Treatment options

Current treatment options for brain AVMs are surgery, embolization and stereotactic radiosurgery. The goal of AVM treatment is to prevent haemorrhage and the choice of treatment depends on many factors, including AVM location (eloquent or non-eloquent brain) and size (Spetzler, R *et al.* 1986; Friedlander, RM 2007; Spetzler, R *et al.* 1992). Small AVMs located at the surface of the brain are suitable for surgery (Moher, J *et al.* 1999). Large AVMs are usually wedge-shaped and extend deeper into the brain; these are more difficult to treat with surgical removal (Moher, J *et al.* 1999). Although surgery prevents haemorrhage, it carries a risk of perioperative death or disability (Spetzler, R *et al.* 1986).

Embolization involves inserting a catheter into an artery, passing it through the body to the AVM feeding arteries in the brain. Agents are then injected to block the vessels and reduce the blood flow to the AVM (Jayaraman, M et al 2008; Han P et al 2003) (Figure 2 and Figure 3). This procedure itself is not usually a cure; often it is performed before surgery to reduce bleeding during the operation (Jayaraman, M et al 2008) or before radiosurgery to reduce the volume to be treated (Lunsford L et al 2008; Zabel-Du Bios A et al 2007). However not all AVM vessels can be reached with catheters and there is a risk of blocking normal arteries. Partial embolization increases the risk of haemorrhage (Jayaraman, M et al 2008; Pierot, L et al 2005; Han, P et al 2003).

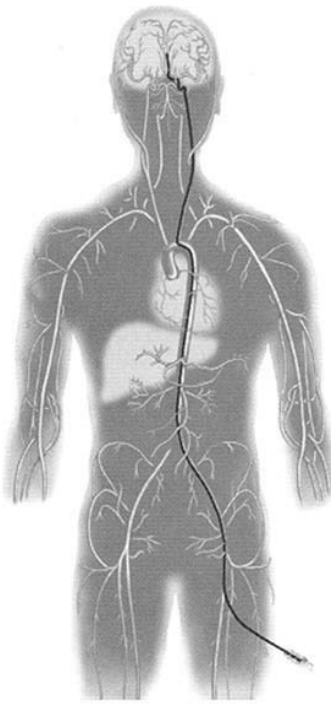


Figure 2. Embolization of brain AVM is performed under X-ray guidance. A small catheter is inserted through the femoral artery in the groin and navigated to the brain arteries (<http://www.aneurysm-stroke.com/av-malformation.php>)

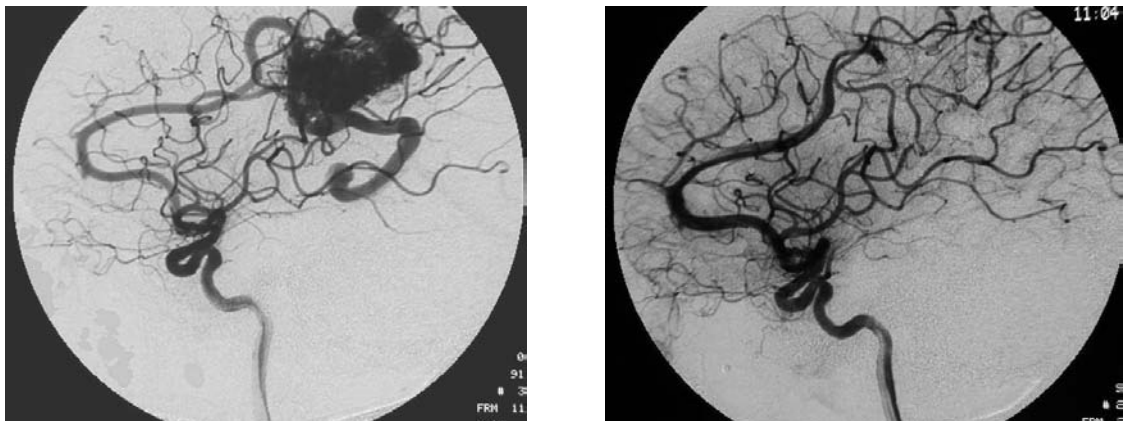


Figure 3. Cerebral angiograms demonstrating an AVM. Before embolization (left) and post embolization (right). [<http://www.aneurysm-stroke.com/av-malformation.php>]

Stereotactic radiosurgery is a procedure that delivers a single, localized, high dose of radiation to the target through the intact skull using a linear accelerator (LINAC) or Gamma Knife (Lunsford L et al 2008; Phillips M et al 1994) (Figure 4). This treatment is suitable for lesions < 3 cm in diameter and located in eloquent areas where surgery can cause neurological

deficits (Friedlander M 2007). Radiosurgery involves placing a frame on the patient's head followed by a CT or MRI to locate the target, then dose planning via a computer and delivering high intensity x-rays by the LINAC or gamma-rays by the Gamma Knife system (Lunsford L et al 2008; Phillips, M et al 1994) (Figure 5). The radiation delivers a high dose to the target volume and a low dose to the surrounding healthy brain tissues (Phillips, M et al 1994). The typical dose for AVMs is 20 – 25 Gy.



Figure 4. Elekta linear accelerator (left) [Elekta Synergy]. Gamma knife RZ (right) [Macquarie University Hospital]

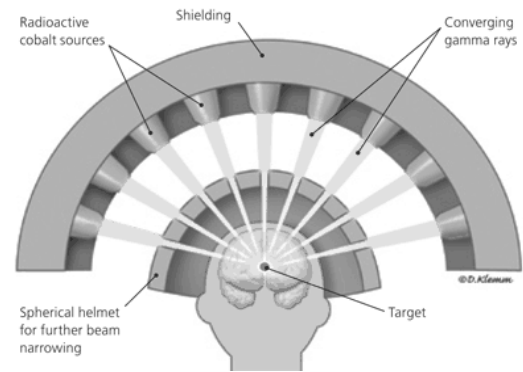
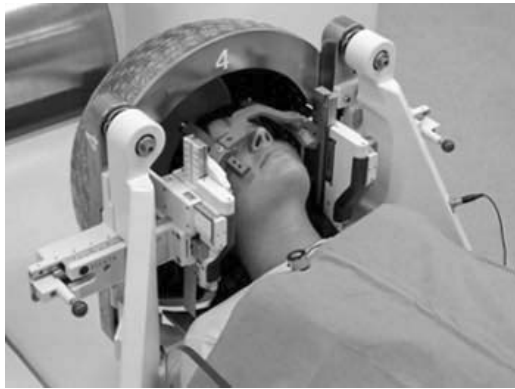


Figure 5. Patient wearing a metal frame for radiosurgery by Gamma Knife. 192 radioactive beams are focused on the target in the brain (right) [Journal of the American Academy of Physicians, 2008]

Compared to other treatments, the immediate risk at the time of the radiosurgery is very low. However, vascular occlusion after radiosurgery can take up to 3 years to complete, and patients remain at risk of haemorrhage during this time (Friedman, W et al 1998; Maruyama, K et al 2005).

Approximately one third of AVMs are unsuitable for current treatment methods, such as the large AVM shown in Figure 6. Therefore there is a need for a new treatment that is safer and more effective than current treatment methods for large and deep lesions (Han P et al 2003; Ferch R et al 2003)

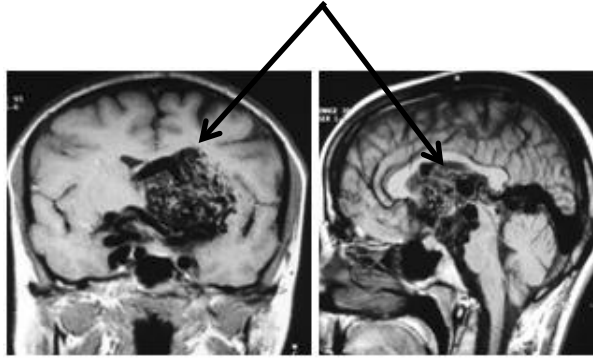


Figure 6. T1-weighted coronal and sagittal MRIs demonstrating a large untreatable AVM that involves the midbrain and thalamus, in a young male patient. (Courtesy of Prof. Marcus Stoodley, Macquarie University).

1.1.2. Development of new treatments for brain AVMs

Work has been conducted over the last decade on developing molecular therapies to promote thrombosis in AVM vessels post radiosurgery. Endothelial biology and responses to radiation have been extensively studied (Tu, J et al 2005 and 2006; Storer, K et al 2007) and an animal model of AVM has been developed that closely resembles human brain AVMs. It has an arterial feeder, a branching and reconnecting system of arterialised veins (the nidus) and a draining vein (Yassari, R et al 2004) (Figure 7). The model has been validated for its structural similarity and molecular characteristics to human AVMs (Storer, K et al 2007; Tu, J et al 2010) (Figure 8). These hemodynamic, structural and molecular similarities make this model the most suitable for molecular studies and the best available for studying the response of AVM endothelium to radiosurgery, to ensure that the changes observed in the rat model are indicative of those that occur in human AVMs.

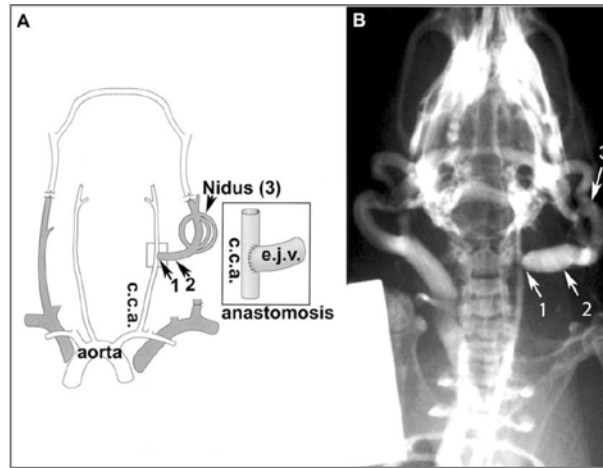


Figure 7. A: Schematic showing the rat model of AVM. A carotid-jugular anastomosis creates an arterial feeder (1), an arterIALIZED vein (2), a nidus (3), and a draining vein (4). B: trans-femoral carotid arteriogram demonstrating the model AVM (Tu, J et al 2010).

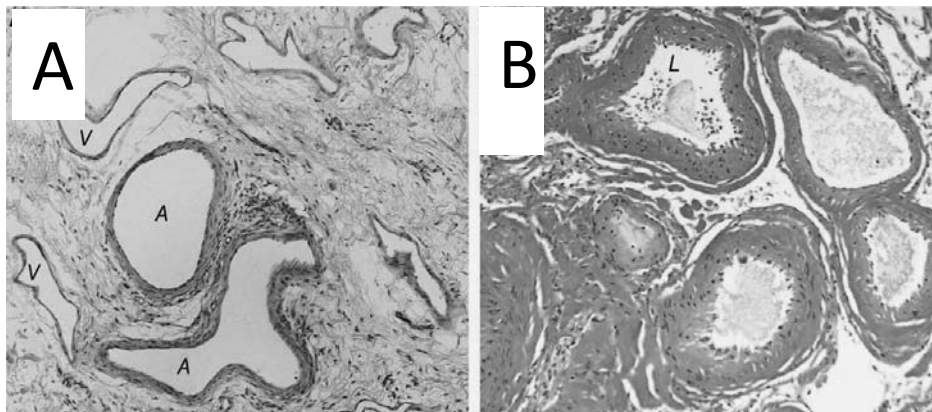


Figure 8. Histological comparison between the arteriovenous fistula (AVF) nidus, and a human AVM nidus. A: AVF nidus 21 days after creating the fistula showing arterialized vessels (A) and venous vessels (V). B: Human AVM nidus showing the lumen (L) (Tu, J et al 2010).

A technique of delivering radiosurgery to the animal model was then established (Figure 9) and thrombosis was stimulated in the animal model of AVM after radiosurgery by administering lipopolysaccharide (LPS) and tissue factor (TF), which is a non-ligand type of vascular targeting (Storer, K et al 2007) (Figure 10).

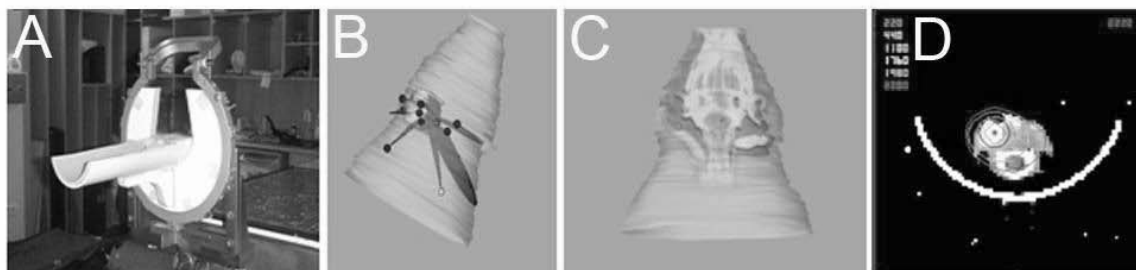


Figure 9. Radiosurgery of the rat AVM model. A: frame attached to stereotactic ring used for human LINAC-based radiosurgery. B & C: AVM model nidus located using CT scan. D: Axial image of CT scan of rat with the AVM targeted for radiosurgery (Storer, K et al 2007)

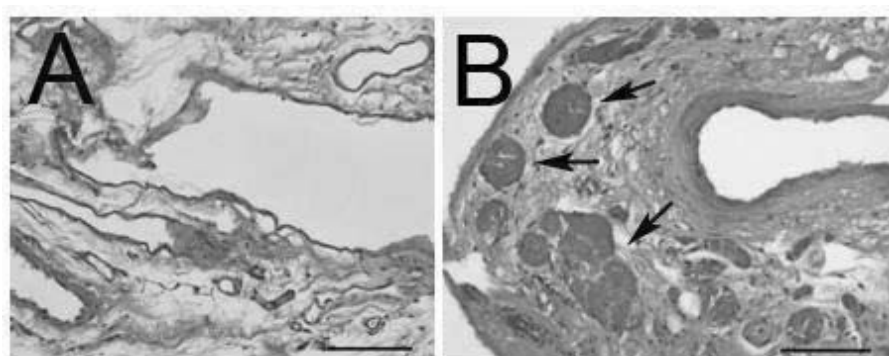


Figure 10. A: Section of irradiated fistula tissue in a rat model of AVM after treatment with saline only, showing no evidence of thrombosis. B: Sections of irradiated fistula tissue in a rat model of AVM after combined treatment with TF and LPS, which induced thrombosis (indicated by arrows) (Storer, K et al 2007).

However this approach wasn't successful in thrombosing large vessels and there are safety concerns regarding injecting humans with LPS (Storer, K et al 2007). A ligand-based vascular targeting approach has the potential to overcome these problems, but requires a luminal surface molecule that discriminates AVM vessels from normal vessels. It is proposed that radiosurgery can stimulate the expression of cell surface discriminating proteins and hence the aim in this project was to identify potential protein targets in AVM endothelium after radiosurgery. These protein candidates could then be investigated for ligand-directed treatment to promote rapid thrombosis. To achieve this goal, a successful identification and capture of cell surface proteins is crucial.

Following is a review of relevant endothelial biology and techniques for isolating membrane proteins. The experimental chapters describe the *in vitro* and *in vivo* biotinylation methodology that was employed to label membrane proteins in a murine cerebral endothelial cell culture and in the animal model of AVM. Membrane proteins in response to irradiation were then identified and analysed utilising proteomics techniques.

1.2. Vascular endothelium

Endothelium is the thin layer of cells lining the circulatory system, cavities of the heart and the inner surface of lymph vessels. The cells that form the endothelium are referred to as endothelial cells. The endothelial cells that are in immediate contact with blood are known as vascular endothelium, while those which are in immediate contact with lymph known as lymphatic endothelial cells (Hwa C et al. 2005; Cines D et al. 1998).

The blood vessel wall is lined by a single layer of endothelial cells; it's separated from the outer layers by a basal lamina. (Alberts B et al 2002) (Figure 11).

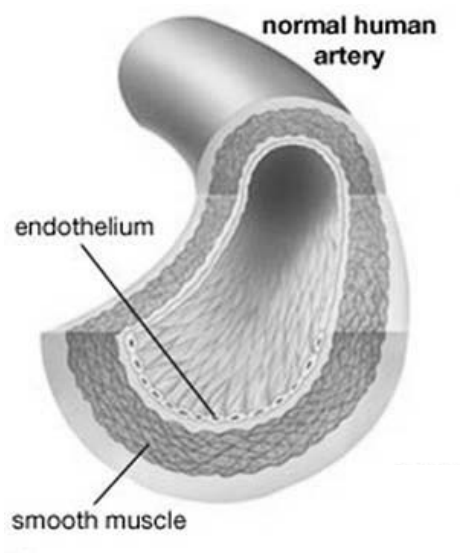


Figure 11. The endothelium and smooth muscle in human artery (Tapp Medical, (<http://www.tappmedical.com/>))

The endothelial cell has three surfaces: a non-thrombogenic luminal surface that contributes to thromboresistant properties, an adhesive subluminal surface that adheres to connective tissue, and a cohesive surface that joins neighbouring cells to one another by cell junctions (tight and gap) (Stefanini, M et al, 2009).

1.2.1. Function of vascular endothelium

Endothelial cells are involved in many vascular biological processes, such as the regulation of blood and nutrient substances flow, formation of new blood vessels, inflammation, thrombosis and fibrinolysis (Fishman A 1982; Cines D et al. 1998). The loss of proper endothelial function leads to several vascular diseases, such as hypertension, coronary heart disease and hypercholesterolemia (Munzel, T et al 2008; Ganz, P et al 2013). Damaged endothelial cells can lose their thromboresistance ability (Bevilacqua, M et al 1984; 1986).

1.2.2. Thrombogenesis

When circulating blood is exposed to a disrupted endothelial surface, it initiates the formation of thrombus. Thrombus in an artery is comprised of a tightly packed network of platelets and fibrin, while in a vein it is comprised of a looser network of erythrocytes, leukocytes, and fibrin (Folk E et al 1985; Halton M et al 1989). The size and composition of the thrombus is determined by changes in blood flow, thrombogenicity of the vascular surfaces, and concentration of plasma components (Furman M et al 1998).

In arterial thrombosis, the following critical events occur: platelet deposition, activation of coagulation factors, followed by formation of fibrin. Platelets attached to a disrupted endothelial surface adhere and aggregate and form an enlarged platelet mass. Coagulation factors are then attached to the damaged vascular cells followed by the generation of a fibrin network (Furman M et al 1998; Stabenfeldt S et al 2010).

1.2.3. Thromboresistant properties of vascular endothelium

Endothelial cells synthesize, secrete and regulate procoagulants, anticoagulants, fibrinolytic proteins, prostanoids and connective tissue components (Gross P et al 2000; Piper P et al 1971). The most important function of the vascular endothelium is preventing the

development of nonphysiologic thrombosis (thrombosis in the wrong place) that can be fatal (Becker R 1992). Many factors contribute to the natural thromboresistant properties of the vascular endothelium, including:

- ***Plasminogen activators***

Serine protease plasmin is an enzyme that proteolytically breaks down fibrin and fibrinogen (Becker R 1992; Gross P et al 2000). The release of these activators is stimulated by heparin, thrombin, aggregating platelets, interleukin and epinephrine (Stein C et al 1998).

- ***Heparin-like molecules***

Endothelial cells synthesize heparin-like molecules with anticoagulant properties that mediate vascular thromboresistance through the interaction of heparin-like bodies with anti-thrombin and heparin cofactor II, located on the endothelial surface (Stern D et al 1985).

- ***Antithrombin III***

Antithrombin III is a plasma glycoprotein that neutralizes most coagulation proteins, such as thrombin and factors XIIa, XIa, IXa and VIIa by covalently binding at their active sites (Stern D et al 1985; Stern D et al 1987)

- ***Annexin V***

Annexins are non-glycosylated proteins, bind to negatively charged phosphatidylserine and phosphatidylethanolamine. Annexin V is an important endothelial surface anticoagulant protein. It has the ability to replace phospholipid-dependent coagulation factors and minimize the adhesion of platelet (Beacker R 1992).

1.2.4. Endothelial response to irradiation

Studies of endothelial cells and their response to irradiation have been largely based on the *in vitro* cultured human umbilical vein endothelial cells (HUVECs). This culture technique was developed in the 1970s (Jaffe E et al 1973; Gimbrone M et al 1974). However endothelium is very heterogeneous; varied exposure to environmental stimuli may be the cause of this heterogeneity (Owman C et al 1998). Cultured endothelial cells from the brain and other organs express different cell surface markers and enzymes (Owman C et al 1998). Many exogenous factors also affect the endothelial cell phenotype, such as soluble growth inhibitors and promoters and proteins such as thrombin and plasmin, and circulating cells such as smooth muscle cells (Cines D et al 1998).

Different expression patterns of endothelial proteins in response to irradiation have been shown in previous studies on human and animal cell cultures *in vitro* and *in vivo*. This may be due to the fact that endothelial cells respond differently to irradiation at different doses. Although it's not clearly understood, in low doses they mainly decrease in expression, and some undergo apoptosis at doses 15–25 Gy, while at doses higher than 100 Gy they undergo hypertrophy (Rubin D, 1997). In 2013 a study by Rombouts C et al, showed for the first time, that low doses of irradiation caused DNA damage (double -strand breaks) in human vascular endothelial cell line EA.hy926 and HUVAC, that may led to endothelial cells apoptosis at low doses of irradiation (Rombouts C et al 2013). Previous studies showed increase expression of some proteins in response to irradiation, such as profilin-1, potassium voltage gated channel protein, and chloride intracellular channel proteins 4 (Das T et al 2010 ; De Costa et al, 2002 ; Pardo and Stuhmer, 2014 ; Kim S et al, 2010). In general, endothelial cells are more resistant to radiation *in vivo* than *in vitro* because of the protection provide by the matrix surrounding vessels (Rubin D 1997).

1.2.5. Selected endothelial vascular molecules and their response to irradiation

- **PECAM-1**

PECAM-1 or CD31 is a vascular endothelial cell adhesion molecule encoded by the human PECAM1 gene on chromosome 17 (Gumina RJ et al. 1996) (Figure 12). It makes up the majority of endothelial cell intercellular junctions (Varon D et al.1998).

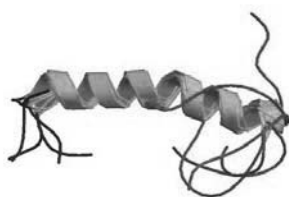


Figure 12. Structure of PECAM-1 in human. (PhosphoSitePlus, <http://www.phosphosite.org/proteinAction.do?id=2301&showAllSites=true>)

In humans it is expressed in platelets, macrophages, lymphocytes, megakaryocytes, osteoclasts and neutrophils. PECAM is a membrane protein and plays a role in integrin-mediated cell adhesion, apoptosis, cell migration, negative regulation of immune cell signalling and thrombosis (Newman PJ et al. 1990; Entrez Gene). The multiple isoforms expressed in vascular beds of various tissues are generated by alternative splicing (Varon D et al. 1998). Previous *in vitro* studies in human and animal cell cultures showed that when endothelial cells were exposed to irradiation doses from 10 – 20 Gy, the expression levels of PECAM increased (Guagler MH et al, 2004).

- ***Cadherin-5***

Cadherin-5 or CD144 is another vascular endothelial cell adhesion molecule, belonging to the family of cadherins and encoded by the CDH5 gene on chromosome 16 (Suzuki et al 1991) (Figure 13 and 14).

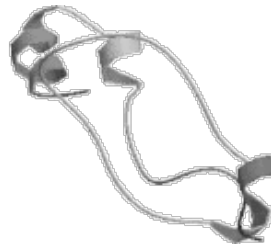


Figure 13. Structure of cadherin-5 [www.USCNK.com]

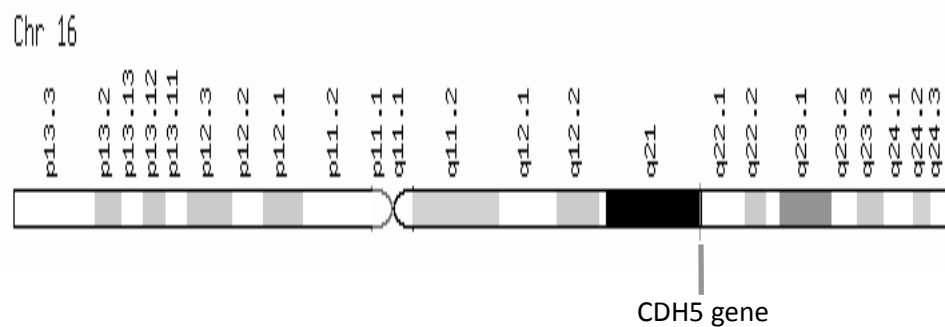


Figure 14. CDH5 gene location on the long arm of chromosome 16 (six cadherin cluster), (www.genecard.org)

Cadherins are calcium-dependent cell adhesion proteins. They control the cohesion and organization of the intercellular junctions. Cadherin-5 specifically decreases intracellular permeability to high molecular weight molecules and minimizes cell migration and is absolutely required for proper vascular development and sustaining newly formed vessels (Breviario et al. 1995; Crosby CV et al 2004). Cadherin-5 response to irradiation is similar to that of PECAM-1 (Akimoto et al 1998).

- ***Integrins***

Integrins are a large family of heterodimeric transmembrane receptor proteins that mediate cell to cell interactions and cell to matrix interactions. Beside their adhesive function, they play important roles in cell signalling, migration, platelet adhesion and thrombus formation at the blood vessel wall (Harris ES et al 2000; Cordes et al 2002). Integrins contain two chains: large alpha and small beta subunits (Figure 15). They form many subfamilies by association of beta-1 and beta-2 with different alpha 1-11 subunits, *e.g.* Integrin alpha-4/beta-1 is a receptor for VCAM-1, it is responsible for lymphocyte adhesion to vascular endothelium and recruitment of leukocytes to inflamed tissues. (Humphries MJ 2000; Harris ES et al 2000).

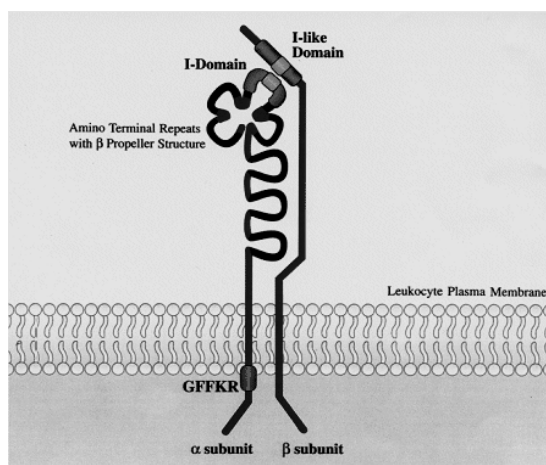


Figure 15. Structure of integrin. (www.cs.stedwards.edu)

In 2002 a study by Cordes N et al, showed that integrin beta-1 was upregulated post irradiation in human lung carcinoma cells *in vitro* (Cordes N et al. 2002).

1.3. Membrane proteins

Membrane proteins are proteins associated with cell or organelle membranes. They are located in the phospholipids' bilayer and have many important biological functions. They include cell adhesion molecules, receptors, enzymes and transport proteins (Von Heijne G, 2006). In 1972, Singer J and Nicolson G, proposed the fluid mosaic model to describe the structure of the cell membrane. They viewed the cell membrane as two-dimensional solutions, comprises of proteins, lipids and carbohydrates that pave the cell surface just like mosaic tiles. This complex structure allows the proteins to perform variety of functions (Singer J and Nicolson G, 1972). Some membrane proteins interact with the extracellular matrix and some with the cytoplasm. Based on their relationship to the lipid bilayer, membrane proteins can be classified as: integral proteins, peripheral proteins, and lipid bound proteins (Gerald K, 2009).

Integral proteins are located within the lipid bilayer. To isolate these proteins from the cell membrane, harsh detergents are needed to disrupt the lipid bilayer. Integral proteins are normally transmembrane proteins, they cross the lipid bilayer once or multiple times adopting an alpha-helical structure. The first are referred to as single pass membrane proteins and the second as multi pass membrane proteins (Lee AG, 2005) (Figure 16). Therefore transmembrane proteins can function inside as well as outside of the cell.

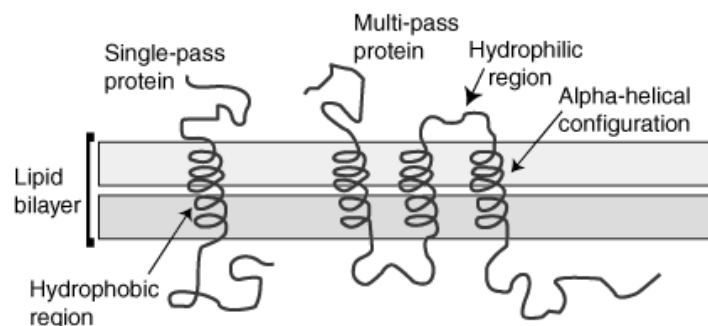


Figure 16. Integral membrane proteins. (www.sparknotes.com)

Peripheral proteins are attached to the exterior of the lipid bilayer; therefore they can be isolated without the need for harsh detergents. Lipid bound proteins are entirely located within the lipid bilayer (Gerald K, 2009; Lee AG, 2005) (Figure 17).

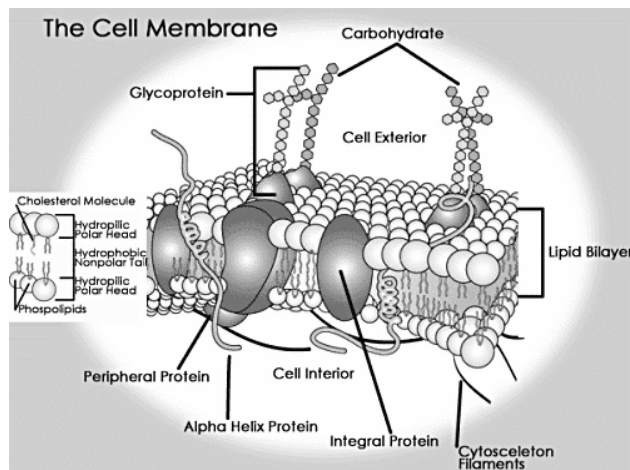


Figure 17. Cell membrane and classes of membrane proteins. The cell membrane is covered by carbohydrate chains on its outer surface, called the glycocalyx. (Spark notes).

Because of the important biological functions of membrane proteins, they are the targets of many pharmaceutical companies investing in development and drug discovery. The two major groups of membrane proteins targeted for drug development are the transmembrane proteins, specifically G protein coupled receptors (GPCRs), and ion channels. (Filmore D, 2004).

Almost 30–40 % of current drugs target GPCRs because of their major involvement in the physiological processes of the cell. The activation or inhibition of GPCRs depends on the type of ligand they bind to (Millar P et al 2010; Rubenstien A 1998). For example, ion channels transport the ions calcium, chloride sodium and potassium across the cell membrane.

Modifying or blockage of these ion channels is the key used in drug development for many diseases such as cancer and multiple sclerosis (Eijkelkamp N et al 2012; Verkman A et al 2009).

1.3.1. Membrane protein extraction

Membrane proteins are difficult to isolate because of their association with the lipid bilayer and with other proteins. Most membrane proteins are not water soluble, and require harsh detergents to become soluble in aqueous solutions (Lin S. et al 2009). Isolation of membrane proteins is the key to successful protein characterization by mass spectrometry; therefore the selection of suitable detergents for solubilisation and purification is a critical step (Arnold T. et al 2008; Lin S. et al 2009).

Detergents penetrate between the membrane bilayers to form mixed micelles with isolated membrane proteins and phospholipids (Neugebauer, J. 1990). Detergents can be classified as: (i) nonionic detergents (such as Triton X-100, NP-40, Tween-20 and Tween-80); (ii) zwittergent (zwitterionic) detergents (such as CHAPS, CHAPSO and Sulfobetaine 3-16); and (iii) ionic detergents (such as SDS) (Helenius, A. et al 1975). Selection of the detergent depends on the type of membrane, the critical micelle concentration (CMC) and the molecular weight of the detergent, the solubilization buffer, temperature, ionic strength, aggregation number and if the detergent has to be removed at a later stage (Neugebauer, J. 1990; Tanford, C. et al 1976). Table 1 represents some of the common detergents and their properties.

Table 1. Selected common detergents and their properties

Detergents	Type	Aggregation number	CMC value mM (% w/v)	Molecular weight
Triton X-100	Nonionic	140	0.24 (0.0155)	647 g
NP-40	Nonionic	149	0.29 (0.0179)	617 g
Tween 80	Nonionic	60	0.01 (0.0016)	1310 g
SDS	Anionic	62	6-8 (0.17-0.23)	288 g
CHAPS	Zwitterionic	10	8-10 (0.5-0.6)	615 g
Brij-58	Nonionic	70	0.08 (0.0086)	1120 g
CHAPSO	Zwitterionic	11	8-10 (~0.505)	631 g

Aggregation number = the number of detergent molecules per micelle; CMC = the range of detergent's critical concentration above which micelles will form

(Calbiochem: <http://wolfson.huji.ac.il/purification/PDF/detergents/CALBIOCHEM-DetergentsIV.pdf>)

Membrane protein isolation also requires high technology instrumentations, such as an ultracentrifuge, which is capable of spinning a rotor at very high speeds to generate acceleration as high as 1,048,000 g and an ultrasonic probe sonicator which uses very high sound energy to agitate the sample (Figure 18).

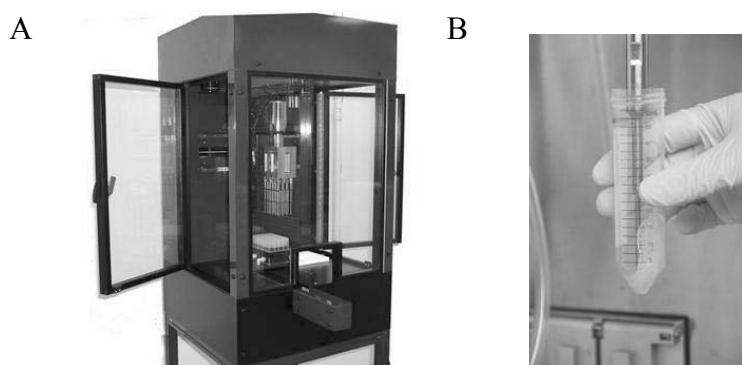


Figure 18: A. Scinomix ultrasonic probe sonicator (Scinomix); B. Probe sonication of a sample.

1.4. Protein labelling

Proteins are labelled in many ways for the purpose of detection and purification. Protein labeling methodologies involve the use of labelled enzymes, biotin, and fluorescent probes (Wombacher R et al 2011). They are conjugated to antibodies such as avidin, streptavidin and other proteins and used in many detection systems. *In vitro* and *in vivo* protein labelling methods have been developed, however optimization is required before employing to a specific cell or tissue.

Primary amines (-NH₂) present at the N-terminus and lysine residues are frequently used as targets for protein labelling. The higher the molecular weight of a protein the more primary amines are available for labelling, e.g. bovine serum albumin contains 59 primary amines; 30 – 35 of them are available on the surface (G-Biosciences). Primary amines are favourable because they are abundant, reactive and found on the surface of proteins.

1.4.1. Biotinylation

Biotinylation is the process of covalently attaching biotin to proteins. Biotin (B7 vitamin), binds with high affinity to avidin and streptavidin proteins. This extraordinary affinity of biotin for these proteins allows biotin-containing molecules to be bound distinctly with avidin/streptavidin conjugates (Barat B et al 2007; De Boer et al 2003). This specific interaction is a very useful tool in molecular biology to detect and isolate membrane proteins.

Amine specific biotinylation is attaching biotin to the amine group of target proteins. Based on water solubility, amine biotinylation reagents are divided into two groups: sulfo-NHS esters and NHS esters. Sulfo-NHS-esters are most frequently used as biotinylation reagents because they are water soluble and they do not penetrate the cell membrane as long as the cell remains intact (Barat B et al 2007; Zhang L et al 1999) (Figure 19).

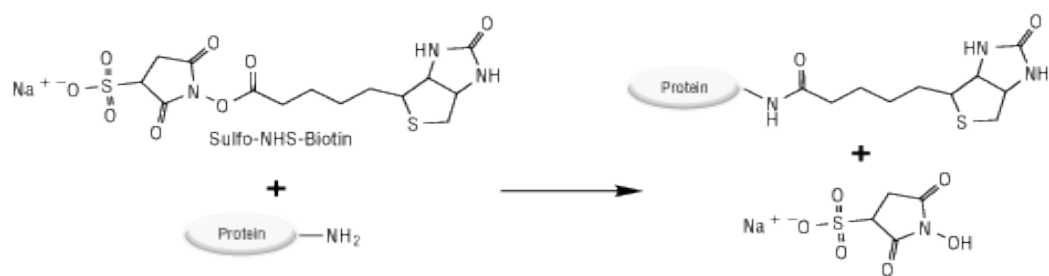


Figure 19. Sulfo-NHS-biotin reacts with the primary amine of lysine residue of the target protein to form a stable product. Sulfo-NHS is released as byproduct. (Thermo Scientific, <http://www.piercenet.com>).

1.5. Proteomics

Proteomics is the identification of proteins in a tissue or cell, and the determination of their function, structure and modifications (Wilkins et al. 1997; Baxevanis et al. 2005; Gygi and Aebersold 2000). The term proteome was coined by Marc Wilkins to describe all the proteins expressed by a genome (Wilkins et al. 1997). It is considered to be the next step in modern biology. Proteomics is dynamic compared to genomics because it changes constantly to reflect the cell's environment. The main objectives in the field of proteomics are: (i) identify all proteins; (ii) analyse differential protein expression in different samples; (iii) characterise proteins by identifying and studying their function and cellular localisation; and (iv) understand protein interaction networks (Palagi M et al. 2006).

Proteomics relies on successful protein separation and purification techniques, mass spectrometry analysis, bioinformatics, and gene and protein databases (Palagi M et al. 2006).

Sample preparation is the most critical and challenging task in any successful proteomics project (Hall et al. 1993). Isolation of proteins involves releasing proteins by breaking the cell wall and solubilizing the proteins in a buffer for fractionation and analysis (Bodzon-Kulakowska A. et al. 2007). Isolation methods can vary from simple solubilisations to more complex extractions based on the tissue and cell types. The difficulties involving in the

purification methods and recovery of protein are the major obstacles to characterization assays, especially of low abundance proteins such as membrane proteins (Carlas B, et al. 2007).

Mass spectrometry (MS) is an important tool in the field of proteomics for protein identification and quantification. The mass spectrometer is composed of an ion source, a mass analyser, and a detector (Figure 20). The principle of MS is comprised of ionizing compounds to generate charged molecules then measuring their mass/charge ratios (m/z). The peptides' masses are then sent to databases, such as MASCOT, to compare with the masses of all known peptides (Kusher B et al. 2005).



Figure 20. Schematic of the basic components of a mass spectrometer.

If the protein does not exist in a database then a tandem mass spectrometry (MS/MS) is used to identify proteins based on the masses of their components. Ions of interest are elected based on their (m/z) ratios from the first MS run, then fragmented and separated based on their individual (m/z) ratios by another MS run to obtain sequence information (Chowdhury SK et al. 1990; Kuster B et al. 2005) (Figure 21).

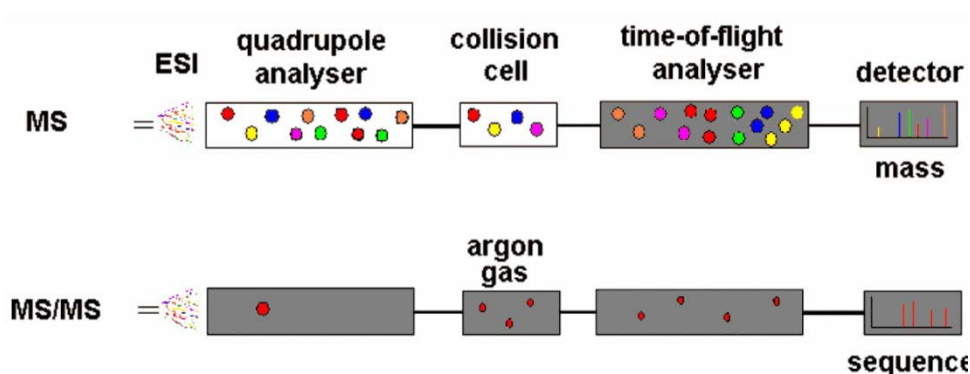


Figure 21. Q-TOF mass spectrometer, when operating in MS mode the sample is ionized and passed through the first quadrupole analyser then into the second time-of-flight analyser to

separate the ions based on their m/z ratios. The Q-TOF is then switched into MS/MS mode where a static gas is introduced to fragment the ions and generate MS/MS spectrum to obtain sequence information and confirm protein identity.

(<http://www.astbury.leeds.ac.uk/facil/MStut/mstutorial.htm>)

1.5.1. Proteomics in medicine

Proteomics plays an important role in medical research, such as in drug discovery and diagnostics, because of the link between proteins, genes and diseases (Petricoin EF et al. 2002). Understanding protein functions helps to understand diseases. Most current drugs are either proteins or they target specific proteins in the body (Wulfschlegel JD et al. 2003).

Identifying unique protein expression associated with specific diseases is a very important and promising area in the field of clinical proteomics (Lopez E et al. 2012). Neuroproteomics is a rising application in the study of brain disorders (Grant SG et al. 2001). Proteomics analysis of brain tissue is an essential part of neuroscience research, although it faces many challenges, importantly the difficulty of obtaining sufficient sample for mass spectrometry analysis, which requires at least 30 nanograms of protein. Usually 30 – 40% of proteins are lost during the sample preparation process, therefore low abundance proteins will not always be detected (Ball et al, 2010; Butcher J 2007). The availability of animal models may solve these problems in some cases (Ball et al 2010).

1.5.2. Quantitative proteomic techniques

Quantitative proteomics technology contributes to studies aimed at revealing disease pathways, biomarker discovery and drug development (Jeffery, C. et al 2006).

- ***Isobaric Tag for Relative and Absolute Quantitation (iTRAQ)***

iTRAQ is a technique used to identify and quantify proteins from different biological samples in a single experiment (Pandhal, J. *et al.* 2008). It is a widespread method for protein and peptide labelling, and has many applications in clinical studies (DeSouza, L. *et al.* 2005; Abdi, F. *et al.* 2006; Song, X. *et al.* 2008). It uses isotope labelling of the N-terminus and side chain amines of peptides. Samples are then pooled and fractionated by chromatography then analysed by mass spectrometry (Song, X. *et al.* 2008). After fragmentation, the attached tag generates low molecular mass ions that allows the relative quantification of the peptides and the proteins they are derived from using software such as Protein Pilot (Song, X. *et al.* 2008) (Figure 22).

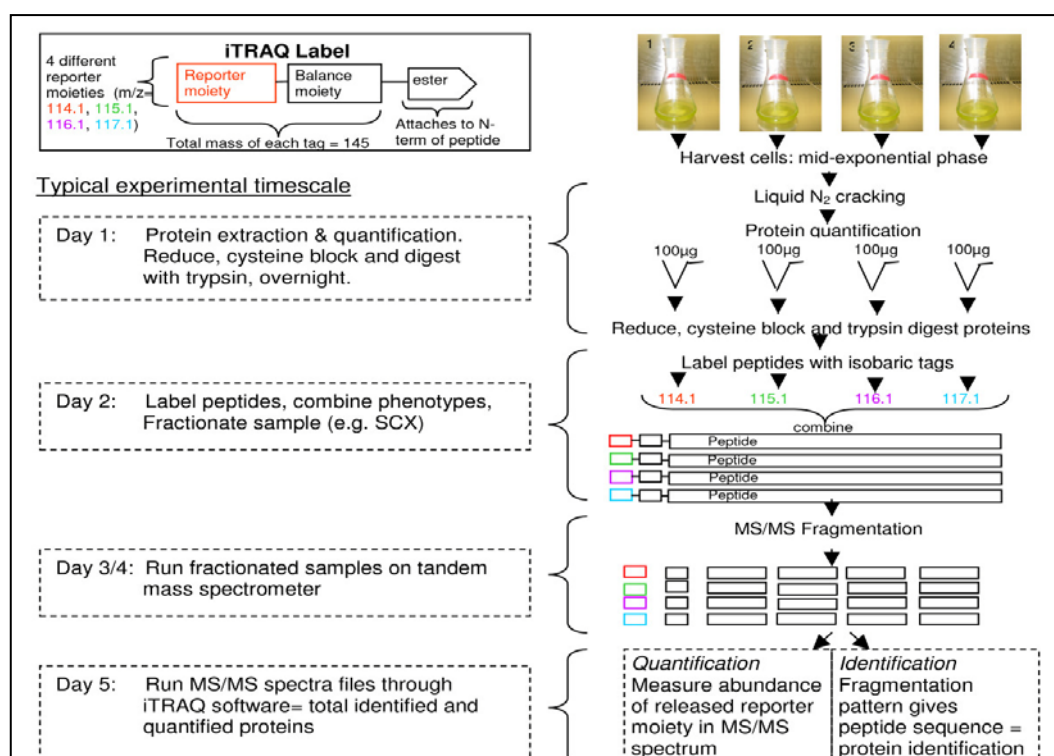


Figure 22. Overview of proteomic analysis using iTRAQ reagents. Proteins are extracted from four samples and digested with trypsin to generate peptides. Peptides are then labelled with iTRAQ isobaric tags; pooled for fractionation and analysed by MS/MS. Isobaric tag intensity correlates to peptide abundance hence it's used for protein quantitation (Pandhal, J. *et al.* 2008).

- ***Mass spectrometry expression (MS^E)***

Most label-based quantitative proteomic techniques, such as iTRAQ, SILAC and radiolabelling, require complex sample preparation which can be very expensive and time consuming (Vibhuti J et al 2009). MS^E is a new method for absolute quantification and identification of proteins from MS data of tryptic peptides without requiring the use of any labelling methods (Jeffery, C. et al 2006). The advantages of this new technique are: (i) improved sequence and proteome coverage; (ii) quantitative accuracy; and (iii) lower false positive rates. These advantages are most dramatic for low abundant proteins such as membrane proteins (Jeffery, C et al 2005; 2006).

The typical MS/MS instruments look at all precursor masses over a defined mass range then select the top five for specific sequential fragmentation scans. The MS^E instruments abandon the selection of a precursor ion for individual fragmentation and fragment everything, as a result the exact mass precursor and fragment ion spectra for every detectable component in the samples are identified and quantified in a single analysis. With this technique 90% of the data are reproducible with 70% of the quantitative data reproducibility and 20 % variability only (Kramer G et al 2015).

In summary, the endothelium is very heterogeneous and its response to irradiation varies from one cell type to another. Radiosurgery induces changes in AVM endothelium that allow discrimination from normal endothelial vessels. Identifying unique membrane proteins expressed on the endothelium after irradiation is essential to successfully develop molecular therapy for brain AVMs.

Chapter 2: *In vitro* biotinylation protocol optimizations of murine endothelial cell cultures (bEnd3)

2.1 Introduction

To study the response of membrane proteins to irradiation in the murine endothelial cell cultures (bEnd.3), a successful protocol for labelling of the membrane proteins was necessary. *In vitro* biotinylation protocol optimizations were therefore carried out to label membrane proteins. The protocol used was modified from (Scheurer, S. *et al.* 2005) and (Roesli, C. *et al.* 2006). Optimizations were carried out using standard proteins (bovine serum albumin and alpha-casein proteins), *Ecoli* and bEnd.3 cultures.

2.2. In vitro biotinylation of bEnd.3 cultures - first trial

2.2.1. Materials and methods

2.2.1.1. Mouse endothelial cell cultures (bEnd.3)

Cryopreserved bEnd.3 cells purchased from (American type culture collection, VA, USA) were cultured in Dulbecco's Modified Eagle's Medium (DMEM) with 4.5 g /L D-glucose, 4mM L-glutamine, and 0.11 g/L sodium pyruvate (Invitrogen Gibco, CA, USA) containing 10% foetal bovine serum albumin (Invitrogen, Gibco), hepes (Sigma Aldrich, MO, USA) and antibiotics (Invitrogen , Gibco) in a 5% CO₂ atmosphere at 37° C. Cells were seeded in 75 cm² tissue culture flasks containing 15 – 17 mL of the growth media until about 80% confluent with medium renewal every 2 – 3 days.

2.2.1.2. Cell density and total protein concentrations

Cell density and total protein concentration assessments were carried out on bEnd.3 cells cultured in 75 cm² culture flasks. Cell density was determined on a Neubaour haemocytometer counting chamber (Sigma, Aldrich, MO, USA). Cell density was approximately 1×10⁵ cells/mL. Cells viability was assessed with Trypan Blue Solution (0.4%) (Sigma, Aldrich, MO,USA).

Total protein concentrations of cell cultures were determined using a Micro BCA Protein Assay Kit (Pierce IL, USA) and bovine serum albumin was used to generate standard curves. Total protein concentration was 1.6 mg/mL.

2.2.1.3. *In vitro* biotinylation

In vitro biotinylation was performed on two 75 cm² flasks following a modified protocol from Scheurer, S. *et al.* (2005) and Roesli, C. *et al.* (2006). Each flask was washed once with PBS pH7.4. Fifteen millilitres of PBS containing 67µM EZ-link (Sulfo-NHS-SS-Biotin) (Pierce, IL, USA) were added to the flasks and incubated for 5 min at room temperature. The biotinylation reaction was terminated by adding Tris Hcl pH 7.5 to a final concentration of 670 µM. After 5 min incubation the cells were washed once with PBS and harvested with 10 mL PBS containing 67µM oxidized glutathione (Sigmas, Aldrich, MO, USA). Cells were pelleted by centrifugation at 1600 g × 5 min and lysed with 1 mL of lysis buffer containing [2% w/v NP40, 0.2% w/v SDS, 100 µM oxidized glutathione and protease inhibitor (Complete, EDTA-free, Roche, Switzerland)] and incubated on ice for 30 minutes.

Biotinylated proteins were captured on streptavidin sepharose high performance (GE health care, Australia). Five hundred microlitres of streptavidin sepharose were washed three times with buffer **A** containing (1% w/v NP40, 0.1% w/v SDS in PBS) before adding to cell lysates. Pooled lysates were incubated with washed streptavidin sepharose for 2 h in a cold room. Streptavidin sepharose was pelleted by centrifugation 1600 g × 5min. Unbound proteins were removed by washing three times with buffer **A**, once with buffer **B** (0.1% w/v NP40, 0.5 M NaCl in PBS) and once with 50 mM Tris-Hcl pH 7.5.

Captured proteins were incubated with 0.4 mL of (5% 2 –mercapthanol in PBS) for 15 minutes on ice to elute proteins. This step was repeated three times. Eluates were collected by centrifugation (1600g × v1 minute) and pooled. Eluted proteins were precipitated by

adding 200 μ L of Tri-chloroacetic acid (TCA) to a final concentration of 10% and incubated for 30 min on ice. Proteins were pelleted (10,000 g \times 5 min) and washed with 1 mL ethanol and air dried.

2.2.1.4. Digestion of eluted proteins and LC-MS/MS analysis

The TCA precipitate (pellet) was dissolved in 50 μ L of 50 mM Ammonium Biocarbonate and 300 ng trypsin was added and incubated overnight at 37°C and analysed by LC-MS/MS. Forty microliters of the sample were injected onto a peptide trap (Michrome peptide Captrap) for preconcentration then desalted with 0.1% formic acid, 2% ACN, at 500 mL/min. The peptide trap was then switched into line with the analytical column. Peptides were eluted from the column by a linear solvent gradient, with steps, from H₂O:CH₃CN (100:0, + 0.1% formic acid) to H₂O:CH₃CN (10:90, + 0.1% formic acid) at 500 mL/min over an 80 min period. The LC eluent was subjected to positive ion nanoflow electrospray MS analysis on QSTAR Elite, which was operated in an information dependent acquisition mode (IDA).

In IDA mode a TOFMS scan was acquired (m/z 400-1600, 0.5s), with the three largest multiply charged ions (counts > 50) sequentially subjected to MS/MS analysis. MS/MS spectra were accumulated for 2 s (m/z 100-1600).

2.2.1.5. Data processing

The LC-MS/MS data were submitted to Mascot for protein identification using the SwissProt database containing *Mus musculus* protein entries. Biotinylated lysine and amino terminus were considered as static modifications. Peptide ion scores above 35 were reported giving a probability of correct identification ($P < 0.05$).

2.2.2. Results

Only fewer proteins of bEnd.3 cultures were identified by mass spectrometry (Figure 23), therefore further protocol optimization was necessary. Below are described the subsequent *in vitro* biotinylation optimizations that were carried out using bovine serum albumin (BSA), alpha casein protein (α -casein) and *Ecoli*, before the second *in vitro* biotinylation attempt on bEnd3 cultures.

Mascot Search Results

User : Margaret
 Email :
 Search title : D:\PE Sciex Data\Projects\LCMS QSTAR 100305\Data\APAF_Client\Margaret_band3_13Apr2010.wiff (sa
 MS data file : \\mASSPEC1\ms data\mARK m\MARGARET BAND3 13aPR2010.MGF
 Database : NCBI nr 20090611 (9029658 sequences; 3093850741 residues)
 Taxonomy : Mus. (144777 sequences)
 Timestamp : 13 Apr 2010 at 23:27:08 GMT
 Enzyme : Trypsin
 Variable modifications : Oxidation (M)
 Mass values : Monoisotopic
 Protein Mass : Unrestricted
 Peptide Mass Tolerance : \pm 300 ppm
 Fragment Mass Tolerance : \pm 0.6 Da
 Max Missed Cleavages : 1
 Instrument type : Default
 Number of queries : 1055
 Protein hits :

gi 4103156	hair keratin basic 5; keratin Hb5 [Mus musculus]
gi 47059013	keratin 73 [Mus musculus]
gi 12852157	unnamed protein product [Mus musculus]
gi 12843914	unnamed protein product [Mus musculus]
gi 22164776	keratin 6L [Mus musculus]
gi 51092303	Tryp10-like trypsinogen [Mus musculus]
gi 149234275	PREDICTED: eEF1A2 binding protein [Mus musculus]
gi 398168	keratin 2 epidermis [Mus musculus]
gi 38566224	Slc22a17 protein [Mus musculus]
gi 74210080	unnamed protein product [Mus musculus]
gi 149272669	PREDICTED: similar to Syop3 like Y-linked [Mus musculus]
gi 74148380	unnamed protein product [Mus musculus]
gi 148681362	mCG140375 [Mus musculus]
gi 99032654	Chain A, X-Ray Structure Of A Hypothetical Protein From Mouse Mm.209172
gi 29747865	Tcp10b protein [Mus musculus]

Select Summary Report

Select Summary (protein hits) ☐ [Help](#)

Significance threshold $p < 0.05$ Max. number of hits AUTO

Standard scoring ☐ MudPIT scoring ☒ Ions score or expect cut-off 0 Show sub-sets 0

Show pop-ups ☒ Suppress pop-ups ☐ Require bold red ☐

Figure 23. Mascot search results of bEnd.3 cells, first trial. Sixteen proteins only were identified

2.3. *In vitro* biotinylation of BSA and α -casein proteins

2.3.1. *Materials and methods*

2.3.1.1. *In vitro* biotinylation

Twenty access fold of biotin was added to BSA and α -casein proteins as follows. Sixty millilitres and 283 μ L of (0.6 μ M and 2.8 μ M) of EZI-Link (Sulfo-NHS-SS-Biotin), (Pierce) were added to 30 nM of BSA, and 141 nM of α -casein respectively. After 5 min incubation at room temperature, the biotinylation reaction was terminated by adding Tris-HCl pH 7.5 and oxidised glutathione to a final concentration of 6 μ M and 0.6 μ M respectively for BSA and 28 μ M and 2.8 μ M respectively for α -casein. Samples were incubated for 15 minutes at room temperature.

2.3.1.2. *One dimensional electrophoreses*

Seventeen microliters from both samples were collected and mixed with 5 μ L of sample buffer LDS \times 4 (Invitrogen, CA, USA) and heated for 5 min at 60°C. One dimensional SDS-PAGE was performed using 12% Tris-HCl pre casts gels (Invitrogen, CA, USA) for approximately 1 h at 30 V. Protein bands were visualised by Coomassie Blue staining and excised using a scalpel blade. Bands were digested overnight with trypsin, and analysed by MALDI-TOF mass spectrometry.

2.3.1.3. *MALDI-TOF mass spectrometry*

Matrix Assisted Laser Desorption Ionisation (MALDI) mass spectroscopy was performed using the 4800 plus MALDI TOF/TOF Analyser (AB Sciex). A Nd:YAG laser (355 nm) was used to irradiate the sample. Spectra were acquired in reflectron MS scan mode in a mass range of 700–3500 Da. The instrument switched to MS/MS mode where the strongest eight peptides from the MS scan were isolated and fragmented by collision induced dissociation,

and re-accelerated to measure their masses and intensities. A near point calibration was applied to give a typical mass accuracy of 50 ppm or better.

2.3.1.4. Data processing

The LC- MS/MS data were submitted to Mascot (Matrix, London, UK) for protein identification using the SwissProt database containing *Human* protein entries. Biotinylated lysine and amino terminus were considered as static modifications. Peptide ion scores above 35 were reported giving a probability of correct identification ($P < 0.05$).

2.3.2. Results

Mass spectrometry analysis identified the biotinylated peptides in both α -casein and BSA proteins [Figure 4 (A: B) and

Figure (A: B)]. Figure 24A and 25A shows the peptides that matched BSA and α -casein in Mascot search results with a score of 661 and 34% sequence coverage for BSA and a score of 482 and 44% sequence coverage for α -casein, while figures 24B and 25B show the matched peptide spectrum of BSA and α -casein with ion scores of 109 and 131 respectively. Tables 2 and 3, represent the peptide sequences that matched BSA and α -casein, $p < 0.05$.

Protein View

Match to: **ALBU_BOVIN** Score: 661 Expect: 5.2e-062

Serum albumin OS=Bos taurus GN=ALB PE=1 SV=4

Found in search of \\Massspec1\MS_DATA\4800+ Users\Users\Matt F\MF040510\ppw_Al_127294141400.txt

Nominal mass (M_r): 69248; Calculated pI value: 5.82

NCBI BLAST search of **ALBU_BOVIN** against nr

Unformatted sequence string for pasting into other applications

Taxonomy: Bos taurus

Variable modifications: Carbamidomethyl (C), Oxidation (M)

Cleavage by Trypsin: cuts C-term side of KR unless next residue is P

Sequence Coverage: 34%

Matched peptides shown in Bold Red

```

1 MKWTFISLL LLFSSAYSRG VFRDTHKSE IAHRFKDLGE EHFKGLVLIA
51 FSQYLQCCPF DEHVKLVNEL TEFKTCVAD ESHAGCEKSL HTLFGDELCK
101 VASLRETYGD MADCEKQEP ERNECFLSHK DSDPDLPLK PDPNTLCDEF
151 KADEKKFWGK YLYEIARRHP YFYAPELLYY ANKYNGVFQE CCQAEDKGAC
201 LLPKIETMRE KVLASSARQR LRCASIQKFG ERALKAWSVA RLSQKFFKAE
251 FVEVTKLVTD LTKVHKSCCH GDLLSCADDR ADLAKYICDN QDTISSKLKE
301 CCKKPLLEKS HCIAEVEKDA IPENLPPLTA DFAEDKDVCK NYQEAKDAFL
351 GSFLYEYSRR HPEYAVSVLL RLAKVEATL EECCAKDDPH ACYSTVFDKL
401 KHLVDEPQNL IKQNCDFEK LGEYGFQNAL IVRYTRKVPQ VSTPTLVEVS
451 RSLGKVGTRC CTKPESEEMP CTEDYLSLIL NRLCVLHEKT PVSEKVIKCC
501 TESLVNRRPC FSALTPDET YPKAFDEKLF TFHADICTLP DTEKQIKKQT
551 ALVELLKHKP KATEEQKTV MENFVAFVDK CCAADDKEAC FAVEGPKLVV
601 STQTALA

```

Show predicted peptides also

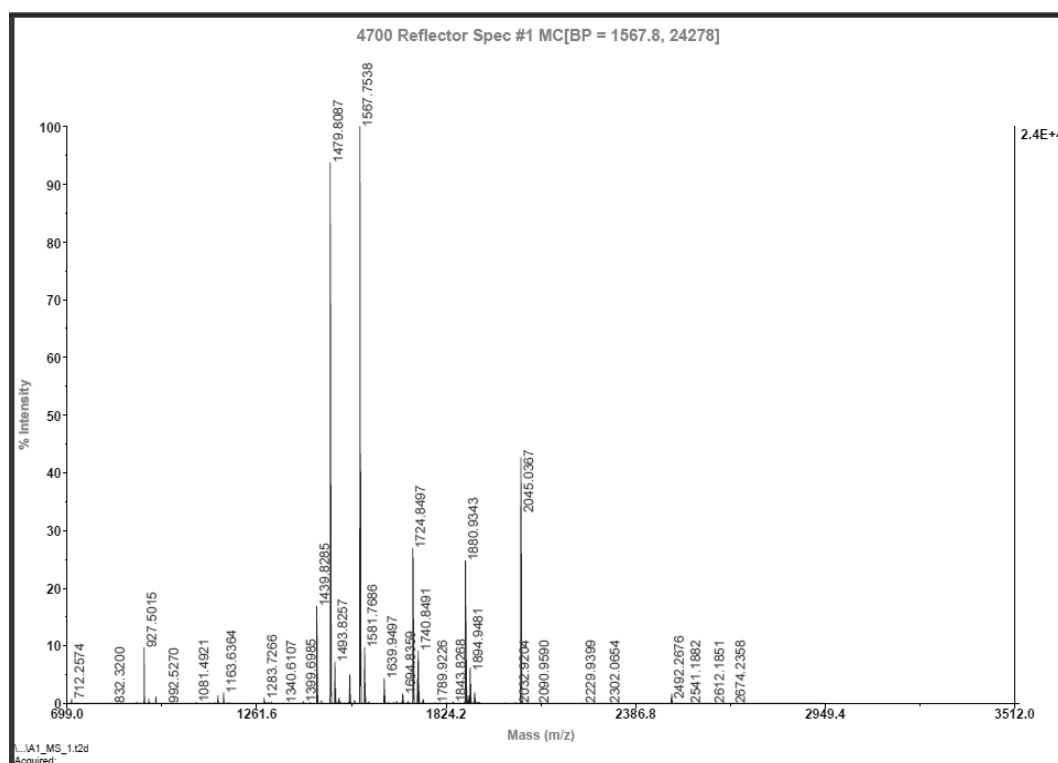


Figure 24. A: Mascot search results for BSA, matched peptides are in bold red. B: Matched peptide spectrum with ion score of 109

Table 2. Peptide sequences that matched BSA, their query numbers and ion scores, $p < 0.05$

Query	Matched sequences	Ion scores
433	K.LGEYGFQNALIVR.Y	109
482	R.MPCTEDYLSLILNR.L	123
482	R.MPCTEDYLSLILNR.L	84
183	R.RHPYFYAPELLYYANK.Y	84
359	K.DAFLGSFLYEYSR.R	125
371	R.RHPEYAVSVLLR.L	39
523	R.RPCFSALTPDETYVK.A	56

Table 3. Peptide sequences matched alpha casein, their query and ion scores, $p < 0.05$

Query	Matched sequences	Ions scores
37	K.HPIKHQGLPQEVLENENLLR.F	40
37	K.HQGLPQEVLENENLLR.F	131
49	R.FFVAPFPEVFGK.E	28
115	R.YLGYLEQLLR.L	94

25A

MATRIX

SCIENCES

Mascot Search Results

Protein View

Match to: **CASA1_BOVIN** Score: 482 Expect: 4.1e-044
Alpha-S1-casein OS=Bos taurus GN=CSN1S1 PE=1 SV=2
Found in search of \\Massspec1\MS_DATA\4800+ Users\Users\Matt F\MF040510\ppw_A2_127294141401.txt

Nominal mass (M_r): 24513; Calculated pI value: 4.98
NCBI BLAST search of **CASA1_BOVIN** against nr
Unformatted [sequence string](#) for pasting into other applications

Taxonomy: [Bos taurus](#)

Variable modifications: Carbamidomethyl (C), Oxidation (M)
Cleavage by Trypsin: cuts C-term side of KR unless next residue is P
Sequence Coverage: **44%**

Matched peptides shown in Bold Red

1 MKLLILTCLV AVALARPKHP IKHQGLPQEV LENENLLRFFV APFPEVFGKE
51 KVNELSKDIG SESTEDQAME DIKQMEAESI SSSEIVPNS VEQKHQKED
101 VPSERYLGYL EQLLRLKKYK VPQLEIVPNS ABERLHSMKE GIHAQQKEPM
151 IGVNQELAYF YPELFRQFYQ LDAYPSGAWY VVPLGTQYTD APSFSDIPNP
201 IGSENSEITL MPLW

Show predicted peptides also

Sort Peptides By

☒ Residue Number
☐ Increasing Mass
☐ Decreasing Mass

Start - End	Observed	Mr(expt)	Mr(calc)	ppm	Miss	Sequence
19 - 37	2235.2710	2234.2637	2234.2283	16	1	K.HPIKHQGLPQEVLENENLLR.F (Ions score 40)
19 - 37	2235.2710	2234.2637	2234.2283	16	1	K.HPIKHQGLPQEVLENENLLR.F (No match)
23 - 37	1759.9749	1758.9676	1758.9377	17	0	K.HQGLPQEVLENENLLR.F (Ions score 131)
23 - 37	1759.9749	1758.9676	1758.9377	17	0	K.HQGLPQEVLENENLLR.F (No match)
38 - 49	1384.7491	1383.7418	1383.7227	14	0	R.FFVAPFPEVFGK.E (Ions score 28)
38 - 49	1384.7491	1383.7418	1383.7227	14	0	R.FFVAPFPEVFGK.E (No match)
95 - 105	1337.7073	1336.7000	1336.6735	20	1	K.HIQKEDVPSER.Y (No match)
106 - 115	1267.7291	1266.7218	1266.6972	19	0	R.YLGYLEQLLR.L (Ions score 94)
106 - 115	1267.7291	1266.7218	1266.6972	19	0	R.YLGYLEQLLR.L (No match)
119 - 134	1872.0182	1871.0109	1870.9788	17	1	K.YKVPQLEIVPSARER.L (No match)

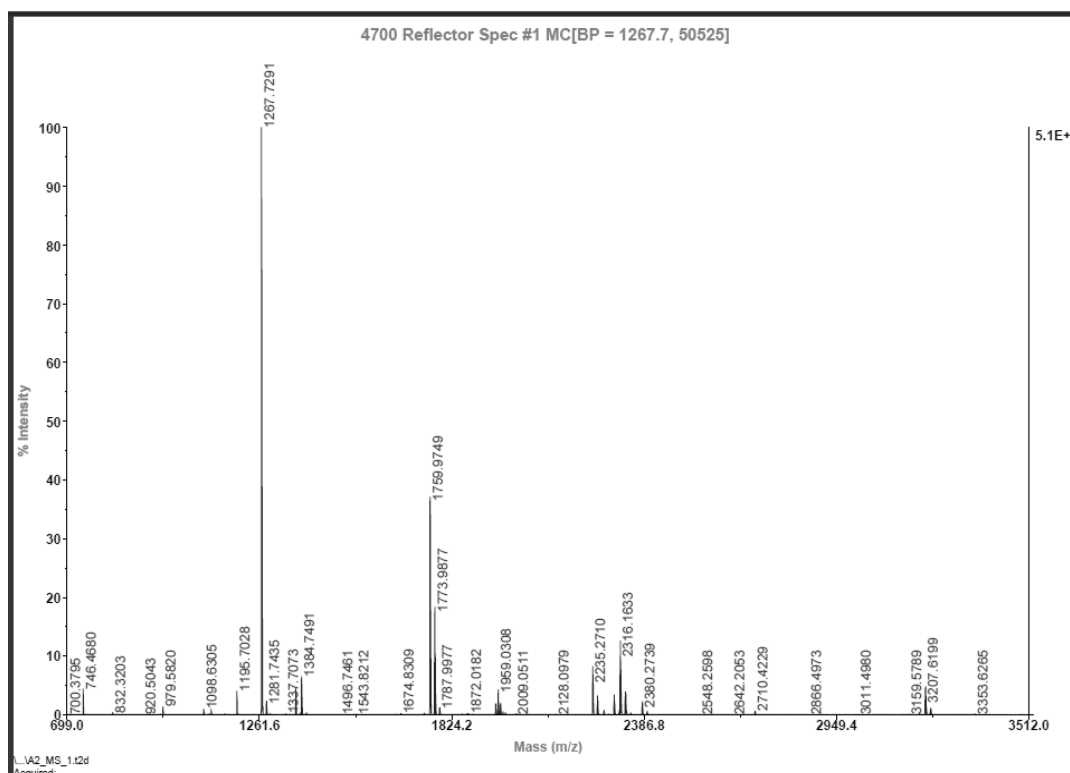


Figure 25. A: Mascot search results for protein alpha casein, matched peptides are in bold red. B: Matched peptide spectrum with ion score of 131.

2.4. *In vitro* biotinylation of BSA and *E.coli* - First trial

The aim of this optimization trial was to examine the efficient detection of biotinylated BSA proteins in the presence of a high amount of un-biotinylated *E.coli* proteins in the same sample mixture. This was important since future experiments would rely on the efficient detection of biotinylated proteins in a complex mixture.

2.4.1. Materials and methods

2.4.1.1. Total protein concentration of *E.coli*.

Total protein concentration was performed on *E.coli* whole cell lysate using the Bradford assay with Bio-Rad protein assay kit (Bio-Rad, Castle Hill, NSW). Bovine serum albumin was used to generate standard curves. Total protein concentration of *E.coli* was 1.37 mg/mL.

2.4.1.2. *In vitro* biotinylation of BSA

In vitro biotinylation was performed using another form of biotin derivative, (Sulfo-NHS-LC-Biotin), instead of the Sulfo-NHS-SS-Biotin previously used, because the latest wasn't available in the Mascot search parameters.

One and half nM of BSA was biotinylated with 30 nM (20 access fold) of EZI-Link (Sulfo-NHS-LC-Biotin) (Pierce) and incubated for 5 min at room temperature. The biotinylation reaction was terminated with 0.3 μ M Tris-HCl pH 7.5 and incubated for 15 min at room temperature. Ten access fold of *E.coli* was added to the biotinylated BSA to test the successful capture of biotinylated BSA in the presence of un-biotinylated *E.coli* proteins.

2.4.1.3. *Capture of biotinylated BSA*

Biotinylated BSA was captured on streptavidin sepharose high performance (GE health care, Australia). Six hundred and forty microlitres of streptavidin sepharose were washed three times with buffer **A** containing (1% w/v NP40, 0.1% w/v SDS in PBS) before adding to the protein mixture, then incubated with washed streptavidin sepharose for 2 h at room temperature. Streptavidin sepharose was pelleted by centrifugation at $1600\text{ g} \times 5\text{ min}$. Unbound proteins were removed by washing three times with buffer **A**, once with buffer **B** (0.1% w/v NP40, 2 M NaCl in PBS) and three times with digestion buffer (50 mM ammonium bicarbonate).

2.4.1.4. *Protein digestion, purification and LC-MS/MS analysis*

Proteins were digested overnight with trypsin as described earlier and purified with OMIX C18 tips (Varian) as follows: protein digests were acidified with 25% trifluoroacetic acid (TFA), the OMIX tip was washed with 100 μ L of 90% acetonitrile and 0.1% TFA by aspiration and discarding the solvent five times. Equilibrations were then performed by aspirating 100 μ L of 0.1 % TFA and discarding the solvent five times. The tip was applied to

the pre-treated sample, dispense and aspirate 100 μ L for up to 10 cycles. The tip then was rinsed three times with 0.1% TFA and the sample eluted by aspiration of 100 μ L of 50% acetonitrile and 0.1% TFA. The sample was dried by Speed Vac for 20 minutes before being subjected to LC-MS/MS analysis as described in section **2.2.1.4**. The data were processed as described in section **2.3.1.4**.

2.4.2. Results

Mass spectrometry analysis successfully identified biotinylated BSA proteins in a mixture of un-biotinylated *E.coli* proteins. Figure 26A is the Mascot search result showing the identified BSA in the fourth hit among all other *E.coli* proteins. Figure 26B shows the peptides that matched BSA in Mascot search results with a score of 448 and 26% sequence coverage, while figure 26C is the matched peptide spectrum of BSA with ion scores of 118. Table 4 represents the peptide sequences that matched BSA, their numbers and ion scores, $p < 0.05$.

Table 4. Peptide sequences that matched BSA, their numbers and ion score

Query	Matched sequences	Ion scores
607	K.LVVSTQTALA	65
557	K.KQTALVELLK.H	60
412	K.HLVDEPQNLIK.Q	53
482	R.MPCTEDYLSLILNR.L	118
451	R.KVPQVSTPTLVEVSR.S	93
336	K.DAIPENLPPLTADFAEDK.D	73
183	R.HPYFYAPELLYYANK.Y	75
557	K.QTALVELLK.H	65
359	K.DAFLGSFLYEYSR.R	76
580	K.TVMENFVAFVDK.C	80
44	K.DLGEEHFK.G	29
75	K.LVNELTEFAK.T	28
167	K.YLYEIAR.R	34
256	K.AEFVEVTK.L	44

Mascot Search Results

```

: margaret
:
:
: Margaret_17May2010.mgf
: SwissProt 2010x (519348 sequences; 183273162 residues)
: 24 Dec 2010 at 02:09:39 GMT
:
: BFTU_SALAR Elongation factor Tu OS=Salmonella arizonae (strain ATCC BAA-7
: BFTU_SHIBS Elongation factor Tu OS=Shigella boydii serotype 4 (strain Sh2
: TCFR1_HUMAN TGF-beta receptor type-1 OS=Homo sapiens GN=TCFBR1 PE=1 SV=1
: ALBU_BOVIN Serum albumin OS=Bos taurus GN=ALB PE=1 SV=4
: BFTU1_PHOLI Elongation factor Tu 1 OS=Photorhabdus luminescens subsp. laun
: BFTU_SODGM Elongation factor Tu OS=Sodalis glossinidius (strain morsitans
: BLAT_ECOLX Beta-lactamase TEM OS=Escherichia coli GN=bla PE=1 SV=1
: G3P1_ESCFE Glyceraldehyde-3-phosphate dehydrogenase A (Fragment) OS=Esche
: G3P CITFE Glyceraldehyde-3-phosphate dehydrogenase (Fragment) OS=Citroba
: BFTU_HABIE Elongation factor Tu OS=Haemophilus influenzae (strain PittEE)
: BFTU1_YERP3 Elongation factor Tu 1 OS=Yersinia pseudotuberculosis serotype
: BFTU1_YERR8 Elongation factor Tu 1 OS=Yersinia enterocolitica serotype O:6
: DNAK_ECOHS Chaperone protein dnaK OS=Escherichia coli O9:H4 (strain HS) G
: BCCP_ECOLI Biotin carboxyl carrier protein of acetyl-CoA carboxylase OS=E
: GST26_SCHJA Glutathione S-transferase class-mu 26 kDa isozyme OS=Schistos
: ACON2_ECOLI Aconitate hydratase 2 OS=Escherichia coli (strain K12) GN=acnE
: SUCC_ECOWW Succinyl-CoA ligase [ADP-forming] subunit beta OS=Escherichia
: RPOA_ECOHS DNA-directed RNA polymerase subunit alpha OS=Escherichia coli
: IDH_ECOLI Isocitrate dehydrogenase [NADP] OS=Escherichia coli (strain K1
: ATPB_ECOWW ATP synthase subunit beta OS=Escherichia coli (strain K12 / MC
: SAV_STRAV Streptavidin OS=Streptomyces avidinii PE=1 SV=1
: IF2_ECO24 Translation initiation factor IF-2 OS=Escherichia coli O139:H2
: RPOB_ECOWW DNA-directed RNA polymerase subunit beta OS=Escherichia coli
: BFTU_BUCAI Elongation factor Tu OS=Buchnera aphidicola subsp. Acyrthosiph
: CLPB_ECOLI Chaperone protein ClpB OS=Escherichia coli (strain K12) GN=clpB
: GLPK_SHIDS Glycerol kinase OS=Shigella dysenteriae serotype 1 (strain Sd1
: RPOC_ECOWW DNA-directed RNA polymerase subunit beta' OS=Escherichia coli
: FTSH_BUCAP Cell division protease ftsH OS=Buchnera aphidicola subsp. Schi
: IBPA_ECOWW Small heat shock protein ibpA OS=Escherichia coli (strain K12)
: BFTU_DESVH Elongation factor Tu OS=Desulfovibrio vulgaris (strain Hildenb
: RL4_CITK8 S0S ribosomal protein L4 OS=Citrobacter koseri (strain ATCC 252
: RHO_ECOLI Transcription termination factor rho OS=Escherichia coli (stra
: BFTU_AERS4 Elongation factor Tu OS=Aeromonas salmonicida (strain A448) GN
: USG_ECOLI USG-1 protein OS=Escherichia coli (strain K12) GN=usg PE=1 SV=
: BGAL_ECOHS Beta-galactosidase OS=Escherichia coli O9:H4 (strain HS) GN=la
: AHPC_ECOLI Alkyl hydroperoxide reductase subunit C OS=Escherichia coli (s

```

MATRIX SCIENCE Mascot Search Results

Protein View

Match to: **ALBU BOVIN** Score: **448**
 Serum albumin OS=Bos taurus GN=ALB PE=1 SV=4
 Found in search of Margaret_17May2010.mgf

Nominal mass (M_r): **69248**; Calculated pI value: **5.82**

NCBI BLAST search of **ALBU BOVIN** against nr
 Unformatted sequence string for pasting into other applications

Taxonomy: Bos taurus

Cleavage by Trypsin: cuts C-term side of KR unless next residue is P
 Sequence Coverage: **26%**

Matched peptides shown in Bold Red

```

1 MKWVTFISLL LLFSSAYSRG VFRDTHKSE IAHRFKDLGE EHFGLVLIA
51 FSQYLQQCPF DEHVKLVLNEL TEFKTCVAD ESHAGCEKSL HTLFGDELCK
101 VASLRETYGD MADCCCKQEP ERNECFLSHK DDSPDLPLK PDPNLCDEF
151 KADEKKFWGK YLYEIARRHP YFYAPPELLYY ANKYNGVFQE CCQAEKGGAC
201 LLPKIETMRE KVLASSARQR LRCASIQKFG ERALKAWSVA RLSQKFPKAE
251 FVEVTKLVTD LTKVHKECCH GDLECCADDR ADLAKYICDN QDTISSKLKE
301 CCDKPLLEKS HCIAEVEKDA IPENLPPLTA DFAEDKDVCK NYQEAQDAFL
351 GSFLYYSRRR HPEYAVSVLL RLAKYEATL EECCKADDPH ACYSTVFDKL
401 KHLVDEPQNL IKQNCQDFEK LGEYGFQNAL IVRYTRKVPQ VSTPTLVEVS
451 RSLGKVGTRC CTKPESERMP CTEDYLSLIL NRLCVLHEKT PVSEKVTKCC
501 TESLVNRRPC FSALTPDETY VPKAFDEKLF TFHADICTLP DTEKQIKKQT
551 ALVELLKHKP KATEEQLKTV MENFVAFVDK CCAADDKEAC FAVEGPKLVV
601 STQTALA

```

Show predicted peptides also

Sort Peptides By

☒ Residue Number ☐ Increasing Mass ☐ Decreasing Mass

Start - End	Observed	Mr (expt)	Mr (calc)	ppm	Miss	Sequence	
37 - 44	487.7317	973.4488	973.4505	-2	0	K.DLGEEHFK.G	(Ions score 29)
66 - 75	582.3105	1162.6065	1162.6234	-14	0	K.LVNELTEFAK.T	(Ions score 58)
66 - 75	582.3379	1162.6613	1162.6234	33	0	K.LVNELTEFAK.T	(Ions score 28)
66 - 75	582.3493	1162.6841	1162.6234	52	0	K.LVNELTEFAK.T	(Ions score 41)
161 - 167	464.2446	926.4746	926.4861	-12	0	K.YLYEIAR.R	(Ions score 34)

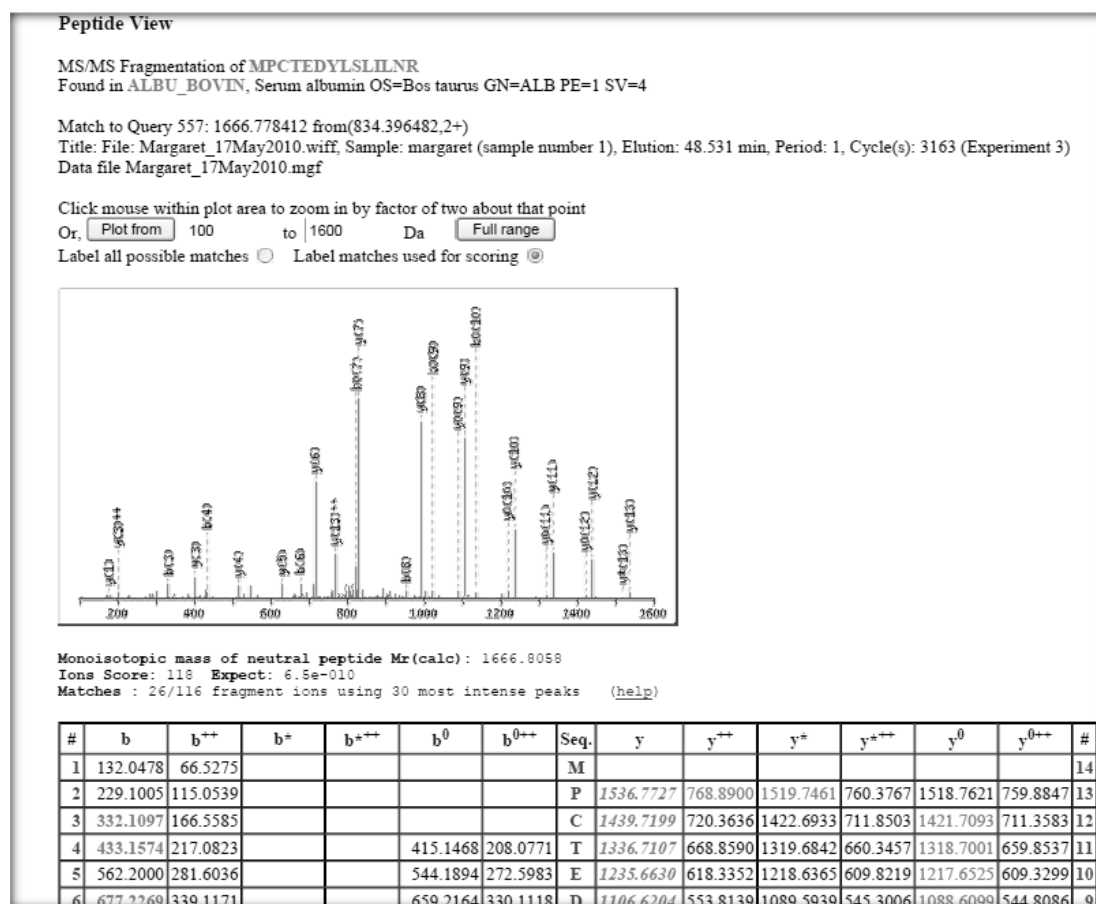


Figure 26. A: Mascot search results identified BSA (the fourth on the list). B: Protein View of BSA matched peptides in bold red. C: Peptide spectrum with ion scores of 118

Although the results above indicated the successful capture of biotinylated proteins, further optimizations on the protocol were performed to examine different parameters, such as biotin type, concentration, and incubation conditions, to reach optimal protein biotinylation and identification.

2.5. *In vitro* biotinylation of BSA and *E.coli* - Second trial

2.5.1. *Materials and methods*

2.5.1.1. *In vitro* biotinylation of BSA

Two samples of BSA were prepared as follows: 1.5 nM of BSA was biotinylated with 30 nM (20 access fold) of EZI-Link (Sulfo-NHS-LC-Biotin), (Pierce) and incubated for 5 minutes at room temperature. The second 1.5 nM of BSA was biotinylated with 60 nM of EZI-Link (40 access fold) and incubated for 15 minutes at room temperature. The biotinylation reactions were terminated with 0.3 μ M and 0.6 μ M Tris-HCl pH 7.5 respectively and incubated for 15 min at room temperature. Almost 30 access fold of *E.coli* was then added to the second sample (the 40 access fold of biotinylated BSA).

2.5.1.2. *Capture of biotinylated BSA*

The 40 access fold biotinylated BSA was captured on streptavidin sepharose (GE health care, Australia). Six hundred and forty microlitres of streptavidin sepharose were washed three times with buffer **A** containing (1% w/v NP40, 0.5% w/v SDS in PBS) before adding to the protein mixture, then incubated with washed streptavidin sepharose for two hours in room temperature. Streptavidin sepharose was pelleted by centrifugation 1600 g \times 5minutes.

Unbound proteins were eliminated by washing three times with buffer **A**, once with buffer **B** (0.1% w/v NP40, 0.5 M NaCl in PBS) and three times with digestion buffer (50 mM ammonium bicarbonate).

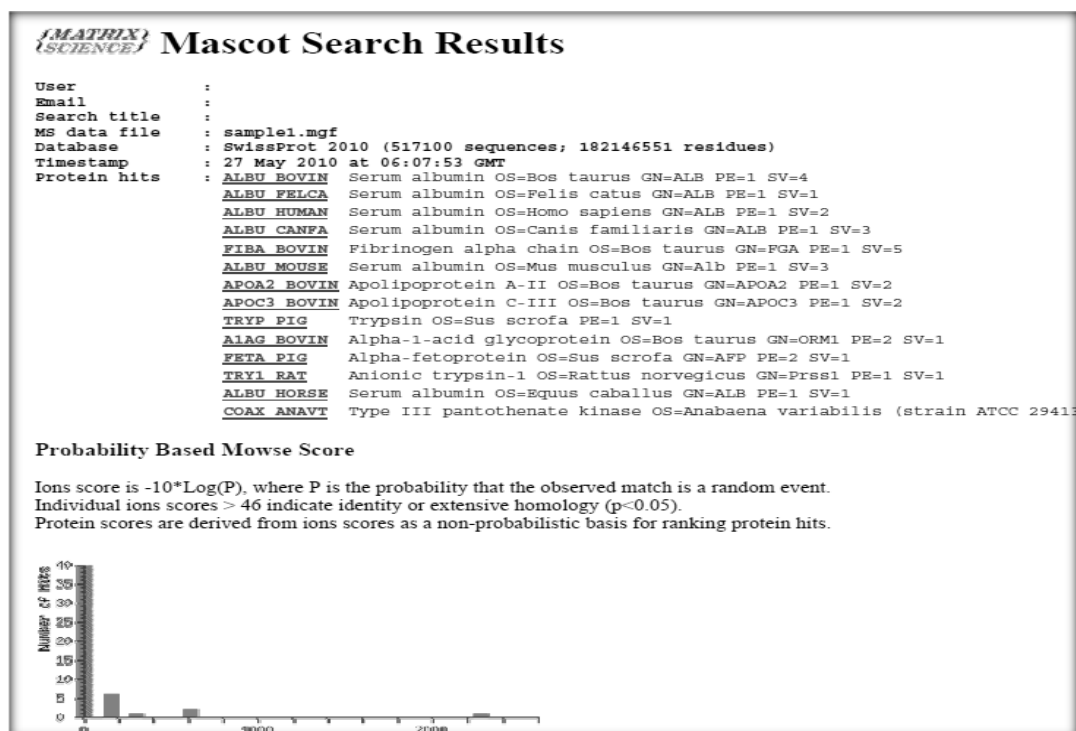
The 20 access fold biotinylated BSA was not captured on streptavidin sepharose. After the biotinylation termination reaction, BSA was digested with trypsin overnight.

2.5.1.3. Protein digestion, purification and LC-MS/MS analysis

Both BSA samples were digested overnight with trypsin and purified with OMIX C18 tips, as described in section 2.4.1.4. Samples were then dried by Speed Vac for 20 min before being subjected to LC-MS/MS analysis as described in section 2.2.1.4, and data analysis as described in section 2.3.1.4.

2.5.1. Results

The aim of this experiment was to examine the effect of different biotin concentrations and incubation periods on BSA biotinylation and capture, in the presence and absence of unbiotinylated *E.coli* proteins. Mass spectrometry successfully detected biotinylated BSA in both samples (Figure 17 and Figure 28). Figure 27A is the mascot search results showing the identified BSA that was biotinylated with 20 access fold of biotin with 5 min incubation, in the absence of unbiotinylated *E.coli* proteins. Figure 27B shows the peptides that matched BSA in mascot search results with a score of 2506 and 55% sequence coverage, while figure 27C is the matched peptide spectrum of BSA with an ion score of 129. Table 5 represents the sequences that matched BSA, $p < 0.05$.



Protein View

Match to: ALBU BOVIN Score: 2506
 Serum albumin OS=Bos taurus GN=ALB PE=1 SV=4
 Found in search of sample1.mgf

Nominal mass (M_r): 69248; Calculated pI value: 5.82
 NCBI BLAST search of ALBU BOVIN against nr
 Unformatted sequence string for pasting into other applications

Taxonomy: Bos taurus

Variable modifications: NHS-LC-Biotin (K)
 Cleavage by Trypsin: cuts C-term side of KR unless next residue is P
 Sequence Coverage: 55%

Matched peptides shown in Bold Red

```

1 MHWTFISLL LLFSSAYSRG VFRDTHKSE IARRFKDLGE EHFKGLVLIA
51 FSOYLQCCPF DEHVKLNLNEL TFAKTCVAD ESHAGCEKSL HTLPGDELCK
101 VASLRETYGD MADCCCKQEP ERNECFLSHK DDSPOLPKLK PDPNTLCDEF
151 KADEKKFWGK YLYEIARRHP YFYAPRLLYY ANKYNQVFQE CCQAEKGCAC
201 LLPKIETWRE KVLASSARQR LRCASIQKPG ERALKAWSVA RLSQKFFKAE
251 FVEVTKLAVD LTKVHKECCH GDLLECADDR ADLAKYICDN QDTISSKLKE
301 CCKKPLEKS HCIAEVRKDA IPENLPFLTA DFAEDKDVCK NYQEAKDAFL
351 GSFLEYEYRR HPEYAVSVLL RLAKYEATL EECCAKDDPH ACYSTVDFKL
401 KHLVDEPQNL IKQNCDOPEK LGYGFQNAL IVRYTRKVPQ VSTPTLVEVS
451 RSLKVGCTRC CTKPESERMP CTEDYLSLIL NRLCVLHKKI PVSEKVTKCC
501 TESLVNRRPC PSALTPOETY VKAFDEKLF TPHADICTLP DTEKQIKKQT
551 ALVELLKHKP KATEBQLKTV MENFVAFVDK CCAADKEAC FAVEGPKLVV
601 STOTALA
  
```

Show predicted peptides also

Sort Peptides By ☒ Residue Number ☐ Increasing Mass ☐ Decreasing Mass

Start - End	Observed	Mr (expt)	Mr (calc)	ppm	Miss	Sequence
35 - 44	417.1854	1248.5344	1248.6139	-64	1	R.FKDLGEEHFK.G (Ions score 46)
35 - 44	417.1970	1248.5692	1248.6139	-36	1	R.FKDLGEEHFK.G (Ions score 62)
35 - 44	417.2067	1248.5982	1248.6139	-13	1	R.FKDLGEEHFK.G (Ions score 49)
37 - 44	487.7024	973.3903	973.4505	-62	0	K.DLGEEHFK.G (Ions score 27)
45 - 65	812.3675	2434.0808	2434.2355	-64	0	K.GLVLIAFSQYLQCCPFDEHVK.L (Ions score 64)
45 - 65	812.3918	2434.1536	2434.2355	-34	0	K.GLVLIAFSQYLQCCPFDEHVK.L (Ions score 51)
45 - 65	812.4188	2434.2345	2434.2355	-0	0	K.GLVLIAFSQYLQCCPFDEHVK.L (Ions score 66)
89 - 100	454.8753	1361.6039	1361.6649	-45	0	K.SLHTLPGDELCK.V (Ions score 60)
131 - 138	443.7028	885.3910	885.4080	-19	0	K.DDSPOLPK.L (Ions score 33)
139 - 151	507.2317	1518.6731	1518.7388	-43	0	K.LKPDPTNLTCDERK.A (Ions score 14)
139 - 155	491.4757	1961.8736	1961.9404	-34	1	K.LKPDPTNLTCDERKAEK.K (Ions score 53)
161 - 167	464.2283	926.4420	926.4861	-48	0	K.YLYEIAR.R (Ions score 53)
168 - 183	682.2877	2043.8412	2044.0206	-88	1	R.RHPYFYAPRLLYYANK.Y (Ions score 17)

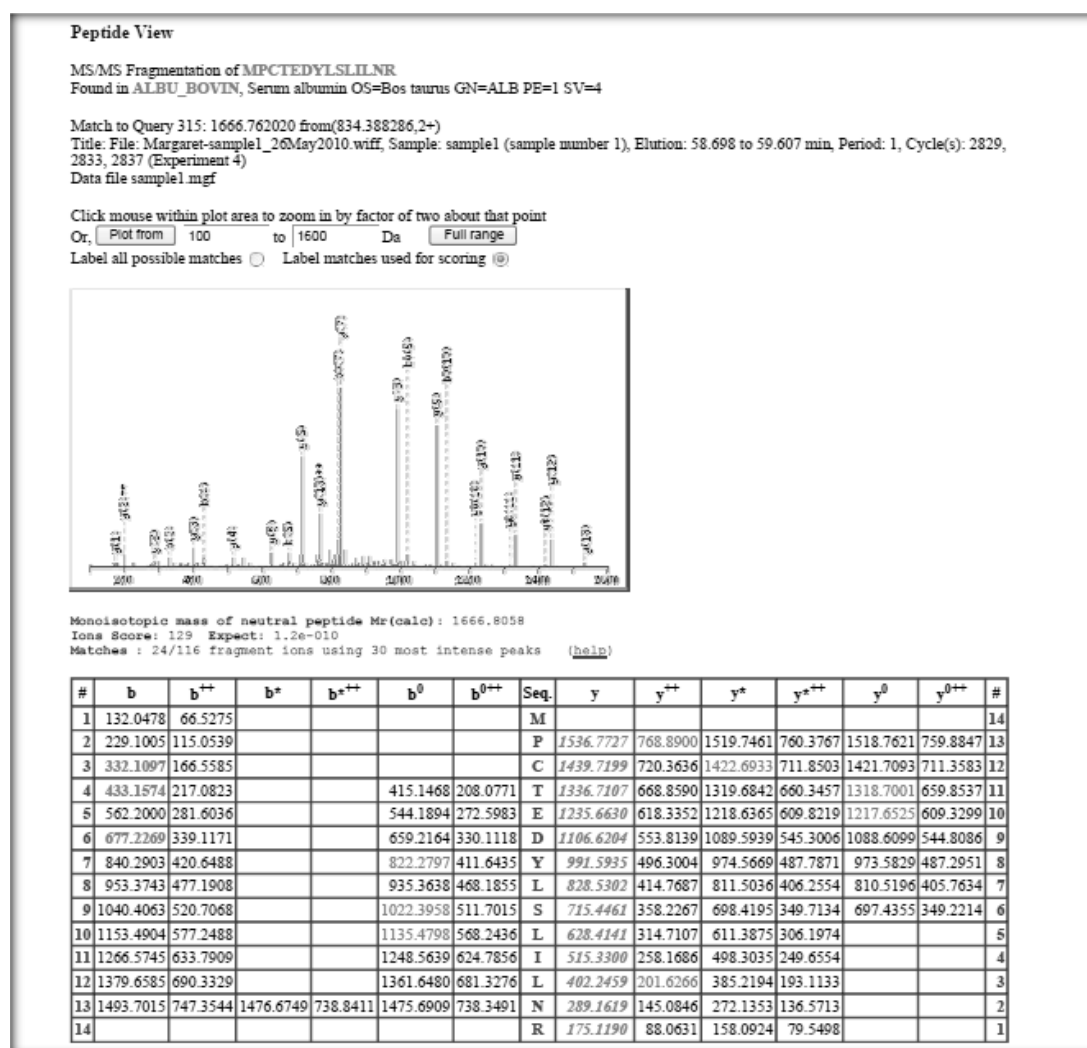


Table 5. Peptide sequences matched BSA, their query and ion scores, $p < 0.05$

Query	Matched sequences	Ion scores
155	R.HPEYAVSVLLR.L	123
103	K.KQTALVELLK.H	90
104	K.KQTALVELLK.H	64
105	K.KQTALVELLK.H	55
10	R.LSQKFPK.A	47
31	K.YLYEIAR.R	53
66	K.LVVSTQTALA	60
58	K.LVVSTQTALA	59
299	R.KVPQVSTPTLVEVSR.S	78
215	R.KVPQVSTPTLVEVSR	129
107	K.KQTALVELLK.H	49
154	R.HPEYAVSVLLR.L	60
169	K.HLVDEPQNLIK.Q	67
317	R.MPCTEDYLSLILNR.L	110
318	R.MPCTEDYLSLILNR.L	107
315	R.MPCTEDYLSLILNR.L	84
298	R.KVPQVSTPTLVEVSR.S	90
278	K.DAFLGSFLYEYSR.R	85
257	K.VPQVSTPTLVEVSR.S	84
296	KVPQVSTPTLVEVSR.S	77
239	K.LGEYGFQNALIVR.Y	111
173	K.HLVDEPQNLIK.Q	79
319	R.MPCTEDYLSLILNR.L	106

Figure 28A below represent the Mascot search result showing the identified BSA that was biotinylated with 40 access fold of biotin with 15 min incubation, in the presence of unbiotinylated *E.coli* proteins. Figure 28B shows the peptides that matched BSA in the Mascot search results with a score of 261 and 13% sequence coverage, while Figure 28C is the matched peptide spectrum of BSA with an ion score of 129. Table 6 represent the sequences that matched BSA with $p < 0.05$.

Mascot Search Results																																																																			
User	:																																																																		
Email	:																																																																		
Search title	:																																																																		
MS data file	: sample2.mgf																																																																		
Database	: SwissProt 2010 (517100 sequences; 182146551 residues)																																																																		
Timestamp	: 27 May 2010 at 06:16:01 GMT																																																																		
Protein hits	: <table> <tr> <td><u>TGFR1_BOVIN</u></td><td>TGF-beta receptor type-1 OS=Bos taurus GN=TGFR1 PE=2 SV=1</td></tr> <tr> <td><u>GST26_SCHJA</u></td><td>Glutathione S-transferase class-mu 26 kDa isozyme OS=Schistosoma japonicum PE=1 SV=3</td></tr> <tr> <td><u>SAV_STRAV</u></td><td>Streptavidin OS=Streptomyces avidinii PE=1 SV=1</td></tr> <tr> <td><u>ALBU_BOVIN</u></td><td>Serum albumin OS=Bos taurus GN=ALB PE=1 SV=4</td></tr> <tr> <td><u>ACBA_ECOLI</u></td><td>Isocitrate lyase OS=Escherichia coli (strain K12) GN=aceA PE=1 SV=1</td></tr> <tr> <td><u>BLAT_ECOLX</u></td><td>Beta-lactamase TEM OS=Escherichia coli GN=bla PE=1 SV=1</td></tr> <tr> <td><u>RS2_ECO27</u></td><td>30S ribosomal protein S2 OS=Escherichia coli O127:H6 (strain E2348/69 / EPEC) GN=rpsB PE=3 SV=1</td></tr> <tr> <td><u>TRYP_PIG</u></td><td>Trypsin OS=Sus scrofa PE=1 SV=1</td></tr> <tr> <td><u>DHSA_ECOLI</u></td><td>Succinate dehydrogenase flavoprotein subunit OS=Escherichia coli (strain K12) GN=sdhA PE=1 SV=1</td></tr> <tr> <td><u>ALBU_CANFA</u></td><td>Serum albumin OS=Canis familiaris GN=ALB PE=1 SV=3</td></tr> <tr> <td><u>ALBU_PIG</u></td><td>Serum albumin OS=Sus scrofa GN=ALB PE=1 SV=2</td></tr> <tr> <td><u>ALBU_FELCA</u></td><td>Serum albumin OS=Felis catus GN=ALB PE=1 SV=1</td></tr> <tr> <td><u>ALBU_MOUSE</u></td><td>Serum albumin OS=Mus musculus GN=Alb PE=1 SV=3</td></tr> <tr> <td><u>CLPX_ABRHH</u></td><td>ATP-dependent Clp protease ATP-binding subunit clpX OS=Aeromonas hydrophila subsp. hydrophila (strain ATCC 7966 / N</td></tr> <tr> <td><u>CLPX_ANAPZ</u></td><td>ATP-dependent Clp protease ATP-binding subunit clpX OS=Anaplasma phagocytophilum (strain HZ) GN=clpX PE=3 SV=1</td></tr> <tr> <td><u>CLPX_PARUW</u></td><td>ATP-dependent Clp protease ATP-binding subunit clpX OS=Protochlamydia amoebophila (strain UWE25) GN=clpX PE=3 SV=1</td></tr> <tr> <td><u>CLPX_ANATD</u></td><td>ATP-dependent Clp protease ATP-binding subunit clpX OS=Anaerocellum thermophilum (strain DSM 6725 / Z-1320) GN=clpX</td></tr> <tr> <td><u>BCCP_ECOLI</u></td><td>Biotin carboxyl carrier protein of acetyl-CoA carboxylase OS=Escherichia coli (strain K12) GN=accB PE=1 SV=1</td></tr> <tr> <td><u>SPG1_STRSG</u></td><td>Immunoglobulin G-binding protein G OS=Streptococcus sp. group G GN=spg PE=1 SV=1</td></tr> <tr> <td><u>K2C1_HUMAN</u></td><td>Keratin, type II cytoskeletal 1 OS=Homo sapiens GN=KRT1 PE=1 SV=6</td></tr> <tr> <td><u>DNAK_ECOHS</u></td><td>Chaperone protein dnaK OS=Escherichia coli O9:H4 (strain HS) GN=dnaK PE=2 SV=1</td></tr> <tr> <td><u>EFTU_ABRHH</u></td><td>Elongation factor Tu OS=Aeromonas hydrophila subsp. hydrophila (strain ATCC 7966 / NCIB 9240) GN=tuf1 PE=3 SV=1</td></tr> <tr> <td><u>EFTU1_YERRE</u></td><td>Elongation factor Tu 1 OS=Yersinia enterocolitica serotype O:8 / biotype 1B (strain 8081) GN=tuf1 PE=3 SV=1</td></tr> <tr> <td><u>DHSA_SALTY</u></td><td>Succinate dehydrogenase flavoprotein subunit OS=Salmonella typhimurium GN=sdhA PE=3 SV=1</td></tr> <tr> <td><u>ODO1_ECO57</u></td><td>2-oxoglutarate dehydrogenase E1 component OS=Escherichia coli O157:H7 GN=suca PE=3 SV=1</td></tr> <tr> <td><u>DNAK_YERPA</u></td><td>Chaperone protein dnaK OS=Yersinia pestis bv. Antiqua (strain Antiqua) GN=dnaK PE=2 SV=1</td></tr> <tr> <td><u>RL11_CITK8</u></td><td>50S ribosomal protein L11 OS=Citrobacter koseri (strain ATCC BAA-895 / CDC 4225-83 / SGSC4696) GN=rpLK PE=3 SV=1</td></tr> <tr> <td><u>GST27_SCHMA</u></td><td>Glutathione S-transferase class-mu 26 kDa isozyme OS=Schistosoma mansoni PE=2 SV=1</td></tr> <tr> <td><u>IP2_STRM5</u></td><td>Translation initiation factor IF-2 OS=Stenotrophomonas maltophilia (strain R551-3) GN=infB PE=3 SV=1</td></tr> <tr> <td><u>G3P1_ECO57</u></td><td>Glyceraldehyde-3-phosphate dehydrogenase A OS=Escherichia coli O157:H7 GN=gapA PE=3 SV=2</td></tr> <tr> <td><u>HSLU_ECOBW</u></td><td>ATP-dependent hsl protease ATP-binding subunit hslU OS=Escherichia coli (strain K12 / BW2952) GN=hslU PE=3 SV=1</td></tr> <tr> <td><u>SYV_ECOLI</u></td><td>Valyl-tRNA synthetase OS=Escherichia coli (strain K12) GN=vals PE=1 SV=2</td></tr> <tr> <td><u>SYV_ERWCT</u></td><td>Valyl-tRNA synthetase OS=Erwinia carotovora subsp. atroseptica GN=vals PE=3 SV=1</td></tr> </table>	<u>TGFR1_BOVIN</u>	TGF-beta receptor type-1 OS=Bos taurus GN=TGFR1 PE=2 SV=1	<u>GST26_SCHJA</u>	Glutathione S-transferase class-mu 26 kDa isozyme OS=Schistosoma japonicum PE=1 SV=3	<u>SAV_STRAV</u>	Streptavidin OS=Streptomyces avidinii PE=1 SV=1	<u>ALBU_BOVIN</u>	Serum albumin OS=Bos taurus GN=ALB PE=1 SV=4	<u>ACBA_ECOLI</u>	Isocitrate lyase OS=Escherichia coli (strain K12) GN=aceA PE=1 SV=1	<u>BLAT_ECOLX</u>	Beta-lactamase TEM OS=Escherichia coli GN=bla PE=1 SV=1	<u>RS2_ECO27</u>	30S ribosomal protein S2 OS=Escherichia coli O127:H6 (strain E2348/69 / EPEC) GN=rpsB PE=3 SV=1	<u>TRYP_PIG</u>	Trypsin OS=Sus scrofa PE=1 SV=1	<u>DHSA_ECOLI</u>	Succinate dehydrogenase flavoprotein subunit OS=Escherichia coli (strain K12) GN=sdhA PE=1 SV=1	<u>ALBU_CANFA</u>	Serum albumin OS=Canis familiaris GN=ALB PE=1 SV=3	<u>ALBU_PIG</u>	Serum albumin OS=Sus scrofa GN=ALB PE=1 SV=2	<u>ALBU_FELCA</u>	Serum albumin OS=Felis catus GN=ALB PE=1 SV=1	<u>ALBU_MOUSE</u>	Serum albumin OS=Mus musculus GN=Alb PE=1 SV=3	<u>CLPX_ABRHH</u>	ATP-dependent Clp protease ATP-binding subunit clpX OS=Aeromonas hydrophila subsp. hydrophila (strain ATCC 7966 / N	<u>CLPX_ANAPZ</u>	ATP-dependent Clp protease ATP-binding subunit clpX OS=Anaplasma phagocytophilum (strain HZ) GN=clpX PE=3 SV=1	<u>CLPX_PARUW</u>	ATP-dependent Clp protease ATP-binding subunit clpX OS=Protochlamydia amoebophila (strain UWE25) GN=clpX PE=3 SV=1	<u>CLPX_ANATD</u>	ATP-dependent Clp protease ATP-binding subunit clpX OS=Anaerocellum thermophilum (strain DSM 6725 / Z-1320) GN=clpX	<u>BCCP_ECOLI</u>	Biotin carboxyl carrier protein of acetyl-CoA carboxylase OS=Escherichia coli (strain K12) GN=accB PE=1 SV=1	<u>SPG1_STRSG</u>	Immunoglobulin G-binding protein G OS=Streptococcus sp. group G GN=spg PE=1 SV=1	<u>K2C1_HUMAN</u>	Keratin, type II cytoskeletal 1 OS=Homo sapiens GN=KRT1 PE=1 SV=6	<u>DNAK_ECOHS</u>	Chaperone protein dnaK OS=Escherichia coli O9:H4 (strain HS) GN=dnaK PE=2 SV=1	<u>EFTU_ABRHH</u>	Elongation factor Tu OS=Aeromonas hydrophila subsp. hydrophila (strain ATCC 7966 / NCIB 9240) GN=tuf1 PE=3 SV=1	<u>EFTU1_YERRE</u>	Elongation factor Tu 1 OS=Yersinia enterocolitica serotype O:8 / biotype 1B (strain 8081) GN=tuf1 PE=3 SV=1	<u>DHSA_SALTY</u>	Succinate dehydrogenase flavoprotein subunit OS=Salmonella typhimurium GN=sdhA PE=3 SV=1	<u>ODO1_ECO57</u>	2-oxoglutarate dehydrogenase E1 component OS=Escherichia coli O157:H7 GN=suca PE=3 SV=1	<u>DNAK_YERPA</u>	Chaperone protein dnaK OS=Yersinia pestis bv. Antiqua (strain Antiqua) GN=dnaK PE=2 SV=1	<u>RL11_CITK8</u>	50S ribosomal protein L11 OS=Citrobacter koseri (strain ATCC BAA-895 / CDC 4225-83 / SGSC4696) GN=rpLK PE=3 SV=1	<u>GST27_SCHMA</u>	Glutathione S-transferase class-mu 26 kDa isozyme OS=Schistosoma mansoni PE=2 SV=1	<u>IP2_STRM5</u>	Translation initiation factor IF-2 OS=Stenotrophomonas maltophilia (strain R551-3) GN=infB PE=3 SV=1	<u>G3P1_ECO57</u>	Glyceraldehyde-3-phosphate dehydrogenase A OS=Escherichia coli O157:H7 GN=gapA PE=3 SV=2	<u>HSLU_ECOBW</u>	ATP-dependent hsl protease ATP-binding subunit hslU OS=Escherichia coli (strain K12 / BW2952) GN=hslU PE=3 SV=1	<u>SYV_ECOLI</u>	Valyl-tRNA synthetase OS=Escherichia coli (strain K12) GN=vals PE=1 SV=2	<u>SYV_ERWCT</u>	Valyl-tRNA synthetase OS=Erwinia carotovora subsp. atroseptica GN=vals PE=3 SV=1
<u>TGFR1_BOVIN</u>	TGF-beta receptor type-1 OS=Bos taurus GN=TGFR1 PE=2 SV=1																																																																		
<u>GST26_SCHJA</u>	Glutathione S-transferase class-mu 26 kDa isozyme OS=Schistosoma japonicum PE=1 SV=3																																																																		
<u>SAV_STRAV</u>	Streptavidin OS=Streptomyces avidinii PE=1 SV=1																																																																		
<u>ALBU_BOVIN</u>	Serum albumin OS=Bos taurus GN=ALB PE=1 SV=4																																																																		
<u>ACBA_ECOLI</u>	Isocitrate lyase OS=Escherichia coli (strain K12) GN=aceA PE=1 SV=1																																																																		
<u>BLAT_ECOLX</u>	Beta-lactamase TEM OS=Escherichia coli GN=bla PE=1 SV=1																																																																		
<u>RS2_ECO27</u>	30S ribosomal protein S2 OS=Escherichia coli O127:H6 (strain E2348/69 / EPEC) GN=rpsB PE=3 SV=1																																																																		
<u>TRYP_PIG</u>	Trypsin OS=Sus scrofa PE=1 SV=1																																																																		
<u>DHSA_ECOLI</u>	Succinate dehydrogenase flavoprotein subunit OS=Escherichia coli (strain K12) GN=sdhA PE=1 SV=1																																																																		
<u>ALBU_CANFA</u>	Serum albumin OS=Canis familiaris GN=ALB PE=1 SV=3																																																																		
<u>ALBU_PIG</u>	Serum albumin OS=Sus scrofa GN=ALB PE=1 SV=2																																																																		
<u>ALBU_FELCA</u>	Serum albumin OS=Felis catus GN=ALB PE=1 SV=1																																																																		
<u>ALBU_MOUSE</u>	Serum albumin OS=Mus musculus GN=Alb PE=1 SV=3																																																																		
<u>CLPX_ABRHH</u>	ATP-dependent Clp protease ATP-binding subunit clpX OS=Aeromonas hydrophila subsp. hydrophila (strain ATCC 7966 / N																																																																		
<u>CLPX_ANAPZ</u>	ATP-dependent Clp protease ATP-binding subunit clpX OS=Anaplasma phagocytophilum (strain HZ) GN=clpX PE=3 SV=1																																																																		
<u>CLPX_PARUW</u>	ATP-dependent Clp protease ATP-binding subunit clpX OS=Protochlamydia amoebophila (strain UWE25) GN=clpX PE=3 SV=1																																																																		
<u>CLPX_ANATD</u>	ATP-dependent Clp protease ATP-binding subunit clpX OS=Anaerocellum thermophilum (strain DSM 6725 / Z-1320) GN=clpX																																																																		
<u>BCCP_ECOLI</u>	Biotin carboxyl carrier protein of acetyl-CoA carboxylase OS=Escherichia coli (strain K12) GN=accB PE=1 SV=1																																																																		
<u>SPG1_STRSG</u>	Immunoglobulin G-binding protein G OS=Streptococcus sp. group G GN=spg PE=1 SV=1																																																																		
<u>K2C1_HUMAN</u>	Keratin, type II cytoskeletal 1 OS=Homo sapiens GN=KRT1 PE=1 SV=6																																																																		
<u>DNAK_ECOHS</u>	Chaperone protein dnaK OS=Escherichia coli O9:H4 (strain HS) GN=dnaK PE=2 SV=1																																																																		
<u>EFTU_ABRHH</u>	Elongation factor Tu OS=Aeromonas hydrophila subsp. hydrophila (strain ATCC 7966 / NCIB 9240) GN=tuf1 PE=3 SV=1																																																																		
<u>EFTU1_YERRE</u>	Elongation factor Tu 1 OS=Yersinia enterocolitica serotype O:8 / biotype 1B (strain 8081) GN=tuf1 PE=3 SV=1																																																																		
<u>DHSA_SALTY</u>	Succinate dehydrogenase flavoprotein subunit OS=Salmonella typhimurium GN=sdhA PE=3 SV=1																																																																		
<u>ODO1_ECO57</u>	2-oxoglutarate dehydrogenase E1 component OS=Escherichia coli O157:H7 GN=suca PE=3 SV=1																																																																		
<u>DNAK_YERPA</u>	Chaperone protein dnaK OS=Yersinia pestis bv. Antiqua (strain Antiqua) GN=dnaK PE=2 SV=1																																																																		
<u>RL11_CITK8</u>	50S ribosomal protein L11 OS=Citrobacter koseri (strain ATCC BAA-895 / CDC 4225-83 / SGSC4696) GN=rpLK PE=3 SV=1																																																																		
<u>GST27_SCHMA</u>	Glutathione S-transferase class-mu 26 kDa isozyme OS=Schistosoma mansoni PE=2 SV=1																																																																		
<u>IP2_STRM5</u>	Translation initiation factor IF-2 OS=Stenotrophomonas maltophilia (strain R551-3) GN=infB PE=3 SV=1																																																																		
<u>G3P1_ECO57</u>	Glyceraldehyde-3-phosphate dehydrogenase A OS=Escherichia coli O157:H7 GN=gapA PE=3 SV=2																																																																		
<u>HSLU_ECOBW</u>	ATP-dependent hsl protease ATP-binding subunit hslU OS=Escherichia coli (strain K12 / BW2952) GN=hslU PE=3 SV=1																																																																		
<u>SYV_ECOLI</u>	Valyl-tRNA synthetase OS=Escherichia coli (strain K12) GN=vals PE=1 SV=2																																																																		
<u>SYV_ERWCT</u>	Valyl-tRNA synthetase OS=Erwinia carotovora subsp. atroseptica GN=vals PE=3 SV=1																																																																		

Protein View

Match to: ALBU_BOVIN Score: 261

Serum albumin OS=Bos taurus GN=ALB PE=1 SV=4

Found in search of sample2.mgf

Nominal mass (M_r): 69248; Calculated pI value: 5.82

NCBI BLAST search of ALBU_BOVIN against nr

Unformatted sequence string for pasting into other applications

Taxonomy: Bos taurus

Variable modifications: NHS-LC-Biotin (K),NHS-LC-Biotin (N-term)

Cleavage by Trypsin: cuts C-term side of KR unless next residue is P

Sequence Coverage: 13%

Matched peptides shown in Bold Red

```

1 MKWVTFISLL LFFSSAYSRG VFRRDTHKSE IAHRFKDLGE EHFKGLVLIA
51 FSQYLQQCPF DEHVKLVNEL TEFAKTCVAD ESHAGCEKSL HTLFGDELCK
101 VASLRETYGD MADCCEKQEP ERNECFLSHK DDSPDLPKLK PDPNTLCDEF
151 KADEKKFWGK YLYEIAARRHP YFYAPELLYY ANKYNGVFQE CCQAEDKGAC
201 LLPKIETMRE KVLASSARQR LRCASIQKFG ERAKAWSVV RLSQKFPKAE
251 FVEVTKLVTD LTKVHKECCH GDLLECADDR ADLAKYICDN QDTISSKLKE
301 CCDKPLLEKS HCIAEVEKDA IPENLPPLTA DFAEDKDVCK NYQEAKDAFL
351 GSFLYEYSRR HPEYAVSVLL RLAKEYEATL EECCAADDPH ACYSTVFDFKL
401 KHLVDEPQNL IKQNCDFEKL LGEYGFQNAL IVRYTRKVPQ VSTPTLVEVS
451 RSLGKVGTRC CTKPESERMP CTEDYLSLIL NRLCVLHEKT PVSEKVTKCC
501 TESLVNRRPC FSALTPDETY VPKAFDEKLF TFHADICTLP DTEKQIKKQT
551 ALVELLKHKP KATEEQLKTV MENFVAFVDK CCAADDKEAC FAVEGPKLVV
601 STQTALA

```

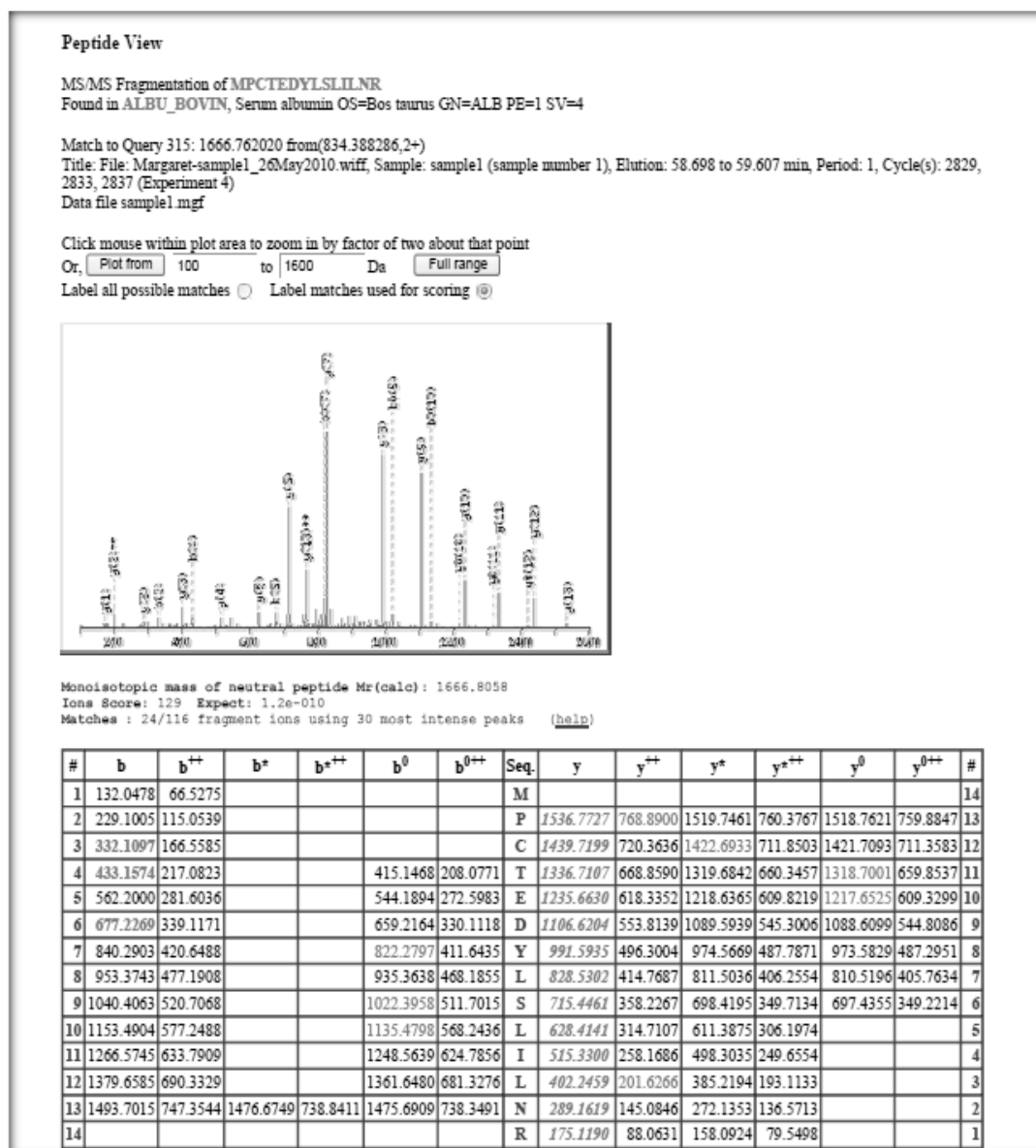


Table 6. Peptide sequences matched BSA, their query numbers and ion scores $p < 0.05$

Query	Matched sequences	Ion scores
561	K.LGEYGFQNALIVR.Y	109
521	K.YICDNQDTISSK.L	62
471	K.HLVDEPQNLIK.Q	51
235	K.QTALVELLK.H	58
389	K.LVNELTEFAK.T	62
147	K.YLYEIAR.R	48
144	K.YELHYDVLLV	50

2.6. *In vitro* biotinylation of BSA with different biotin concentrations - Third trial

2.6.1. *Materials and methods*

2.6.1.1. *In vitro* biotinylation

Three new optimisation experiments were carried out on BSA using different biotin concentrations and incubations conditions, in addition to alkylation and reduction that was performed first on the three BSA samples to expose as many free amines on the N-terminus and lysine residues to biotin as possible. The reduction reaction was carried out by adding 1mM of DTT to all three (1.5 nM BSA) samples. Samples were then incubated for 30 min at room temperature, followed by alkylation with 5 mM of iodoacetamide and incubation for 10 min at room temperature.

The first BSA sample was biotinylated with 30 nM of EZI-Link (20 access fold) and incubated for 15 minutes at room temperature. The second BSA sample was biotinylated with 30 nM of EZI-Link again but incubated for 30 minutes. The third BSA sample was biotinylated with 136 nM of EZI-Link (90 access fold) and incubated for 25 minutes at room temperature. The biotinylation reaction was terminated with 0.3 μ M of Tris-Hcl for the first two samples and with 1.36 μ M for the 3rd sample. All samples were then digested with trypsin overnight, purified with OMIX tips as described at section 2.4.1.4 and analysed with LC-MS per section 2.2.1.4. Table 7 is a summary of the three samples' reaction conditions.

Table 7. Different BSA biotinylation conditions.

Samples	Biotin conc.	Biotin fold	Incubation	Tris-Hcl
S1	30 nM	x20	15	0.3 μ M
S2	30 nM	x20	30	0.3 μ M
S3	136 nM	x90	25	1.36 μ M

2.6.2. Results

Mass spectrometry successfully detected biotinylated BSA in all three samples (Figure 29, Figure 30 and Figure 31). Figure 29A is the Mascot search result showing the peptides that matched BSA in S1, with a score of 1102 and 30% sequence coverage, while figure 29B is the matched peptide spectrum of BSA with ion score of 110. Table 8 represents the sequences that matched BSA in S1 with $p < 0.05$.

Protein View

Match to: **ALBU_BOVIN** Score: 1102

Serum albumin OS=Bos taurus GN=ALB PE=1 SV=4

Found in search of sample1.mgf

Nominal mass (M_r): **69248**; Calculated pI value: 5.82

NCBI BLAST search of **ALBU_BOVIN** against nr

Unformatted sequence string for pasting into other applications

Taxonomy: Bos taurus

Variable modifications: NHS-LC-Biotin (K), NHS-LC-Biotin (N-term)

Cleavage by Trypsin: cuts C-term side of KR unless next residue is P

Sequence Coverage: 30%

Matched peptides shown in Bold Red

```

1 MKWVTFISLL LLFSSAYSRG VFRRDTHKSE IAHRFKDLGE EHFKGLVLIA
51 FSQYLQQCPF DEHVKLVLNEL TEFATKCVAD ESHAGCEKSL HTLFGDELCK
101 VASLRETYGD MADCCEKQEP ERNECFLSHK DDSPDLPLKL PDPNTLCDEF
151 KADEKKFWGK YLYEIARRHP YFYAPELLYY ANKYNGVFQE CCQAEDKGAC
201 LLPKIETMRE KVLASSARQR LRCASIQKFG ERAKAWVA RLSQKFPKAE
251 FVEVTKLVTD LTKVHKECCH GDLLCADDR ADLAKYICDN QDTISSKLKE
301 CCDKPLLEKS HCIAEVEKDA IPENLPPLTA DFAEDKDVCK NYQEAQDAFL
351 GSFLYEYSRR HPEYAVSVLL RLAKEYEATL EECCAADDPH ACYSTVFDKL
401 KHLVDEPQNL IKQNCQDFEK LGEYGFQNAL IVRYTRKVPQ VSTPTLVEVS
451 RSLGKVGTRC CTKPESERMP CTEDYLSLIL NRLCVLHEKT PVSEKVIKCC
501 TESLVNRRPC FSALTPDETY VPKAFDEKLF TFHADICTLP DTEKQIKKQT
551 ALVELLKHKP KATEEQKKTV MENFVAFVDK CCAADDKEAC FAVEGPKLVV
601 STQTALA

```

Show predicted peptides also

Sort Peptides By

☒ Residue Number ☐ Increasing Mass ☐ Decreasing Mass

Peptide View

MS/MS Fragmentation of KVPQVSTPTLVEVSR

Found in ALBU_BOVIN, Serum albumin OS=Bos taurus GN=ALB PE=1 SV=4

Match to Query 597: 1638.908338 from(820.461445,2+)

Title: File: Margaret_10June2010_sample1.wiff, Sample: sample1 (sample number 1), Elution: 31.747 min, Period: 1, Cycle(s): 2627 (Experiment 2)

Data file sample1.mgf

Click mouse within plot area to zoom in by factor of two about that point

Or, Plot from 100 to 1600 Da Full range

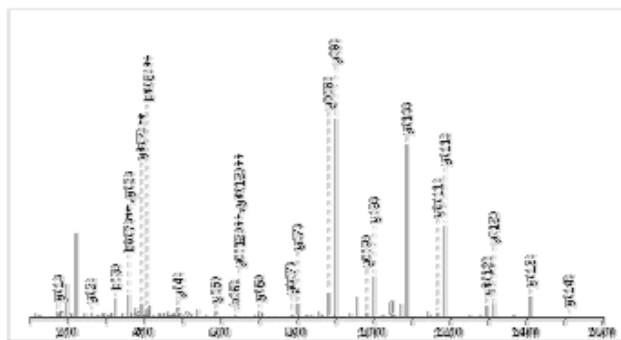
Label all possible matches ☐ Label matches used for scoring ☒

Table 8. Peptide sequences matched BSA in S1, their query and ion scores with $p < 0.05$

Query	Matched sequences	Ion scores
556	K.DAFLGSFLYEYSR.R	110
557	K.DAFLGSFLYEYSR.R	89
559	K.VDFLGSFLYEYSR.R	72
597	K.DAFLGSFLYEYSR.R	67
598	R.KVPQVSTPTLVEVSR.S	91
702	R.KVPQVSTPTLVEVSR.S	113
729	R.HPYFYAPELLYYANK.Y	95
751	K.DAIPENLPPLTADFAEDK.D	75
751	R.RHPYFYAPELLYYANK.Y	55
363	R.RHPYFYAPELLYYANK.Y	49
402	K.HLVDEPQNLIK.Q	64
444	K.TVMENFVAFVDK.C	78
514	K.VPQVSTPTLVEVSR.S	109
386	R.HPEYAVSVLLR.L	68
445	K.TVMENFVAFVDK.C	75

Figure 30A is the Mascot search result showing the peptides that matched BSA in S2, with a score of 989 and 30% sequence coverage, while Figure 30B is the matched peptide spectrum of BSA in S2 with ion score of 107. Table 9 represents the sequences that matched BSA in S2 with $p < 0.05$.

Protein View

Match to: ALBU_BOVIN Score: 989

Serum albumin OS=Bos taurus GN=ALB PE=1 SV=4

Found in search of sample2.mgf

Nominal mass (M_r): 69248; Calculated pI value: 5.82

NCBI BLAST search of ALBU_BOVIN against nr

Unformatted sequence string for pasting into other applications

Taxonomy: Bos taurus

Variable modifications: NHS-LC-Biotin (K), NHS-LC-Biotin (N-term)

Cleavage by Trypsin: cuts C-term side of KR unless next residue is P

Sequence Coverage: 30%

Matched peptides shown in Bold Red

```

1 MKWVTFISLL LLFSSAYSRG VFRDTHKSE IAHRFKDLGE EHFKGLVLIA
51 FSQYLQQCPF DEHVKLVNEL TEFAKTCVAD ESHAGCEKSL HTLFGDELCK
101 VASLRETYGD MADCCCEKQEP ERNECFLSHK DDSPDLPKLK PDPNTLCDEF
151 KADEKKFWGK YLYEIARRHP YFYAPELLYY ANKYNGVFQE CCQAEDKGAC
201 LLPKIETMRE KVLASSARQR LRCASIQKFG ERALKAWSVA RLSQKFPKAE
251 FVEVTKLVTD LTRVHKECCH GDLLECADDR ADLAKYICDN QDTISSKLKE
301 CCDKPLLEKS HCIAEVEKDA IPENLPPLTA DFAEDKDVCK NYQEAKDAFL
351 GSFLYEYSRR HPEYAVSVLL RLAKYEATL EECCAADDPH ACYSTVFDKL
401 KHLVDEPQNL IKQNCQFEK LGEYGFQNAL IVRYTRKVPQ VSTPTLVEVS
451 RSLGKVGTRC CTKPESERMP CTEDYLSLIL NRCLVLHEKT PVSEKVTKCC
501 TESLVNRRPC FSALTPDETY VPKAFDEKLF TFHADICTLP DTEKQIKKQT
551 ALVELLKHKP KATEEQLKTV MENFVAFVVK CCAADDKEAC FAVEGPKLVV
601 STQTALA

```

Show predicted peptides also

Peptide View

MS/MS Fragmentation of KVPQVSTPTLVEVSR

Found in ALBU_BOVIN, Serum albumin OS=Bos taurus GN=ALB PE=1 SV=4

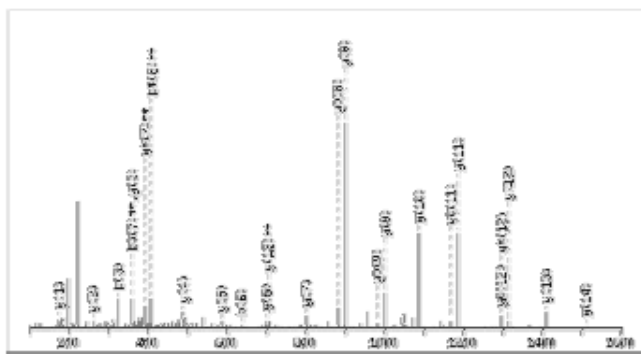
Match to Query 579: 1638.924594 from(820.469573,2+)

Title: File: Margaret_10June2010_sample2.wiff, Sample: sample2 (sample number 1), Elution: 31.381 min, Period: 1, Cycle(s): 2688 (Experiment 2)

Data file sample2.mgf

Click mouse within plot area to zoom in by factor of two about that point

Or, Plot from 100 to 1600 Da Full range

Label all possible matches ☐ Label matches used for scoring ☒

Monoisotopic mass of neutral peptide Mr(calc): 1638.9305

Ions Score: 107 Expect: 4.6e-008

Matches : 25/156 fragment ions using 42 most intense peaks ([help](#))

#	b	b ⁺⁺	b ⁺	b ⁺⁺	b ⁰	b ⁰⁺⁺	Seq.	y	y ⁺⁺	y ⁺	y ⁺⁺	y ⁰	y ⁰⁺⁺	#
1	129.1022	65.0548	112.0757	56.5415			K							15
2	228.1707	114.5890	211.1441	106.0757			V	1511.8428	756.4250	1494.8162	747.9118	1493.8322	747.4197	14
3	325.2234	163.1153	308.1969	154.6021			P	1412.7744	706.8908	1395.7478	698.3775	1394.7638	697.8855	13
4	453.2820	227.1446	436.2554	218.6314			Q	1315.7216	658.3644	1298.6951	649.8512	1297.7110	649.3592	12
5	552.3504	276.6788	535.3239	268.1656			V	1187.6630	594.3352	1170.6365	585.8219	1169.6525	585.3299	11
6	639.3824	320.1949	622.3559	311.6816	621.3719	311.1896	S	1088.5946	544.8009	1071.5681	536.2877	1070.5841	535.7957	10
7	740.4301	370.7187	723.4036	362.2054	722.4196	361.7134	T	1001.5626	501.2849	984.5360	492.7717	983.5520	492.2796	9
8	837.4829	419.2451	820.4563	410.7318	819.4723	410.2398	P	900.5149	450.7611	883.4884	442.2478	882.5043	441.7558	8
9	938.5306	469.7689	921.5040	461.2556	920.5200	460.7636	T	803.4621	402.2347	786.4356	393.7214	785.4516	393.2294	7
10	1051.6146	526.3109	1034.5881	517.7977	1033.6041	517.3057	L	702.4145	351.7109	685.3879	343.1976	684.4039	342.7056	6
11	1150.6830	575.8452	1133.6565	567.3319	1132.6725	566.8399	V	589.3304	295.1688	572.3039	286.6556	571.3198	286.1636	5
12	1279.7256	640.3665	1262.6991	631.8532	1261.7151	631.3612	E	490.2620	245.6346	473.2354	237.1214	472.2514	236.6293	4
13	1378.7940	689.9007	1361.7675	681.3874	1360.7835	680.8954	V	361.2194	181.1133	344.1928	172.6001	343.2088	172.1081	3
14	1465.8261	733.4167	1448.7995	724.9034	1447.8155	724.4114	S	262.1510	131.5791	245.1244	123.0659	244.1404	122.5738	2
15							R	175.1190	88.0631	158.0924	79.5498			1

Figure 30. A: Matched peptides of BSA in sample 2 with score of 989. B: Peptide spectra with ion score of 107.

Table 9. Peptide sequences matched BSA in S2, their query and ion scores with $p < 0.05$

Query	Matched sequences	Ion scores
288	K.VPQVSTPTLVEVSR.S	74
387	K.YGVFLGSFLYEYSR.R	95
535	K.YAFLGSFLYEYSR.R	107
444	K.DAFLGSFLYEYSR.R	53
598	R.KVPQVSTPTLVEVSR.S	91
701	R.VKPQVSTPTLVEVSR.S	115
734	R.HPYFYAPELLYYANK.Y	95
752	K.DAIPENLPPLTADFAE.D	65
755	R.RHPYFYAPELLYYANK.Y	59
463	R.RHPYFYAPELLYYANK.Y	49
404	K.HLVDEPQNLIK.Y	100
514	K.VLEVSTPTLVEVSR.L	104
376	R.HPEYAVSVLLR.C	68
455	K.TVMENFVAFVDK.R	66

Figure 31A represent the Mascot search result showing the peptides that matched BSA in S3, with a score of 1266 and 33% sequence coverage, while figure 31B is the matched peptide spectrum of BSA in S3 with ion score of 109. Table 10 represents the sequences that matched BSA in S3 with $p < 0.05$.

Protein View

Match to: **ALBU_BOVIN** Score: **1266**
 Serum albumin OS=Bos taurus GN=ALB PE=1 SV=4
 Found in search of sample3.mgf

Nominal mass (M_r): **69248**; Calculated pI value: **5.82**
 NCBI BLAST search of **ALBU_BOVIN** against nr
 Unformatted sequence string for pasting into other applications

Taxonomy: Bos taurus

Variable modifications: NHS-LC-Biotin (K), NHS-LC-Biotin (N-term)
 Cleavage by Trypsin: cuts C-term side of KR unless next residue is P
 Sequence Coverage: **33%**

Matched peptides shown in Bold Red

```

1  MKWVTFISLL LFFSSAYSRG VFRDTHKSE IAHRFKDLGE EHFKGLVLIA
51  FSQYLQQCPF DEHVKLVLNEL TEFKTCVAD ESHAGCEKSL HTLFGDELCK
101 VASLRETYGD MADCCCKQEP ERNECFSLHK DDSPDLPLK PDPNTLCDEF
151 KADEKKFWGK YLYEIARRHP YFYAPELLYY ANKYNGVFQE CCQAEDKGAC
201 LLPKIETMRE KVLASSARQR LRCASIQKFG ERALKAWSVA RLSQKFPKAE
251 FVEVTKLVTD LTKVHKECCH GDLLECADDR ADLAKYICDN QDTISSKLKE
301 CCDKPLLEKS HCIAEVEKDA IPENLPPLTA DPAEDKDVCK NYQEAQDAFL
351 GSFLYEYSRR HPEYAVSVLL RLAKYEATL EECCAKDDPH ACYSTVFDKL
401 KHLVDEPQNL IKQNCQFEK LGEYGFQNAL IVRYTRKVPQ VSTPTLVEVS
451 RSLGKVGTRC CTKPESERMP CTEDYLSLIL NRCLVLHEKT PVSEKVTKCC
501 TESLVNRRPC FSALTPDETY VPKAFDEKLF TFHADICTLP DTEKQIKKQT
551 ALVELLKHKP KATEEQLKTV MENFVAFVDK CCAADDKEAC FAVEGPKLVV
601 STQTALA

```

Show predicted peptides also

Peptide View

MS/MS Fragmentation of LGEYGFQNALIVR

Found in ALBU_BOVIN, Serum albumin OS=Bos taurus GN=ALB PE=1 SV=4

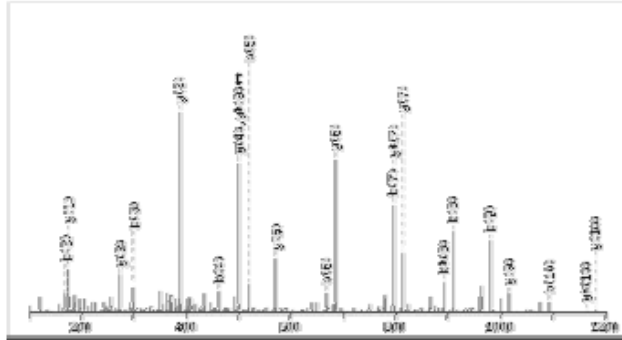
Match to Query 478: 1478.868777 from(493.963535,3+)

Title: File: Margaret_10June2010_sample3.wiff, Sample: sample3 (sample number 1), Elution: 39.28 min, Period: 1, Cycle(s): 2795 (Experiment 3)

Data file sample3.mgf

Click mouse within plot area to zoom in by factor of two about that point

Or, Plot from 100 to 1200 Da Full range

Label all possible matches ☐ Label matches used for scoring ☒

Monoisotopic mass of neutral peptide Mr(calc): 1478.7881

Ions Score: 107 Expect: 3.8e-008

Matches: 22/108 fragment ions using 22 most intense peaks [\(help\)](#)

#	b	b ⁺⁺	b ⁺	b ⁺⁺	b ⁰	b ⁰⁺⁺	Seq.	y	y ⁺⁺	y ⁺	y ⁺⁺	y ⁰	y ⁰⁺⁺	#
1	114.0913	57.5493					L							13
2	171.1128	86.0600					G	1366.7114	683.8593	1349.6848	675.3461	1348.7008	674.8540	12
3	300.1554	150.5813			282.1448	141.5761	E	1309.6899	655.3486	1292.6634	646.8353	1291.6793	646.3433	11
4	463.2187	232.1130			445.2082	223.1077	Y	1180.6473	590.8273	1163.6208	582.3140			10
5	520.2402	260.6237			502.2296	251.6185	G	1017.5840	509.2956	1000.5574	500.7824			9
6	667.3086	334.1579			649.2980	325.1527	F	960.5625	480.7849	943.5360	472.2716			8
7	795.3672	398.1872	778.3406	389.6740	777.3566	389.1819	Q	813.4941	407.2507	796.4676	398.7374			7
8	909.4101	455.2087	892.3836	446.6954	891.3995	446.2034	N	685.4355	343.2214	668.4090	334.7081			6
9	980.4472	490.7272	963.4207	482.2140	962.4367	481.7220	A	571.3926	286.1999	554.3661	277.6867			5
10	1093.5313	547.2693	1076.5047	538.7560	1075.5207	538.2640	L	500.3555	250.6814	483.3289	242.1681			4
11	1206.6154	603.8113	1189.5888	595.2980	1188.6048	594.8060	I	387.2714	194.1394	370.2449	185.6261			3
12	1305.6838	653.3455	1288.6572	644.8322	1287.6732	644.3402	V	274.1874	137.5973	257.1608	129.0840			2
13							R	175.1190	88.0631	158.0924	79.5498			1

Figure 31. A: Matched peptides of BSA in sample 3 with score of 1266. B: Peptide spectra with ion score of 109.

Table 10. Peptide sequences matched BSA in S3, their query and ion scores with $p < 0.05$

Query	Matched sequences	Ion scores
522	R.KVPQVSTPTLVLSR.S	100
540	K.DAFLGSFLYEYSR.R	95
559	K.DAFLGSFLYEYSER.R	84
563	K.DAFLGSFLYEYSR.R	102
598	K.FADLGSFLYEYSR.R	91
701	R.KVPQVSTPTLVEVSR.S	112
756	R.HPYFYAPELLYYANK.Y	95
755	K.DAIPENLPPLTADFAEDK.D	75
751	R.RHPYFYAPELLYYANK.Y	55
423	R.RHPYFYAPELLYYANK.Y	49
402	K.HLVDEPQNLIK.Q	64
443	K.TVMENFVAFVDK.C	108
514	K.VPQVSTPTLVEVSR.S	69
386	R.HPEYAVSVLLR.L	68
278	R.RHPYFYAPELLYYAN.K	40
290	K.TVAFLGSFLYEYSR.R	85
296	K.MFLGSFLYEYSRG.R	73

2.7. *In vitro* biotinylation of BSA using different biotin concentrations with *E.coli*

2.7.1. *Materials and methods*

2.7.1.1. *In vitro* biotinylation

Four more optimisation experiments were carried out on BSA, using different biotin concentrations and conditions to further enhance the biotinylation and capture of proteins in the presence and absence of un-biotinylated *E.coli* proteins. The four samples were prepared as per Table 11. The alkylation, reduction and biotinylation were performed as described earlier in section 2.6.1.1.

Table 11. Four BSA samples reactions

Samples	BSA	Biotin	Access fold of biotin	Incubation	Tris-Hcl
S1	1.5nM	0.03 μ M	$\times 20$	15 min	0.3 μ M
S2	1.5nM	0.15 μ M	$\times 100$	15 min	1.5 μ M
S3	1.5nM	0.3 μ M	$\times 200$	15 min	3 μ M
S4	1.5nM	0.75 μ M	$\times 500$	15 min	7.5 μ M

After 15 min incubation with Tris-HCl, each sample was divided into two halves, the first half (S1A, S2A, S3A, S4A) was digested with trypsin overnight and the second half (S1B, S2B, S3B, S4B) was mixed with 30 access fold of *E.coli* proteins (Table 12), and captured on streptavidin sepharose for 2 h at room temperature, then digested with trypsin overnight. All eight samples were then purified with OMIX tips and analysed with LC-MS/MS as described in sections 2.4.1.4 and 2.2.1.4 respectively.

Table 12. Summary of the two halves of the four BSA samples

No <i>E.coli</i> added	Mixed with <i>E.coli</i>
S1A	S1B
S2A	S2B
S3A	S3B
S4A	S4B

A control sample was also prepared by adding 0.045 μM (30 access fold) of *E.coli* to 1.5 nM of BSA sample without biotinylation reaction, followed by 600 μL of streptavidin sepharose. The control sample was then digested with trypsin overnight and analysed by LC-MS/MS the same as the other eight samples

2.7.1.2 Results

Mass spectrometry data of serum albumin samples mixed with *E.coli* failed to detect biotinylated BSA proteins, except in S1B. Table 13 is the Mascot search results for S1B showing the peptides that matched BSA with a score of 611 and 26% sequence coverage. The remaining three samples (S2B, S3B and S4B) contained polymers which may be of the streptavidin sepharose. However biotinylated BSA proteins were detected in all other four samples that were not mixed with *E.coli* (S1A, S2A, S3A and S4A).

Table 13. Peptide sequences matched BSA in S1B sample, their query numbers and ion scores with $p < 0.05$

Query	Matched sequences	Ion scores
266	K.LVNELTEFAK.T	65
342	K.TVMENFVAFVDK.C	74
343	K.TVMENFVAFVDK.C	62
378	K.LGEYGFQNALIVR.Y	116
398	K.DAFLGSFLYEYSR.R	80
415	R.MPCTEDYLSLILNR.L	95
416	MPCTEDYLSLILNR.L	97
442	K.LFTFHADICTLPDTEK.Q	61
366	R.RHPEYAVSVLLR.L	64
354	K.SLHTLFGDELCK.V	52
399	K.DAFLGSFLYEYSR.R	76
444	R.RHPYFYAPELLYYANK.Y	49

Table 14 is the Mascot search result for S1A showing the peptides that matched BSA with a score of 2276 and 90% sequence coverage. Table 15 is the Mascot search result for S2A showing the peptides that matched BSA with a score of 2284 and 86% sequence coverage. Table 16 is the Mascot search result for S3A showing the peptides that matched BSA with a score of 2082 and 87% sequence coverage, while Table 17 is the Mascot search result for S4A showing the peptides that matched BSA with a score of 2077 and 81% sequence coverage.

Table 14. Peptide sequences that matched BSA in S1A sample, their query numbers and ion scores with $p < 0.05$

Query	Matched sequences	Ion scores
312	K.LGEYGFQNALIVR.Y	112
314	K.LGEYGFQNALIVR.Y	101
316	K.LGEYGFQNALIVR.Y	116
347	K.LKECCDKPLLEK.S	76
356	K.LKHLVDEPQNLIK.Q	70
394	R.KVPQVSTPTLVEVSR.S	98
401	R.MPCTEDYLSLILNR.L	98
418	R.LAKEYEATLEECCA.K.D	64
446	K.CCAADDKEACFAVEGP.K	101
292	R.RHPEYAVSVLLR.L	73
195	K.KQTALVELLK.H	74
260	K.TVMENFVAFVDK.C	52
265	K.TVMENFVAFVDK.C	80
231	K.ECCDKPLLEK.S	58

Table 15. Peptide sequences that matched BSA in S2A sample, their query numbers and ion scores with $p < 0.05$

Query	Matched sequences	Ion scores
243	K.LGEYGFQNALIVR.Y	109
245	K.LGEYGFQNALIVR.Y	128
302	R.KVPQVSTPTLVEVSR.S	100
312	R.MPCTEDYLSLILNR.L	91
313	R.MPCTEDYLSLILNR.L	79
370	K.VASLRETYGDMADCCEK.Q	72
397	ATEEQLKTVMENFVAFVDK.C	80
315	K.YNGVFQECCQAEDK.G	81
353	K.CCAADDKEACFAVEGPK.L	98
228	K.YICDNQDTISSK.L	65
215	R.RHPEYAVSVLLR.L	77
197	K.SLHTLFGDELCK.V	61
233	K.TCVADESHAGCEK.S	54
377	R.RHPYFYAPELLYYANK.Y	56

Table 16. Peptide sequences that matched BSA in S3A sample, their query numbers and ion scores with $p < 0.05$.

Query	Matched sequences	Ion scores
181	R.RHPEYAVSVLLR.L	80
184	R.RHPEYAVSVLLR.L	77
202	K.LGEYGFQNALIVR.Y	112
203	K.LGEYGFQNALIVR.Y	92
357	K.ATEEQLKTVMENFVAFVDK.C	98
328	K.VASLRETYGDMADCCEK.Q	74
269	R.MPCTEDYLSLILNR.L	88
234	K.LKECCDKPLLEK.S	57
204	K.LGEYGFQNALIVR.Y	78
245	K.DAFLGSFLYEYSR.R	80
201	K.LGEYGFQNALIVR.Y	59
206	K.LGEYGFQNALIVR.Y	95

Table 17. Peptide sequences that matched BSA in S4A sample, their query numbers and ion scores with $p < 0.05$.

Query	Matched sequences	Ion scores
211	K.LGEYGFQNALIVR.Y	105
212	K.LGEYGFQNALIVR.Y	109
215	K.LGEYGFQNALIVR.Y	115
214	K.LGEYGFQNALIVR.Y	85
195	R.RHPEYAVSVLLR.L	70
213	K.LGEYGFQNALIVR.Y	81
233	K.VPQVSTPTLVEVSR.S	86
234	K.DAFLGSFLYEYSR.R	79
259	R.KVPQVSTPTLVEVSR.S	79
308	K.CCAADDKEACFAVEGPK.L	108
326	R.RHPYFYAPELLYYANK.Y	54
275	K.YNGVFQECCQAEDK.G	61

Mass spectrometry of the control sample did not identify BSA protein, which is expected, since the BSA was not biotinylated, hence wasn't captured on streptavidin sepharose

Mascot Search Results	
User	: margaret
Email	:
Search title	: control again
MS data file	: Margaret Control.mgf
Database	: SwissProt 2010x (517802 sequences; 182492287 residues)
Timestamp	: 5 Jul 2010 at 02:58:05 GMT
Enzyme	: Trypsin
Variable modifications	: NHS-LC-Biotin (K), NHS-LC-Biotin (N-term)
Mass values	: Monoisotopic
Protein Mass	: Unrestricted
Peptide Mass Tolerance	: ± 100 ppm
Fragment Mass Tolerance	: ± 0.6 Da
Max Missed Cleavages	: 1
Instrument type	: ESI-QUAD-TOF
Number of queries	: 1028
Protein hits	: GST26_SCHJA Glutathione S-transferase class-mu 26 kDa
	<u>TGFR1_HUMAN</u> TGF-beta receptor type-1 OS=Homo sapiens G
	<u>BLAT_ECOLX</u> Beta-lactamase TEM OS=Escherichia coli GN=
	<u>EFTU_SALAR</u> Elongation factor Tu OS=Salmonella arizona
	<u>EFTU_SHIBS</u> Elongation factor Tu OS=Shigella boydii se
	<u>EFTU1_YERES</u> Elongation factor Tu 1 OS=Yersinia enteroc
	<u>IBPA_ECOBW</u> Small heat shock protein ibpA OS=Escherich
	<u>CLPX_ECOBW</u> ATP-dependent Clp protease ATP-binding sub
	<u>EFTU1_PHOLI</u> Elongation factor Tu 1 OS=Photorhabdus lum
	<u>ACV1B_HUMAN</u> Activin receptor type-1B OS=Homo sapiens G
	<u>SAV_STRAV</u> Streptavidin OS=Streptomyces avidinii PE=1
	<u>EFTU_ALTMD</u> Elongation factor Tu OS=Alteromonas macleo
	<u>RPOC_BAUCH</u> DNA-directed RNA polymerase subunit beta'
	<u>ACV1C_HUMAN</u> Activin receptor type-1C OS=Homo sapiens G
	<u>EFTU_HAMD5</u> Elongation factor Tu OS=Hamiltonella defen
	<u>IDH_COXBU</u> Isocitrate dehydrogenase [NADP] OS=Coxiell
	<u>IDH_HELEJ</u> Isocitrate dehydrogenase [NADP] OS=Helicob
	<u>GST27_SCHMA</u> Glutathione S-transferase class-mu 26 kDa
	<u>IDH_ECOLI</u> Isocitrate dehydrogenase [NADP] OS=Escheri
	<u>RHO_ECOLI</u> Transcription termination factor rho OS=Es
	<u>RL28_ECO24</u> 50S ribosomal protein L28 OS=Escherichia c
	<u>EFTU_BAUCH</u> Elongation factor Tu OS=Baumannia cicadell
	<u>IBPA_SERP5</u> Small heat shock protein ibpA OS=Serratia
	<u>GATZ_ECOBW</u> D-tagatose-1,6-bisphosphate aldolase subun

Figure 32. No serum albumin was detected in the control sample, because BSA was not biotinylated, therefore was not captured.

All of above *in vitro* biotinylation optimizations using BSA, alpha casein and *E.coli* indicated successful labelling and capturing of biotinylated proteins, therefore the subsequent biotinylation optimization was performed on bEnd.3 cell cultures since these are the cells that will be used for irradiation experiments.

2.8. *In vitro* biotinylation of bEnd3 cell cultures - new trials

New experiments were carried out to optimize protein labelling and capture in bEnd3 cells, each with a different concentration of biotin and a different number of pooled samples to achieve the optimal biotinylation condition required for membrane protein identification in bEnd3 cell cultures.

2.8.1. *Materials and methods*

2.8.1.1. *In vitro* biotinylation

In vitro biotinylation was performed on five 75 cm² flasks. Each flask was washed four times with PBS pH 7.4. Sixty-seven µM of Sulfo-NHS-LC-Biotin (Pierce, IL, USA) was added to two flasks, while the other three flasks were incubated with 4.2 nM of Sulfo-NHS-LC-Biotin. The biotinylation reaction was terminated by adding Tris-HCl pH 7.5 to a final concentration of 670 µM to the first two flasks and 1.66 µM to the other three flasks. After 15 min incubation the cells were washed three times with PBS and harvested with 1 mL of lysis buffer [containing 2% v/v Triton-X100, 0.2% w/v SDS and protease inhibitor EDTA-free (Complete, Roche, Switzerland)] and kept on ice for 30 min.

After incubation the two samples that were incubated with 67 µM of biotin were pooled in a 10 mL Falcon tube, and the three samples that were incubated with 1.66 µM were pooled in a separate 10 mL Falcon tube (Table 18). A control sample was also prepared by adding 670 µM of Tris-HCl directly to a 75 cm² culture flask, followed by 1 mL of lysis buffer to harvest the cells.

Table 18. The five bEnd3 biotinylation conditions

Samples	Biotin Conc.	Incubation time	Tris-Hcl	Pooled samples
S1	67 μ M	5 min	670 μ M	S1+S2
S2	67 μ M	5 min	670 μ M	
S3	4.2 nM	15 min	1.66 μ M	S3+S4+S5
S4	4.2 nM	15 min	1.66 μ M	
S5	4.2 nM	15 min	1.66 μ M	
Control	---	----	670 μ M	---

Biotinylated proteins were captured on streptavidin sepharose (GE health care, Australia). Five hundred microlitres of streptavidin sepharose were washed three times with buffer **A** (containing 1% v/v Triron–X100, 0.1% w/v SDS in PBS). Pooled lysates were incubated with washed streptavidin sepharose for 2 h in a cold room. Streptavidin sepharose was pelleted by centrifugation with 500 g x 10 min. Unbound proteins were washed away three times with buffer **A**, once with buffer **B** (0.1% v/v Triron–X100, 0.5 M NaCl in PBS) and once with digestion buffer (50 mM of ammonium bicarbonate).

2.8.1.2. Tryptic digestion of biotinylated proteins and LC-MS/MS analysis

Streptavidin sepharose was re-suspended in 200 μ L of digestion buffer. Twenty microlitres of trypsin was then added and incubated overnight at 37° C. The samples were centrifuged at 14,100 xg for 5 minutes at room temperature. Supernatant was collected and fractionated by strong cation exchange chromatography and analysed by LC-MS/MS as described in section 2.2.1.4.

2.8.1.3. Data processing

The LC- MS/MS data were submitted to Mascot (Matrix Science, London, UK) for protein identification using the SwissProt database containing *Mus musculus* protein entries.

Biotinylated lysine and amino terminus were considered as static modifications. Peptide ion scores above 35 were reported giving a probability of correct identification $p < 0.05$.

2.8.2. Results

The mass spectrometry of the pooled sample labelled with 4.2 nM of biotin detected in total 112 proteins. Sixteen of them were membrane proteins (Table 19), while the pooled sample labelled with 67 μ M of biotin identified in total 214 proteins, 35 of them were membrane proteins (Table 20) which was the best data obtained on bEnd3 cultures. The biotin concentration was increased to 490 μ M which led to identification of 39 membrane proteins, however we noticed that the higher the biotin concentration the more cytoplasmic proteins were detected in the MS data, this may be due to the fact that biotin penetrates the cell membrane at very high concentrations.

Table 19. Membrane proteins of bEnd.3 cell cultures identified using 4.2nM of biotin

Cadherin-5	Leukocyte	ICAM-2	Integrin beta-1	CAP-1
Integrin alpha-5	Integrin alpha-6	MUC18	VDAC-1	ESAM
VDAC-3	Annexin A1	RAB10	ILK	Integrin alpha-3
Rab 35				

Table 20. Membrane proteins of bEnd.3 cell cultures identified using 67μM of biotin

Protein name	Uniprot accession #	Membrane protein classification
PECAM-1	Q08481	Single pass type 1
Annexin A2	P07356	Extracellular matrix
Cadherin 5	P33151	Single pass type 1
ICAM-2	P13597	=
MUC18	Q8R2Y2	=
Integrin alpha-5	P11688	=
ESAM	Q925F2	=
Septin 11	B3GNI6	Cytoskeleton
ILK	O55222	Peripheral
Spectrin Beta	Q62261	Cytoskeleton
CAV1	P49817	Peripheral
Annexin A1	P10107	=
Receptor type tyrosin	O15146	Plasma
Integrin alpha-6	Q61739	Single pass type 1
VDAC1	Q60932	Multi pass
CD38	P56528	Single pass type 2
CD102	Q61391	=
PLVAP	Q91VC4	=
Rab-1B	Q9D1G1	Lipid anchor
ITB1	P09055	Single pass type 1
OX-2	B7SDA8	Glycoprotein
DYSF	Q9ESD7	Single pass type 2
RAS1	Q61411	Lipid anchor
GANS1	I0AXZ5	Transmembrane
CD29	P09055	Single pass type 1
G3P	P0A4Q0	Transmembrane
Rab-7a	P51150	peripheral
AP2M1	P84091	=

The control sample did not identify any membrane proteins, only nucleus and cytoplasmic proteins were detected, which was expected since biotin was not added to the sample (Figure 33).

<i>(MATRIX)</i> Mascot Search Results <i>(SCIENCES)</i>	
User	: margaret
Email	:
Search title	: control
MS data file	: MS_S1-26Aug10.mgf
Database	: SwissProt 2010x (519348 sequences; 183273162 residues)
Taxonomy	: Mus musculus (house mouse) (16313 sequences)
Timestamp	: 30 Aug 2010 at 02:47:59 GMT
Enzyme	: Trypsin
Variable modifications	: NHS-LC-Biotin (K), NHS-LC-Biotin (N-term)
Mass values	: Monoisotopic
Protein Mass	: Unrestricted
Peptide Mass Tolerance	: ± 100 ppm
Fragment Mass Tolerance	: ± 0.6 Da
Max Missed Cleavages	: 1
Instrument type	: ESI-QUAD-TOF
Number of queries	: 1023
Protein hits	: <u>MYH9 MOUSE</u> Myosin-9 OS=Mus musculus GN=Myh9 PE=1 SV=4 <u>MYH10 MOUSE</u> Myosin-10 OS=Mus musculus GN=Myh10 PE=1 SV=2 <u>VIME MOUSE</u> Vimentin OS=Mus musculus GN=Vim PE=1 SV=3 <u>ACTB MOUSE</u> Actin, cytoplasmic 1 OS=Mus musculus GN=Actb PE=1 SV=2 <u>PLEC MOUSE</u> Plectin OS=Mus musculus GN=Plec PE=1 SV=2 <u>ACTN4 MOUSE</u> Alpha-actinin-4 OS=Mus musculus GN=Actn4 PE=1 SV=1 <u>ACTA MOUSE</u> Actin, aortic smooth muscle OS=Mus musculus GN=Acta1 PE=1 SV=1 <u>H2B1B MOUSE</u> Histone H2B type 1-B OS=Mus musculus GN=Histh2b1b PE=1 SV=1 <u>LMNA MOUSE</u> Lamin-A/C OS=Mus musculus GN=Lmna PE=1 SV=2 <u>ZO1 MOUSE</u> Tight junction protein ZO-1 OS=Mus musculus GN=Zot1 PE=1 SV=1 <u>SPTB2 MOUSE</u> Spectrin beta chain, brain 1 OS=Mus musculus GN=Sptb2 PE=1 SV=1 <u>ACTBL MOUSE</u> Beta-actin-like protein 2 OS=Mus musculus GN=Actbl PE=1 SV=1 <u>H4 MOUSE</u> Histone H4 OS=Mus musculus GN=Histh4a PE=1 SV=1 <u>MYH11 MOUSE</u> Myosin-11 OS=Mus musculus GN=Myh11 PE=1 SV=1 <u>H2A2B MOUSE</u> Histone H2A type 2-B OS=Mus musculus GN=Histh2a2b PE=1 SV=1 <u>ROA3 MOUSE</u> Heterogeneous nuclear ribonucleoprotein A3 OS=Mus musculus GN=Roa3 PE=1 SV=1 <u>MYH14 MOUSE</u> Myosin-14 OS=Mus musculus GN=Myh14 PE=1 SV=1 <u>H2A2A MOUSE</u> Histone H2A type 2-A OS=Mus musculus GN=Histh2a2a PE=1 SV=1 <u>H13 MOUSE</u> Histone H1.3 OS=Mus musculus GN=Histh1d PE=1 SV=1 <u>SPTA2 MOUSE</u> Spectrin alpha chain, brain OS=Mus musculus GN=Spta2 PE=1 SV=1 <u>DESM MOUSE</u> Desmin OS=Mus musculus GN=Des PE=1 SV=3 <u>EF1A1 MOUSE</u> Elongation factor 1-alpha 1 OS=Mus musculus GN=Ef1a1 PE=1 SV=1 <u>ARPC4 MOUSE</u> Actin-related protein 2/3 complex subunit 4 OS=Mus musculus GN=Arpc4 PE=1 SV=1 <u>CAPEB MOUSE</u> F-actin-capping protein subunit beta OS=Mus musculus GN=Capeb PE=1 SV=1 <u>ROA2 MOUSE</u> Heterogeneous nuclear ribonucleoproteins A2/B1 OS=Mus musculus GN=Roa2 PE=1 SV=1 <u>CAZA2 MOUSE</u> F-actin-capping protein subunit alpha-2 OS=Mus musculus GN=Caza2 PE=1 SV=1

Figure 33. Mascot search results of bEnd3 control sample. No membrane proteins were identified.

The data obtained from 67μM of biotin, indicated the successful *in vitro* biotinylation and capture of membrane proteins of bEnd3 cultures, therefore this protocol was used for the irradiation experiments of bEnd3 cultures described in Chapters 3 and 4.

2.9 Western blot analysis of bEnd.3 cells

Western blotting analysis was carried out on bEnd.3 cell cultures to confirm that the cells maintained their phenotype after multiple passages. Usually endothelial cell markers, MAdCAM-1 and VCAM-1 are expressed on bEnd.3 cells at early passages but not at passages greater than 30 (Sikorski, E et al 1993; Montesano, R et al 1990) therefore, western blot analysis was performed to confirm the presence of these two molecules at passages 29, 31 and 32. The purchased cells from ATCC were at passage 25.

Protein extracts were prepared by lysing bEnd.3 cells in RIPA (Radioimmunoprecipitation) lysis buffer (Invitrogen) containing 1 mM of PMSF (phenylmethylsulfonyl fluoride) to prevent protease degradation. Approximately 10 µg of cell protein was electrophoresed on 4-12 % NuPAGE gels (Invitrogen), using MOPS [3-(N-morpholino) propanesulfonic acid] running buffer (Invitrogen), then transferred into nitrocellulose membranes. Membranes were incubated with the primary antibodies, anti-mouse MAdCAM-1 (1:500) (R&D Systems, Australia) and anti-mouse VCAM-1 (1:500) (R&D Systems, Australia) overnight. Protein expressions were visualized by Amersham ECL Western Blotting Detection and Imaging System (GE Healthcare) with Fuji LAS 3000 camera, (Figure 34 and Figure 35).



Figure 34. Confirmation of the presence of MAdCAM-1 in bEnd.3 cells at passages 29, 31 and 32.

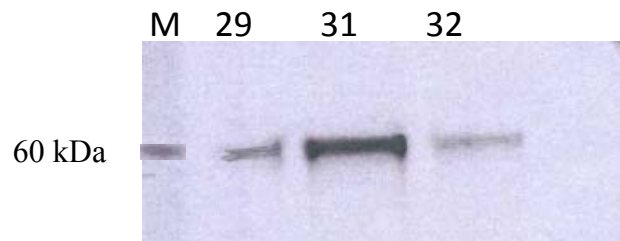


Figure 35. Confirmation of the presence of VCAM-1 in bEnd.3 cells at passages 29, 31 and 32.

Western blot analysis confirmed the presence of endothelial cell markers, MAdCAM-1 and VCAM-1, at passages up to 32. However, the highest passage used in these experiments was 30.

Chapter3. *In vitro* biotinylation and iTRAQ-mass spectrometry of bEnd.3 cells

3.1 Introduction

In vitro biotinylation and iTRAQ-mass spectrometry were used to assess membrane protein changes in bEnd.3 cell cultures in response to irradiation. bEnd.3 cultures were irradiated with 25 Gy and surface biotinylation was performed at 6 h, 24 h, 48 h and 72 h post radiation. Sham-irradiated cell cultures (controls) were treated identically but did not receive any radiation. Biotinylated proteins were then captured on streptavidin resin, digested, and labelled with iTRAQ (Isobaric Tag for Relative and Absolute Quantitation) reagents and pooled. Peptides were separated by strong cation exchange (SCX) chromatography and analysed by nanoLC/ MS to identify and quantify membrane proteins at the same time.

3.2 Materials and Methods

3.2.1 Mouse endothelial cell cultures (bEnd.3)

Cryopreserved bEnd.3 cells obtained from (American Type Culture Collection, VA, USA) were cultured in DMEM with 4.5 g /L D-glucose, 4 mM L-glutamine, and 0.11 g/L sodium pyruvate (Gibco, CA, USA). 10% foetal bovine serum albumin (Invitrogen, Gibco), hepes (Sigma, Aldrich, MO, USA) and antibiotics (Invitrogen, Gibco) were added to the DMEM and incubated in a 5% CO₂ atmosphere at 37° C. Cells were seeded in 75 cm² tissue culture flasks, 15 – 17mL of the growth media was added until about 80% confluence with medium renewal every 2 – 3 days.

3.2.2 Cell density and total protein concentration

bEnd.3 cells were counted using a Bio-Rad Automated Cell Counter TC10 (Bio-Rad, Castle Hill, NSW). Cell viability was assessed with Trypan Blue Solution (0.4%) (Sigma Aldrich, MO, USA). Equal amounts of cells were seeded in each flask. The total protein concentration of cell cultures was determined using Micro BCA kit (Pierce, IL, USA). A standard curve was

generated by using bovine serum albumin. The density of bEnd.3 cells was approximately 1×10^5 cells/mL and total protein concentration was 1.6 mg/mL.

3.2.3 Irradiation of bEnd.3 cells

bEnd.3 cells were irradiated once they reached 80% confluence in their culture flasks with an absorbed dose of 26 ± 5 Gy using 6 MV photons on an Elekta Synergy linear accelerator at Macquarie University Hospital. Cells were returned to the incubator immediately after irradiation.

3.2.4 In vitro biotinylation of bEnd.3 cells

Surface biotinylation was performed on irradiated and non-irradiated bEnd.3 cultures using a modified protocol from (Scheurer, S et al. 2005) and (Roesli, C et al. 2006). Each 75 cm² flask containing approximately 1×10^6 cells was washed four times with PBS pH 7.4. Twenty millilitres of PBS containing 67 μ M Sulfo-NHS-LC-Biotin (Pierce, IL, USA) were added to the flasks and incubated for 5 min at room temperature. The biotinylation reaction was terminated by adding Tris-HCl pH 7.5 to reach a final concentration of 670 μ M. After 5 min incubation the cells were washed four times with PBS and harvested with 2–3 mL of lysis buffer [containing 2% w/v NP40, 0.2% w/v SDS and protease inhibitor (Complete, EDTA-free, Roche, Switzerland)] and kept on ice for 30 min.

3.2.5 Capture of biotinylated proteins

Streptavidin sepharose high performance (GE health care, Australia) were used to capture biotinylated proteins. Five hundred microlitres of streptavidin sepharose were washed first three times with buffer A (containing 1% w/v NP40, 0.5% w/v SDS in PBS). Samples were then incubated with washed streptavidin sepharose for 2 h in room temperature. Streptavidin sepharose was pelleted by centrifugation at $1600 \times g$ for 5 min. Unbound proteins were

eliminated by washing 3 times with buffer A, once with buffer B (0.1% w/v NP40, 0.5 M NaCl in PBS) and once with digestion buffer (0.25 mM TEAB). The protocol was modified from Scheurer, S. *et al.* 2005 and Roesli, C. *et al.* 2006.

3.2.6 Tryptic digestion of biotinylated proteins and iTRAQ labelling

Streptavidin sepharose was re-suspended in 200 µL of digestion buffer. Twenty microlitres of trypsin were added and incubated overnight at 37° C. The samples were centrifuged at 14,100 ×g for 2 min at room temperature. Supernatant was removed and dried in the SpeediVac until complete dryness. Samples were resuspended in 0.5 M TEAB and labelled with iTRAQ 8-plex reagents kit (Applied Biosystems, Foster City, CA) as follows [Sample (6) :113, control (6) :114, sample (24) :115, control (24) :116, sample (48) : 117, control (48) : 118, sample (72) : 119, control (72) : 121]

3.2.7. Strong cation exchange chromatography and Nano-LC ESI MS/MS

iTRAQ labelled samples were pooled in a 1:1 ratio and fractionated by strong cation exchange liquid chromatography (SCX) and the cleaned sample was collected and dried. The cleaned SCX fraction was resuspended in 90 µL of desalting solution containing 0.1% trifluoroacetic acid and 2% acetonitrile 97.9% water. Thirty nine micorilitres of the resuspended solution was loaded on a reverse phase peptide Captrap (Michrom Bioresources) then desalted with the desalting solution at a rate of 10 µL per min for 13 min. The trap was switched on line with a 150 µm x 10 cm C18 3 µm 300A ProteCol column (SGE). The buffer solution A contained 99.9% water, 0.1% formic acid and buffer solution B was increased from 5% to 90% in 120 min in 3 linear gradient steps to elude the peptides. The column was then cleaned with 100% buffer B for 15 min and equilibrated with buffer A for 30 min. The reverse phase nanoLC eluent was subject to positive ion nanoflow electrospray analysis. In IDA (information dependent acquisition) mode a TOFMS scan was acquired (m/z 380-1600 for 0.5 s), with the three most intense multiply-charged ions (with counts > 70) then subjected

to MS/MS analysis. MS/MS spectra were gathered for 2 s in the mass range of m/z 100 – 1600 with a modified (Enhanced All Q2) transition setting to favour low mass ions so that the reporting iTRAQ tag ion (113, 114, 115, 116, 117, 118, 119 and 121) intensities were enhanced for quantitation. (Australian Proteome Analysis Facility, APAF protocol)

3.2.8 Immunocytochemistry

The following protocol was prepared, optimised on bEnd3 cells then used. Cells were grown on cover slips in a 6 well cell culture plates (CELLSTAR, Indiana, USA), and fixed with 4% paraformaldehyde for 6 min. Cells were washed with PBS three times and permeabilized with 0.2% (v/v) Tween-20 in PBS for another 6 min. After washing with PBS X3 and 1% (w/v) bovine serum albumin 3 times, cells were labelled with anti-cadherin-5 (CD144), anti-CD109 (BD Pharmingen) and anti-protein disulfide isomerase (PDI) (Sigma) antibodies. The corresponding secondary antibodies were labelled with Alexa Fluor 488 (Invitrogen) and nuclei were stained with DAPI (Invitrogen). Slides were then mounted with Fluoromount mounting medium (DAKO) and examined with a fluorescence microscope (Leica, Microsystems, Germany). Cells were stained at 6 h, 24 h, 48 h and 72 hrs post irradiation. Control (non-radiated) cells were also stained at each time point.

3.3 Data analysis

The Nano-LC ESI MS/MS data were submitted to ProteinPilot V4.0 software (AB Sciex) for data processing using SwissProt database and *Mus musculus* species. Bias correction was selected. The detected protein threshold (unused ProtScore) was set as > 1.3 , better than 95% confidence with $p\text{-values} < 0.05$ (Figure 36 and Figure 36). The hypothesis being tested for ProteinPilot software was “The actual protein ratio is 1 and the observed protein ratio is different than 1 by chance.” This null hypothesis is not true when the difference in expression

is real. That is, the difference between the observed ratio and 1 is due to something real, not random variation. The smaller the *p-value*, the more likely that expression difference is real.

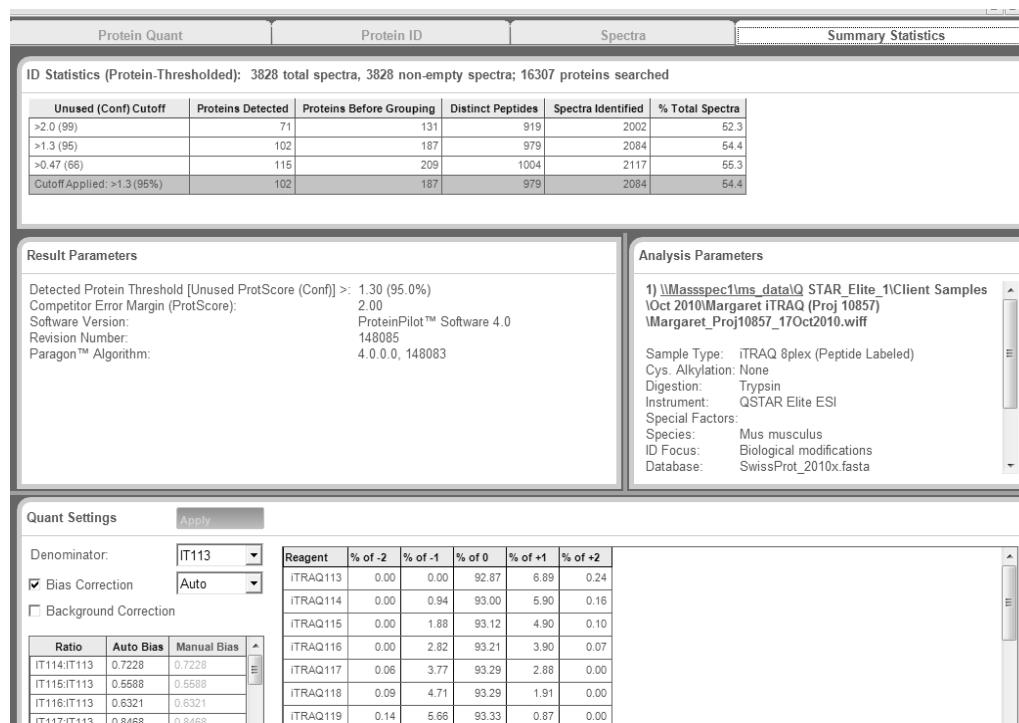


Figure 36. Screen shot of Protein Pilot showing the analysis parameters used. Detected protein threshold (unused ProtScore) set > 1.3 with confidence > 95%.

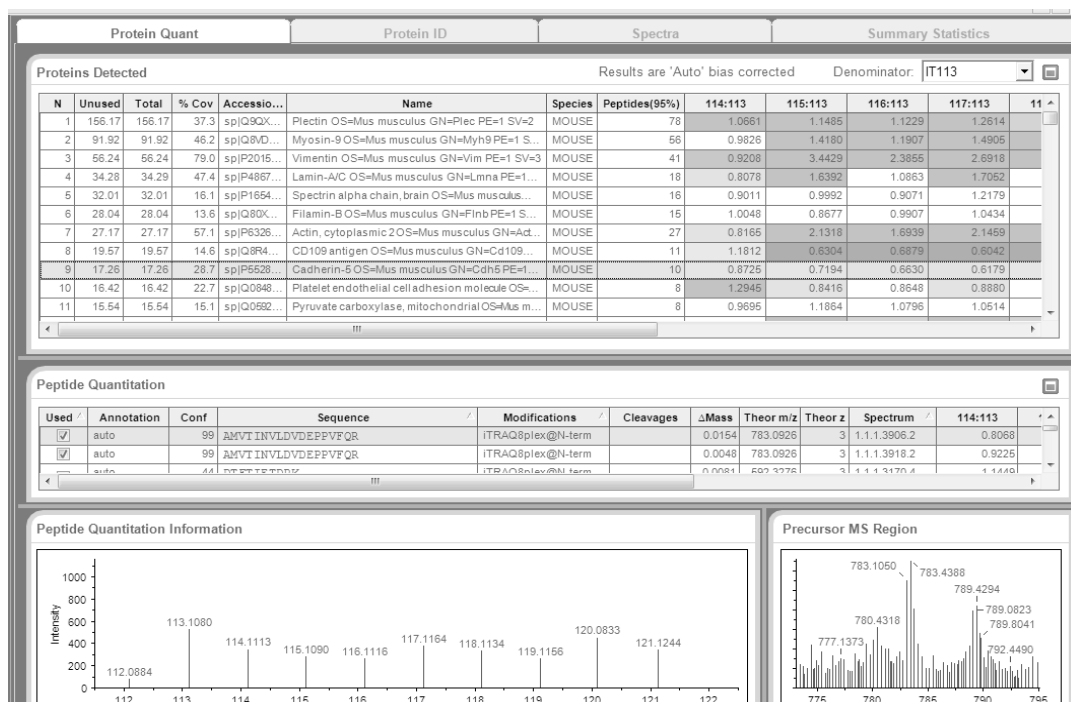


Figure 37. Screen shot of Protein Pilot showing the identified proteins and their peptide information. Red colour indicates up-regulation and blue indicates down-regulation. The intensity of the colouring indicates the certainty of the altered expression. The more certain the up-regulation, the darker are the red cells; the more certain the down regulation, the darker are the blue cells. The colouring is determined by the *p-value*

3.4. Results

bEnd.3 cells were irradiated once they reached 80% confluence in their culture flasks and samples collected at 6 h, 24 h, 48 h and 72 h post irradiation. Non irradiated cells were also collected at these time points. 8-plex iTRAQ-MS was carried out to compare the differences in protein levels between irradiated and control samples at each time point.

3.4.1. iTRAQ-MS analysis

The proteomics quantitative analysis of 8-plex iTRAQ-MS was carried out with three independent biological replicates. From the first iTRAQ-MS experiment, 102 proteins were identified from a total of 3828 spectra. The second iTRAQ-MS identified 132 proteins from a total of 3938 spectra, and the third iTRAQ-MS identified 83 proteins from a total of 5282 spectra. The (supplementary Table 1) includes the expression levels of the proteins that were significantly up or down regulated in at least one of the three iTRAQ-MS experiments at different time points.

Fifty membrane proteins were identified in all three iTRAQ-MS analyses. Table 21 contains the names of these proteins.

Table 21. Membrane proteins of bEnd.3 cell cultures identified by three iTRAQ -MS

Cadherin-5	PECAM	ICAM-2	Integrin beta-1	Integrin alpha-3
Integrin alpha-5	Integrin alpha-6	MUC18	Flamin B	ESAM
Receptor type tyrosin	CD109	Catenin beta-1	Rap-1B	Synaptic vesicle membrane protein
Rab-1A	CD47	Fibronectin	Rab-7a	Rab-1B
A disintegrin and metalloproteinase	Spectrin beta chain	Annexin A2	Multimerin	Spectrin alpha chain
Catenin delta-1	EPCR	Annexin A1	ICAM-2	Septin 11
Protein disulfide-isomerase	Nitric oxide synthase	Epoxide hydrolase 1	OX-2 membrane glycoprotein	Plasmalemma vesicle-associated protein
Collagen alpha-1	Caveolin-1	Galectin-9	Myoferlin	Rab-5C
ADP/ATP translocase	Tabilin-1	C1-rceprot	Bone marrow stromal antigen	Voltage-dependent anion
Laminin subunit alpha-5	Clathrin heavy chain	Plexin-A2	Endoglin	Inter-alpha-trypsin inhibitor heavy chain-H2

The proteomics analysis focused on the proteins that showed differences in expression between irradiated and control samples in at least two out of the three independent iTRAQ-MS runs. Eleven proteins were significantly differentially expressed in at least two out of the three iTRAQ-MS runs at different time points. At 6 h after irradiation, filamin B, protein disulfide isomerase and vimentin were upregulated in irradiated cells. At 24 h, myosin was upregulated in irradiated cells, while at 48 h, lamin, plectin, vimentin, actin cytoplasmic 2 and histone H2A were upregulated in irradiated cells and at 72 h, plectin, vimentin, myosin and histone H4 were upregulated in irradiated cells (Table 22).

Table 22. Average protein expression ratios (control: irradiated), in at least two out of three iTRAQ experiments and the time point at which they showed significant up or down regulation or (fold change) with $p < 0.05$

Protein name	Ave (C:R) 6h	Ave (C:R) 24h	Ave (C:R) 48h	Ave (R:C) 72h
Cadherin-5*			1.29	
CD109*			1.52	
Protein disulfide isomerase*	0.72			
Actin cytoplasmic 2			0.81	
Filamin B	0.82			
Lamin			0.53	
Plectin	1.14		0.86	1.18
Vimentin	0.76		0.41	1.17
Myosin		0.85		1.28
Histon H2A			0.38	
Histon H4				0.42

*Membrane proteins

The membrane proteins that were up-regulated in irradiated samples, compared to the controls at different time points, are of interest in this study since those on the surface of endothelial cells potentially can be targeted by ligands to induce thrombosis in AVM vessels post radiosurgery. We found six upregulated membrane proteins at different time points (Table 23) however, some membrane protein upregulation, although significant at their MS run with a ($p < 0.05$), was only observed in one out of the three iTRAQ-MS runs.

Table 23. Up-regulated membrane proteins of bEnd.3 cells at various time points and their average (irradiated: control) ratios, $p < 0.05$.

Protein name	(R:C) 6h	(R:C) 24h	(R:C) 72h
Cadherin-5		1.60	
PECAM-1		1.45	1.17
Protein disulfide isomerase (PDI)	1.40*	1.45	1.20
CD109	1.28		
Integrin alpha-5	1.21	1.41	
Integrin alpha-6		1.37	

* Average of 2/3 iTRAQ-MS

Figure 38 and 39 are screen shots of Protein Pilot analysis showing PECAM-1 and cadherin-5 expression levels in ratios (irradiated: control), with a 99% confidence interval for both.

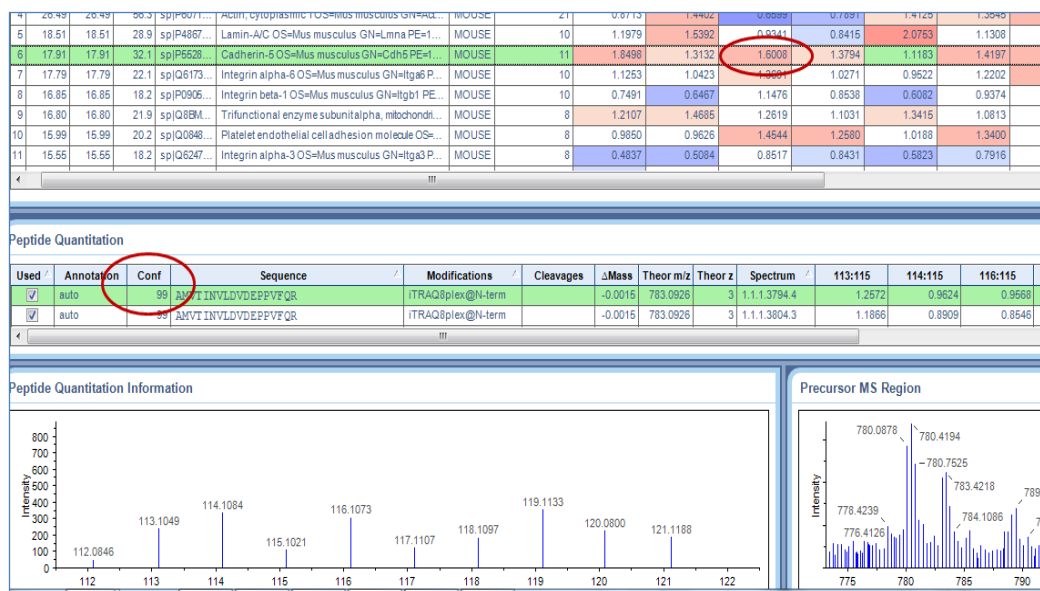


Figure 38. Expression level of PECAM-1 in radiated cells is higher than in controls at 24 h. (R:C) = 1.45 with 99% confidence.

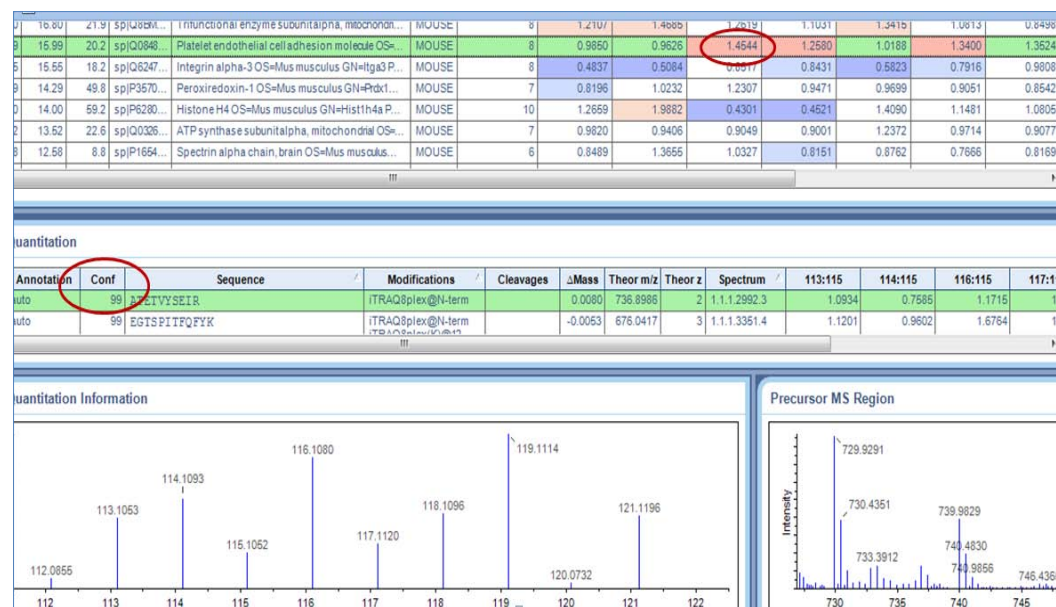


Figure 39. Expression level of Cadh-5 in radiated is higher than controls at 24h. (R:C) = 1.60 with 99% confidence

3.4.2. Immunocytochemistry

Immunocytochemistry and fluorescence microscopy was used to validate the presence and expression of membrane proteins in irradiated and non-irradiated cells.

3.4.2.1. *Cadherin 5*

Cadherin 5 (or CD144) was expressed on the cell membrane of irradiated and non-irradiated cell cultures. The expression intensity in the irradiated cells at 24 h and 48 h was greater than in controls (Figure 40). This observation was in agreement with iTRAQ-MS data at 24 h but not at 48 h which showed decrease in expression levels in irradiated cell (Table 22 and 23).

A change in cell shape was noted after 24 h of irradiation.

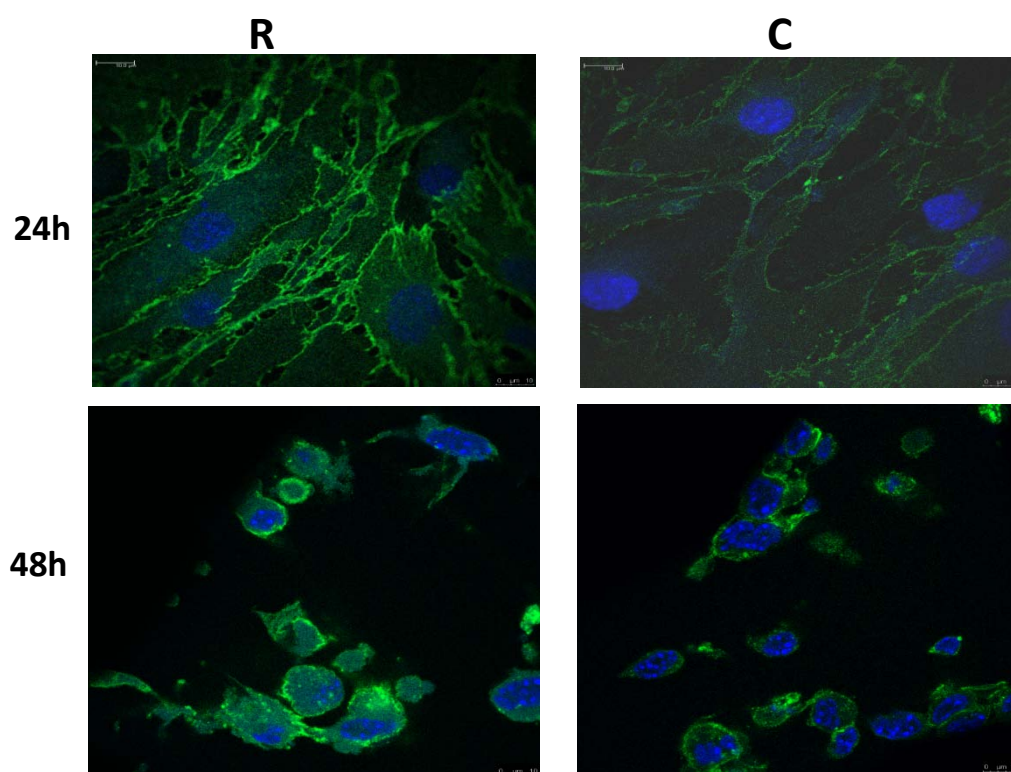


Figure 40. Fluorescent staining of cadherin 5 at 24 h and 48 h post irradiation. Expression levels of this protein were higher in irradiated cell compared to the controls

3.4.2.2. Platelet endothelial cell adhesion molecule-1

PECAM-1 was expressed on the cell membrane of irradiated and non-irradiated cell cultures. PECAM-1 expression intensity on the cell membrane was higher in irradiated cells at 24 h, 48 h and 72 h compared to the controls, however the intensity levels decreased gradually by 48 h and 72 h in irradiated cells. This may due to cell apoptosis, but remained greater than in the controls (Figure 41). The proteomics data at 24 h and 72 h are in agreement with the staining data (Table 23).

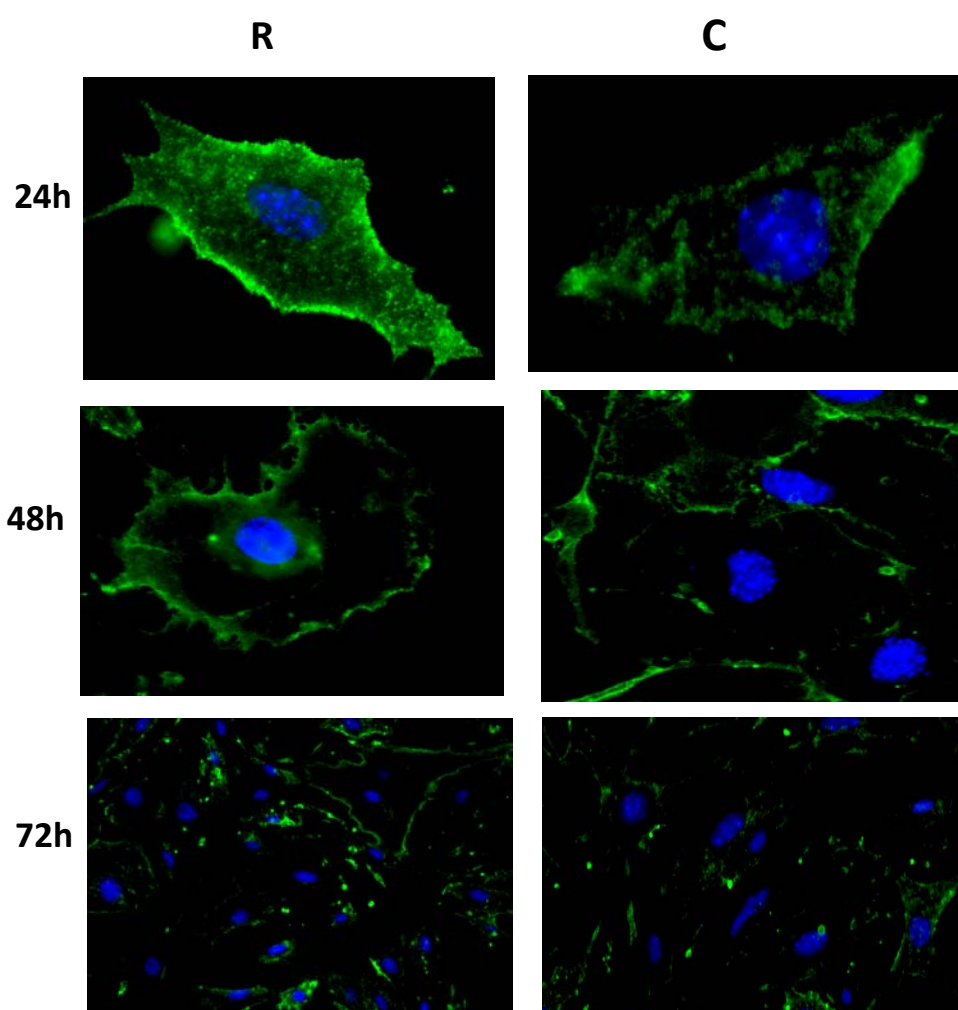


Figure 41. Fluorescent staining of PECAM-1 at 24 h, 48 h and 72 h post irradiation. Expression levels of this protein were higher in irradiated cells compared to the controls at these time points

3.4.2.3. *CD109*

The membrane protein CD109 was mainly expressed in the cytoplasm of irradiated and control cells. The expression intensity in the irradiated cells was higher at 6 h compared to the controls, but lower at 48 h (Figure 42). These data were consistent with the iTRAQ-MS data (Table 22 and 23).

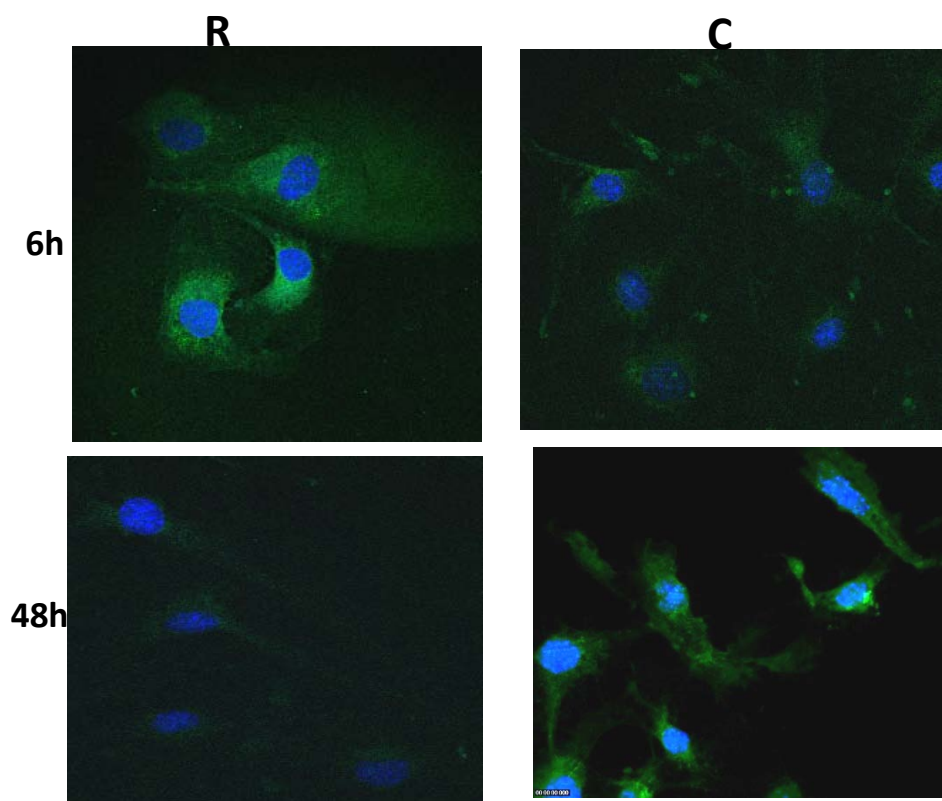


Figure 42. Fluorescent staining of CD109 at 6 h and 48 h post irradiation. Expression levels of this protein increased at 6 h in irradiated cells compared to the controls and decreased at 48 h in irradiated cells.

3.4.2.4. Protein disulfide isomerase (PDI)

PDI was expressed in the cytoplasm of irradiated and control cells. The expression intensity in the irradiated cells was greater than in controls at 6 h, 24 h and 72 h (Figure 43). These data are in agreement with iTRAQ-MS data at those times (Table 23). Unfortunately most irradiated cells died after 72 h.

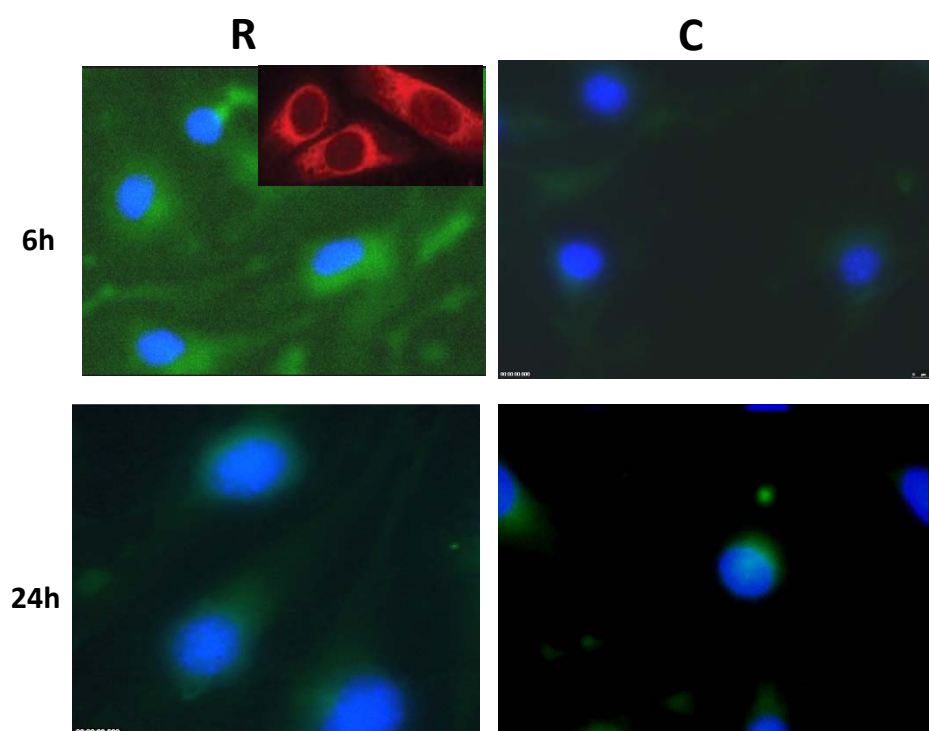


Figure 43. Fluorescent staining of PDI at 6 h and 24 h post irradiation. Expression levels of this protein increased at 6 h and 24 h in irradiated cells compared to the controls. An image of PDI stained with cy5 at 6 h in irradiated cells is also shown.

3.5 Discussion

The use of iTRAQ labelling and mass spectrometry enabled the examination of the differentially expressed membrane proteins between irradiated and non-irradiated murine endothelial cell cultures over time. The immunocytochemistry data validated the presence and expression of those proteins. The membrane proteins that were upregulated in irradiated cells compared to the controls will be investigated as potential targets for the AVM molecular therapy.

Endothelial cells are very heterogeneous and their response to irradiation has been reported previously from *in vitro* and *in vivo* cultured human and animal endothelial cells. After low irradiation doses they mainly decrease their protein expression, and some undergo apoptosis at doses from 15 – 25Gy (Owman C et al 1998; Garlanda C et al 1997; Rubin D 1997).

Fifty membrane proteins were identified from these independent iTRAQ-MS runs, some of those showed increased expression in irradiated cells compared to non-irradiated cells and some showed decrease in expression. The membrane proteins that showed upregulation in irradiated cells at different time points were: PECAM-1, cadherin5, CD109, PDI, integrin alpha 5 and integrin alpha 6. The upregulation of those proteins was confirmed by immunocytochemistry. Platelet endothelial cell adhesion molecule-1 (PECAM-1) is a membrane protein used as a marker to demonstrate the presence of endothelial cells in histological tissues. It is also expressed in certain tumours, which may imply a rapidly growing tumour (Vecchi A, et al 1994; Vanzulli S, et al 1997). PECAM-1 is found on the surface of platelets, neutrophils and monocytes and makes up a large section of endothelial cell intercellular junctions. It is believed that adhesion of platelets to endothelial cells contributes to thrombosis and vascular occlusion post irradiation (Haemost T et al 2004). The proteomics data indicate that PECAM-1 was upregulated in irradiated cells at 24 h and 72 h post irradiation, and the fluorescence staining confirmed these expressions. Therefore PECAM-1 is a worthy candidate for investigation as a target for AVM molecular therapy with

the use of ligands that have been suggested for PECAM-1, such as $\alpha_v\beta_3$ integrin, CD38, CD51 and CD61 (Huss WJ et al 2001; Vecchi A, et al 1994).

Cadherin-5 (or CD144) is another vascular endothelial cell adhesion molecule, belonging to the family of cadherins. Cadherin 5 is required for maintaining a restrictive endothelial barrier and it's essential for proper vascular development (Corada M et al 2001). Previous studies on cadherin 5 response to irradiation showed similar expression to that of PECAM-1 (Akimoto et al 1998). The results here show that cadherin 5 was upregulated at 24 h post irradiation in irradiated cells. Protein disulfide isomerase (PDI), is another membrane protein that showed upregulation in irradiated cells at 6 h, 24 h and 72 h. PDI is an enzyme that acts on the cell surface as a reductase to cleave the disulfide bonds of proteins attached to the cell, while inside the cell it rearranges the disulfide bonds of newly forming proteins (Wilkinson B et al 2004). PDI is also found on the surface of platelets where it plays a role in the activation of integrins that involves rearrangement of disulfide bonds. This activation of integrins to the ligand binding state is an important part of platelet adhesion and secretion (Popielarski M et al 2014; Lahav J et al 2000). No previous evidence is available on the effect of irradiation on PDI expression in endothelial cells, however since this protein expression was upregulated in both proteomics and immunostaining experiments; it is worth pursuing as a potential target for AVM molecular therapy.

Integrins belong to a large family of transmembrane cell adhesion receptors that mediate interactions between adhesion molecules on adjacent cells and on the extracellular matrix. They do exist as heterodimers with alpha and beta subunits, and play different roles in biological processes such as cell migration, wound healing and apoptosis (Popielarski M et al 2014; Xiong P et al 2001). Integrin alpha 5 is a fibronectin receptor, and integrin alpha 6 is a receptor for laminin which is a major protein in the basal lamina (Wu C et al 1993; Lee E et al 1992). Alpha-5 beta-1 integrin mediates the adhesion pathway employed by platelets in the presence of PDI enzyme that facilitates the disulfide exchange on the cell-surface

receptors (Giancotti et al 1999; Essex W et al 1995). In this study the expression levels of integrins alpha 5 and 6 increased in irradiated cells at 6 h and 24 h, making them interesting targets for further investigation for AVM therapy post radiosurgery.

A number of non-membrane proteins also showed significant increased expression in the irradiated cells at different time points. These were: myosin, plectin, vimentin, lamin, actin cytoplasmic 2 and filamin B, which mainly connects cell membrane constituents to the cytoskeleton and maintain cell integrity (Pfendner E et al 2005), while histone proteins, H2A and H4 are involved in the structure of chromatin (Youngson R et al 2006).

Although iTRAQ-MS successfully identified and quantified the differentially expressed proteins on the surface of endothelial cells, the number of identified membrane proteins was small. Therefore, another quantitative proteomics approach known as Mass Spectrometry of Expression (MS^E) was used on bEnd.3 cell cultures with the aim of identifying a larger number of surface proteins, and to further validate the iTRAQ-MS data. The MS^E method is a label-free absolute quantification and identification method of protein analysis from all MS fragments using high performance instruments. The advantages of this technique are: (i) improve sequence and proteome coverage; (ii) quantitative accuracy; and (iii) lower false positive rates (Jeffery, C et al 2005; 2006). These advantages are most dramatic for low abundant proteins such as membrane proteins that we are interested in identifying.

In the next chapter, the experiments conducted on bEnd3 cultures using the quantitative MS^E method will be described in detail. First, optimizations of this method were performed on bEnd.3 cells, followed by the irradiation and proteomics MS^E experiments.

Chapter 4. *In vitro* biotinylation and mass spectrometry expression (MS^E) of bEnd.3 cell cultures post irradiation

4.1 Introduction

To further validate the iTRAQ –LC MS data, and to maximize the number of membrane proteins identified in bEnd3 cultures, an alternative quantitative proteomics technique known as mass spectrometry expression (MS^E) was used to study the differences in expression level of membrane proteins between irradiated and control cell cultures.

Typical MS/MS instruments look at all precursor masses over a defined mass range then select a limited number of the most intense ions for sequential fragmentation scans, while the MS^E instruments abandon the selection of a precursor ion for individual fragmentation and fragments everything within a defined mass window of 50 to 1200 m/z. As a result the exact mass precursor and fragment ion spectra for every detectable component in the samples are measured in a single analysis. (Waters Corporation). With this technique 90% of the data are reproducible with 70% of the quantitative data reproducible and 20% variability (Waters Corporation). This study was conducted at Professor Joseph Loo's lab, at the University of Californian Los Angeles, since his lab was equipped with the latest MS^E instruments from Waters Corporation, which was not available at Macquarie University.

Because of the different nature of data acquisition of MS^E instruments, further *in vitro* biotinylation protocol optimization was performed before employing the MS^E analysis on bEnd.3 cultures. After successful optimization, cell cultures were irradiated with 25 Gy and surface biotinylation was performed at 6 h, 24 h and 48 h post radiation. Non-irradiated cell cultures served as controls. Biotinylated proteins were then captured on streptavidin resin, digested overnight with trypsin, then analysed by MS^E to identify and quantify membrane proteins.

4.2 Materials and Methods of MS^E optimization on bEnd.3

4.2.1 Cell culture irradiation

bEnd.3 cell cultures were prepared as described in chapter 3, section 3.2.1. Three cell cultures were irradiated once they reached 80% confluence in their culture flasks with an absorbed dose of 25 Gy using RS320 research system from (Vraian Medical Systems) that uses a metal ceramic 300kV X-ray tube with an integral high voltage receptacle and cooling system. The system is enclosed in a ray proof housing that contains fittings for water hose connections. The X-ray tube output limits are; Voltage 30 – 310 kV, Current 1.0 mA – 30 mA, Power 3000 W. Cells were returned to the incubator immediately after irradiation. The irradiation was performed at the University of California Los Angeles, Radiation Oncology Department.

4.2.2. *In vitro* biotinylation and MS^E analysis

The initial *in vitro* biotinylation and capture of biotinylated proteins were performed on the cell cultures at 6 h, 24 h and 48 h post irradiation, using the same protocol employed with iTRAQ-MS described in chapter 3, sections 3.2.4 and 3.2.5, to determine the suitability and compatibility of the protocol for MS^E analysis.

After tryptic digestion, chromatographic separation of peptides was achieved using Waters nanoACQUITY UPLC BEH C18 Column (1.7 μ m, 75 μ m x 150 mm, 10 K psi). The mobile phase, used at a flow rate of 0.3 μ L/min, with a gradient of a mixture of (A) 0.1% formic acid in water and (B) 0.1% formic acid in acetonitrile, programmed as follows: initially 97% A for 1 min, reduced to 60% A for 60 min, then decreased to 5% for 2 min, held for 15 min, then increased to 97% A for 3 min. The column temperature was set at 28°C.

Mass spectrometry analysis of tryptic peptides was performed utilizing a Waters Xevo quadrupole time of flight (Q-TOF) mass spectrometer coupled directly to a Waters nanoACQUITY UPLC system. All analysis was performed using positive mode electrospray

ionization (ESI). LC MS data were collected in an alternating low energy MS and elevated energy MS/MS (MS^E) mode of acquisition. In low energy MS mode the data were collected at constant collision energy of 6 eV. In elevated energy MS/MS mode the collision energy was ramped from 15 – 40 eV on laboratory frame energy to collect product ions of all precursors identified from the MS scan.

4.2.3 Data analysis

The LC MS and LC MS/MS data were processed using Proteinlynx global server (PLGS) version 2.5 (Waters Corporation). Protein identification was based on MS/MS peak lists generated by MS^E data independent collision-induced fragmentation using a *Mus musculus* database. Protein identifications were accepted with greater than three fragment ions per peptide, seven fragment ions per protein and one unique peptide per protein identified. Carbamidomethyl cysteine was set as a fixed modification while oxidized methionine was set as variable modification. Trypsin was set as a proteolytic enzyme, and up to two missed cleavages were allowed.

4.2.4 Results

Few peptides were detected in the initial MS^E analysis due to unknown charged molecular species that were present in all samples that prevented efficient peptide ionization (Figure 44). To identify the nature of these molecules, MALDI (Matrix-Assisted Laser Desorption Ionization) analysis was performed. MALDI analysis indicated that the molecules were in fact SDS detergent polymers (Figure 45). Sodium Dodecyl Sulfate is an essential component of the lysis buffer and the washing buffers that used for membrane protein labelling with biotin. Protease inhibitors were not used in this protocol; hence the presence of SDS polymers was from the lysis buffers. Although it did not affect protein identification with the previous LC-MS analysis on Qstar Elite (AB Sciex) instrument, it was clear that the high sensitivity of the

MS^E instrument, Xevo (Waters) could not tolerate the presence of detergents. Therefore the detergent had to be removed completely in order to obtain improved quality MS^E data.

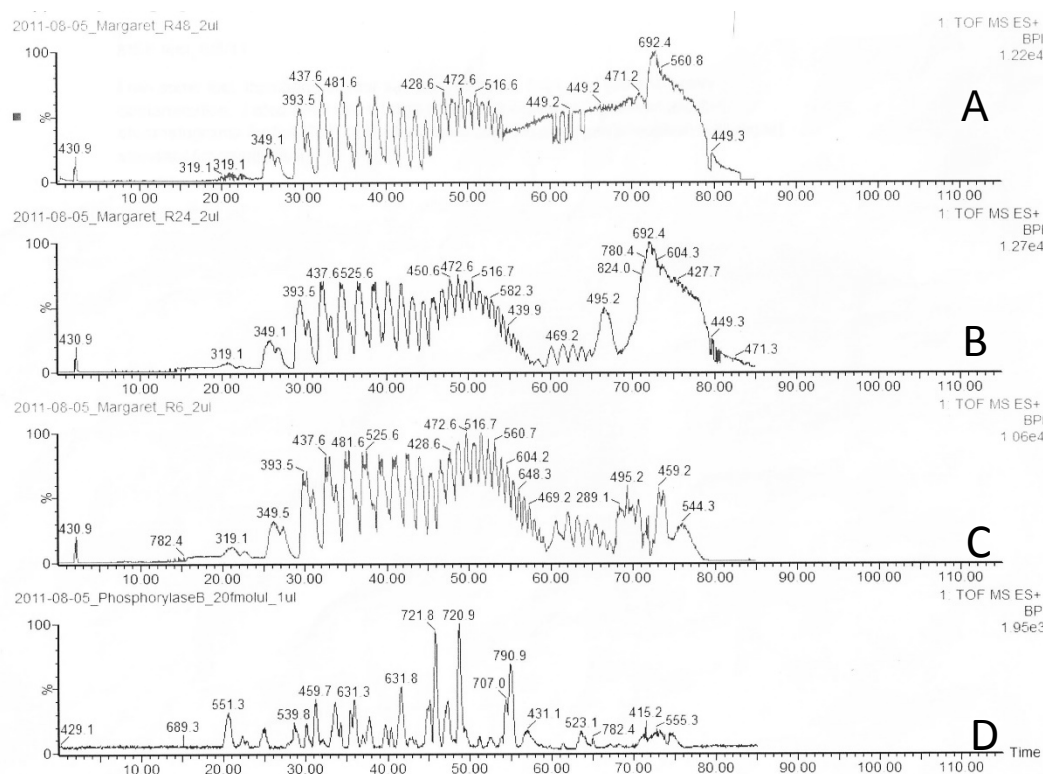


Figure 44. Base peak ion (BPI) chromatograms of bEnd.3 showing heavy contamination at A, B and C compared to standard protein digest (D).

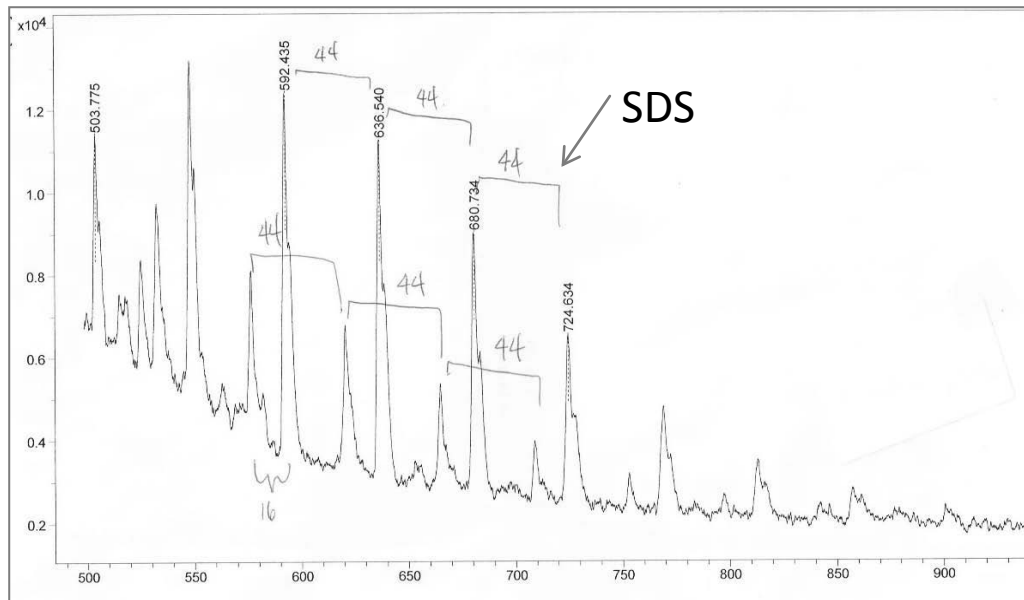


Figure 45. MALDI chromatograms of bEnd3, showing many SDS detergent peaks (44 kDa)

It was clear that a further protocol optimization was necessary. Below are described the optimizations performed to eliminate the effect of the detergents.

4. 3. Optimization of the *in vitro* biotinylation protocol for MS^E analysis

Three optimization experiments were performed for the *in vitro* biotinylation protocol described at sections 3.2.4 and 3.2.5, using *E.coli*, summarized in

Table 24. Optimization of the *in vitro* biotinylation protocol for MS^E analysis using *E.coli*

Protocol A	Protocol B	Protocol C
Repeat the initial protocol then perform *SCX after trypsin digestion. Analyse the sample with MALDI and LCMS	Repeat the initial protocol with increased washing with *Amb from 1 to 8 times, and wash the streptavidin sepharose with PBS 3 times after washing with buffer A. Analyse the sample with MALDI and LCMS	Repeat the initial protocol without the use of any detergents, instead use Amb. Analyse the sample with MALDI and LCMS
*SCX = Strong cation exchange chromatography	*amb = Ammonium bicarbonate	Control sample

4.3.1 Results

LCMS and MALDI chromatograms were mostly clear from detergents (Figures 46, 47, 48 and 49) however, high concentrations of Na⁺ were detected in all sample chromatograms, which may limit the number of proteins identified by LCMS. The total number of proteins identified was 68 with protocol A and 78 with protocol B. The Na⁺ may have originated from the PBS buffer that was used in the protocol.

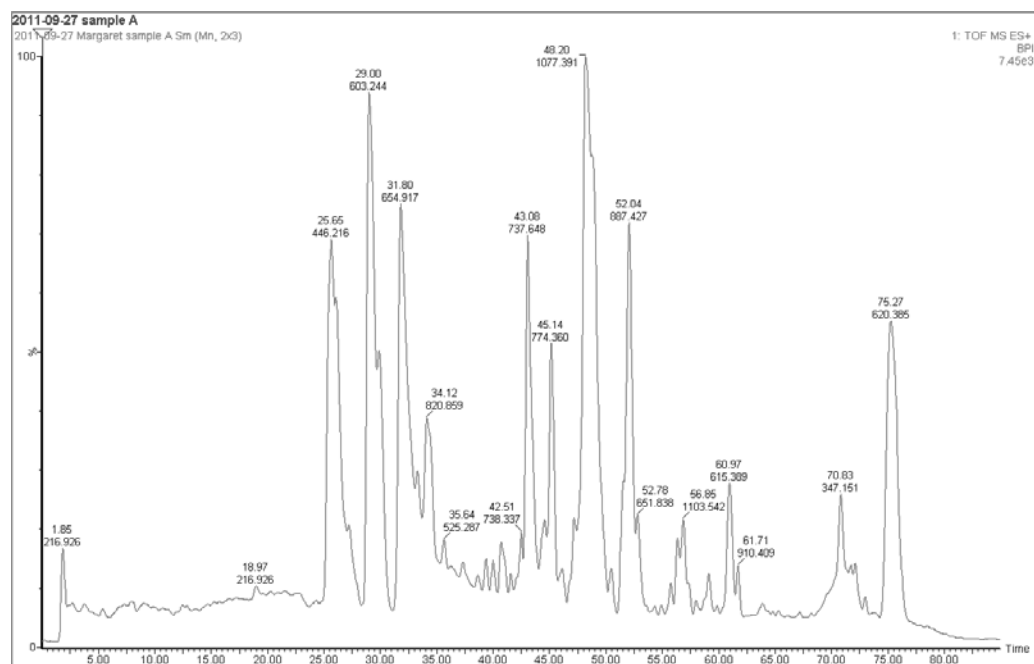


Figure 46. LCMS chromatogram for sample A. No detergents peaks were observed

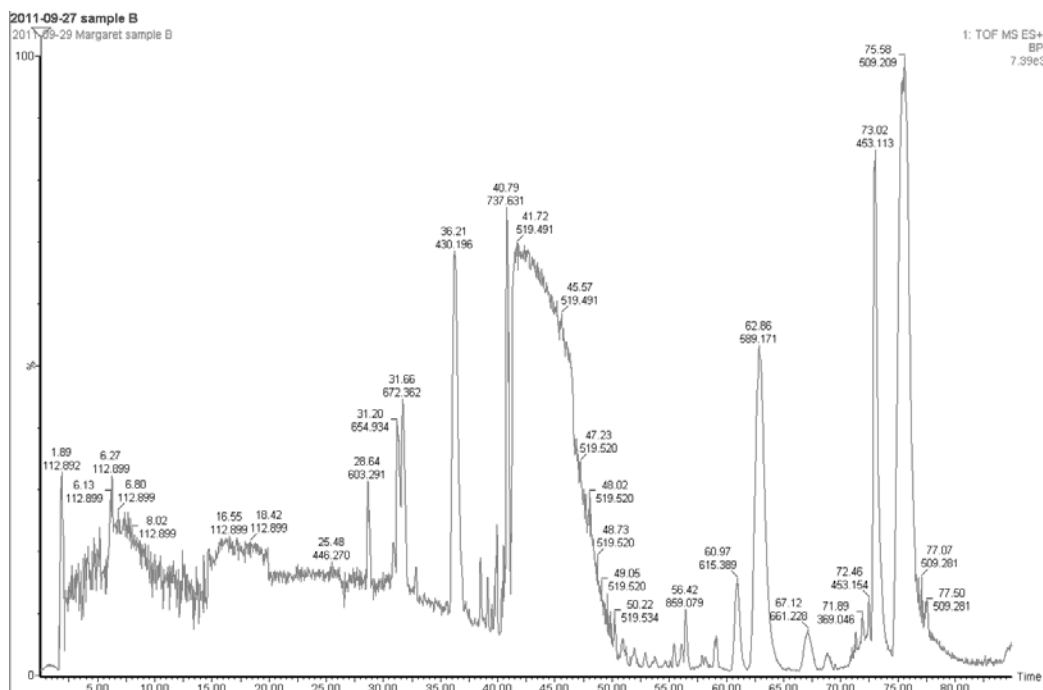


Figure 47. LCMS chromatogram for sample B. Clear from detergents

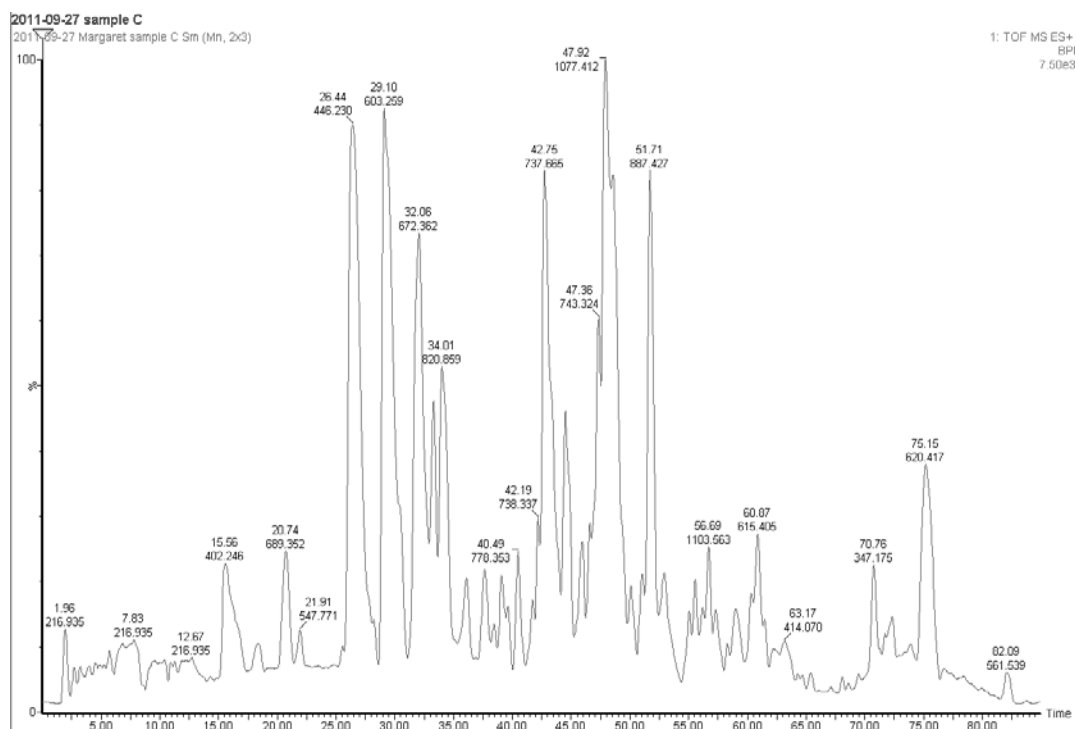


Figure 48. LCMS chromatogram for sample C. No detergents peaks were observed.

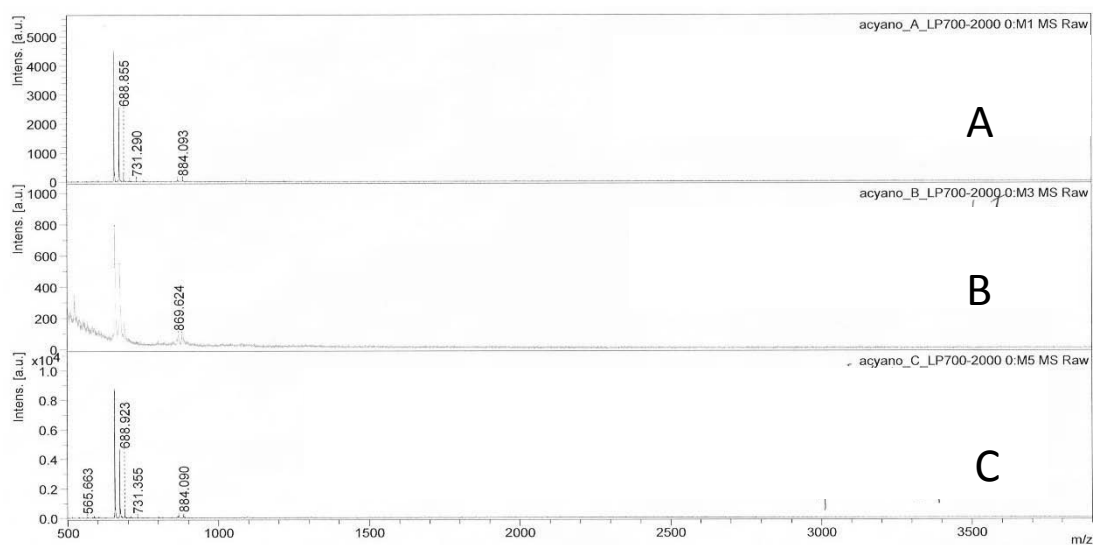


Figure 49. MALDI analysis on samples A, B and C, all were clear from detergents

To eliminate the effect of Na⁺ and further clean the detergents another optimization was performed using bEnd3 cell cultures as follows.

Twenty millilitres of PBS containing 67 μM Sulfo-NHS-LC-Biotin (Pierce, IL, USA) was added to the flask and incubated for 5 min at room temperature. The biotinylation reaction was terminated by adding Tris-HCl pH 7.5 to a final concentration of 670 μM. After 5 min incubation the cells were washed four times with PBS and harvested with 2 – 3 mL of lysis buffer containing 2% v/v TritonX-100, 0.2% w/v SDS and protease inhibitor EDTA-free (Complete, Roche, Switzerland) and kept on ice for 30 min.

Biotinylated proteins were captured on streptavidin sepharose (GE health care). Five hundred microlitres of streptavidin sepharose were washed three times with a buffer containing 1% v/v TX-100, 0.5% w/v SDS in PBS, and then further washed three times with PBS before adding to cell lysates. The samples were incubated with the washed streptavidin sepharose for 2 h at room temperature. Streptavidin sepharose was pelleted by centrifugation at 1600 × g for 5 min. Unbound proteins were removed by washing three times with 1% v/v TritonX-100, once with 0.1% w/v SDS and five times with digestion buffer (50 mM ammonium bicarbonate).

Tryptic digestion of biotinylated proteins and MS^E analysis was performed as described in section 4.2.2 in this chapter and data analysis was performed as described in section 4.2.3 in this chapter.

4.3.2. Results

The MS^E of bEnd3 detected on average 338 proteins from three replicate MS injections. The chromatogram was clear from both detergents and Na⁺ (Figure 50). This latest protocol proved to be effective in eliminating detergents and suitable for analysing with the MS^E instrument. Therefore this protocol was used for the *in vitro* biotinylation study of bEnd 3 cells and MS^E analysis in response to irradiation.

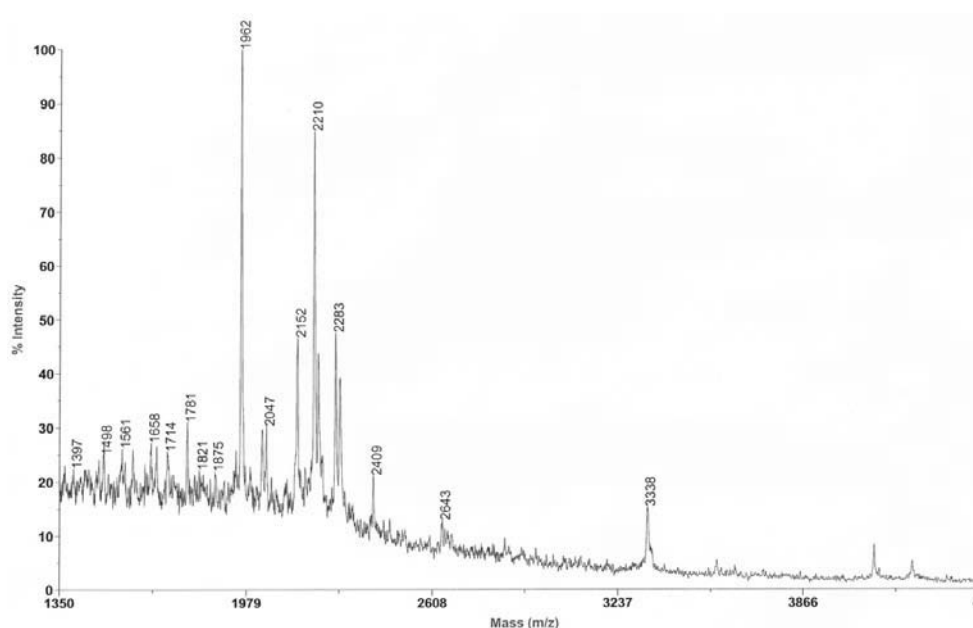


Figure 50. LCMS chromatogram of bEnd3, clear from detergents and sodium ions.

4.4. *In vitro* biotinylation and mass spectrometry expression MS^E of bEnd.3 cell cultures post irradiation

For this study, cultured cells were grown in triplicate, treated by irradiation and samples collected after 6 h, 24 h and 48 h post irradiation. Control, untreated cells were also grown in triplicate and collected at these time points for comparisons. For each time point, MS^E was run in triplicate for both irradiated and control samples. The entire experiment was repeated so that mass spectrometry data were independently obtained twice.

4.4.1 Materials and Methods

4.4.1.1 Mouse endothelial cell cultures (*bEnd.3*)

bEnd.3 cells were cultured as described in section 3.2.1

4.4.1.2 Cell density and total protein concentration

Cell density was counted as described in section 3.3.2. The density of bEnd.3 cells was approximately 1×10^5 cells/mL, and total protein concentration was 1.6 mg/mL.

4.4.1.3 Irradiation of bEnd.3 cells

Cells were irradiated once they reached 80% confluence with an absorbed dose of 25 Gy using a RS320 research system (Vraian Medical Systems), at the UCLA Radiation Oncology Department as described in section 4.2.1. Cells were returned to the incubator immediately after irradiation until their use.

4.4.1.4 In vitro biotinylation of bEnd.3 cells

Surface biotinylation was performed on the endothelial cell cultures using a modified protocol from Scheurer, S *et al.* (2005) and Roesli, C *et al.* (2006). Each 75 cm² flask containing approximately 1×10^6 cells was washed four times with PBS pH 7.4. Twenty millilitres of PBS containing 67 μ M Sulfo-NHS-LC-Biotin (Pierce, IL, USA) were added to the flasks and incubated for 5 min at room temperature. The biotinylation reaction was terminated by adding Tris-HCl pH 7.5 to a final concentration of 670 μ M. After 5 min incubation the cells were washed four times with PBS and harvested with 2– 3 mL of lysis buffer containing 2% v/v TX-100, 0.2% w/v SDS and protease inhibitor EDTA free (Complete, Roche, Switzerland) and kept on ice for 30 min.

4.4.1.5 Capture of biotinylated proteins

Biotinylated proteins were captured on streptavidin sepharose (GE health care). Five hundred microlitres of streptavidin sepharose were washed three times with a buffer containing 1% v/v TX-100, 0.5% w/v SDS in PBS, and then further washed three times with PBS before adding

to cell lysates. Samples then were incubated with washed streptavidin sepharose for 2 h at room temperature. Streptavidin sepharose was pelleted by centrifugation at 1600 ×g for 5 min. Unbound proteins were removed by washing three times with 1% v/v TX-100, once with 0.1% w/v SDS, and five times with digestion buffer (50 mM ammonium bicarbonate).

4.4.1.6 Tryptic digestion of biotinylated proteins and MS^E analysis

Streptavidin sepharose was re-suspended in 200 µL of digestion buffer. Twenty microlitres of trypsin were then added and incubated overnight at 37° C. The samples were centrifuged at 14,100 ×g for 2 min at room temperature and the supernatant was collected.

Chromatographic separation was achieved using Waters nanoACQUITY UPLC BEH C18 Column (1.7 µm, 75 µm x 150 mm, 10 K psi). The mobile phase, used at a flow rate of 0.3 µL/min, with a gradient of a mixture of (A) 0.1% formic acid in water and (B) 0.1% formic acid in acetonitrile was programmed as follows: initial 97% A for 1 min, decreased to 60% A for 60 min, then decreased to 5% for 2 min, held at this for 15 min, again increased to 97% A in 3 min. The column temperature was set at 28°C.

Mass spectrometry analysis of tryptic peptide was performed utilizing Waters Xevo quadrupole time of flight (Q-TOF) mass spectrometer coupled directly to Waters nanoACQUITY UPLC system. Analysis was performed as described above in section 4.2.2.

4.4.2 Data analysis

The LC MS and LC MS/MS data were processed using ProteinLynx Global Server (PLGS) version 2.5 (Waters Corporation) as described above in sections 4.2.3.

4.4.3 Results

To study the effect of irradiation on the murine endothelial cell cultures and to identify the upregulated membrane proteins in response to irradiation, cultured cells were treated by irradiation and samples collected after 6 h, 24 h and 48 h. Control samples were also collected at these time points. The entire experiment was repeated so that mass spectrometry data were obtained independently twice. A total of 36 mass spectrometry runs were analysed from 6 irradiated and 6 control samples, each run in triplicate. The Total number of proteins identified by two MS^E analyses in irradiated and control samples at each time point is presented in (Table 25).

Table 25. Total number of proteins identified by two MS^E analyses in irradiated and control cell cultures (bEnd3)

Time points	Irradiated	Controls
6 h	163	229
24 h	407	371
48 h	216	276

The numbers of membrane proteins detected by the two independent MSE analyses in both irradiated and control samples are presented in (Table 26) below.

Table 26. Numbers of membrane proteins of bEnd3 detected by two independent MS^E analyses in both irradiated

Time points	Membrane proteins in R	Membrane proteins in C
6 h	10	27
24 h	47	31
48 h	18	13

Our proteomics analyses focused on the membrane proteins that were present in both independent MS^E data at three time points. Tables (27, 28 and 29) represent the membrane proteins shared between irradiated (R) and control (C) samples at each time point with their average concentrations on column, average protein masses and number of times identified in the runs. The (supplementary Table 2) includes other membrane proteins identified at 6h in (R) and (C) samples from both MSE^E analyses, but were not shared between them.

Table 27. Membrane proteins identified in irradiated (R) and control (C) samples at 6 h after irradiation, their average masses, average concentration on column (fmol) and number of replication in the MS runs; n = 6 (R); n = 6 (C)

Protein name	MW (Da)	Ave fmol in R	Protein replication	Ave fmol in C	Protein replication
PECAM-1	82118.1	21.7	1	13.5	1
Cadherin 5	88188.2	0.01	1	6.5	1
Annexin A2	38961.4	6.4	1	6.7	1
Multimerin 2	105833.7	0.01	1	6.5	1
Integrin beta 1	91482	0.01	1	6.4	1
Ras related Rab-1B	22358.3	2.4	1	0.01	1
Protein lunapark	47785.1	13.2	1	0.01	1

Table 28. Membrane proteins identified in irradiated (R) and control (C) samples at 24 h after irradiation, their average masses, average concentration on column (fmol) and number of replication in the MS runs; n=6 (R); n=6 (C)

Protein name	MW	Ave fmol in R	Protein replication	Ave fmol in C	Protein replication
PECAM-1	82118.1	67.9	5	52	5
Cadherin 5	88188.2	49	6	16.4	6
Multimerin 2	105833.7	25.4	3	28.9	3
Protein lunapark	47785.1	23.2	1	0.01	1
Endothelial protein C receptor	27668.3	7.2	1	0.01	1
Surface glycoprotein MUC18	72515	0.01	1	13.4	1
Annexin A2	38961.4	9	1	9.4	1
Integrin beta 1	91482	31.7	3	0.01	1
Fibroblast growth factor8	23891.9	19.8	1	0.01	1

Table 29. Membrane proteins identified in irradiated (R) and control (C) samples at 48 h after irradiation, their average masses, average concentration on column (fmol) and number of replication in the MS runs; n=6 (R); n=6 (C)

Protein name	MW	Ave fmol in R	Protein replication	Ave fmol in C	Protein replication
PECAM-1	82118.1	55.4	5	36.7	3
Annexin A2	38961.4	0.01	1	10.4	1
Cadherin 5	88188.2	31.1	3	18.3	1
Multimerin 2	105833.7	19.8	3	21.7	3
Cell surface glycoprot MUC18	72515	15.8	1	0.01	1
Integrin beta 1	91482	15.1	1	0.01	1
Ras related Rab 35	23310.4	10.7	1	0.01	1
Fibroblast growth factor 8	30647.8	0.01	1	4.9	1

Further analysis was focused on the membrane proteins that were present in at least three out of the six runs in R and C groups at each time point. This criterion was observed only at 24 h and 48 h time points, and is presented in Tables (30 and 31) and Figures (51 and 52).

Table 30. Membrane protein upregulation in irradiated (R) vs. control (C) cells at 24 h post irradiation, their accession number, molecular weight, average concentration on column (fmol) and average concentration ratios (irradiated : control); n= 6 (R); n= 6 (C).

Protein name	Accession#	MW	Ave fmol in R	SD	Ave fmol in C	SD	Ave (R:C)	<i>p</i>
PECAM-1	Q08481	82118.14	88.4	57	23.4	26.1	3.8	0.019
Cadherin 5	P55284	88188.25	58.7	33	10.3	10.2	5.7	0.010
Integrin beta1	P09055	91481.98	26.9	16	1.9	0.2	14.2	0.004
EPCR	Q64695	27668.34	35.3	18	2	0.2	17.7	0.058
Multimerin 2	A6H6E2	105833.7	39.3	22	12.4	12.1	3.2	0.033

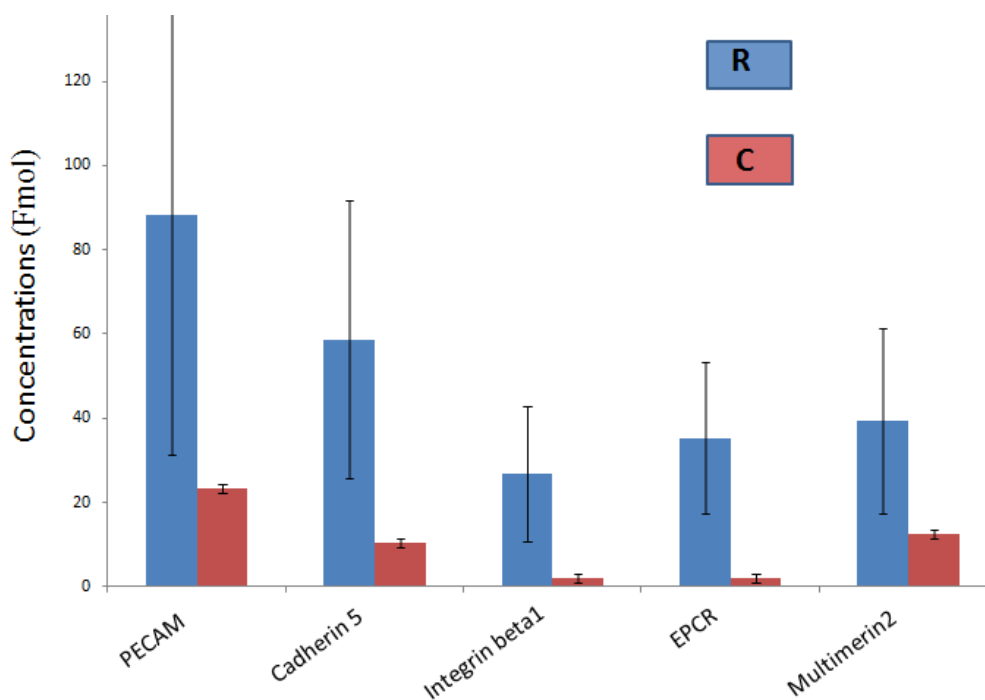


Figure 51. Membrane protein expression in irradiated (R) and control (C) in bEnd3 cells at 24 h post irradiation

Table 31. Membrane protein upregulations in irradiated (R) vs. control (C) cells at 48 h post irradiation, their accession number, molecular weight, average concentration on column (fmol) and average concentration ratios (irradiated : control); n= 6 (R); n= 6 (C)

Protein name	Accession#	MW	Ave fmol in R	SD	Ave fmol in C	SD	Ave (R:C)	<i>p</i>
PECAM-1	Q08481	82118.14	45.0	23.0	19.2	17.9	2.3	0.056
Cadherin 5	P55284	88188.25	16.8	15.7	5.1	6.5	3.3	0.136
Multimerin 2	A6H6E2	105833.7	11.4	9.5	11.8	11.1	1.0	0.938

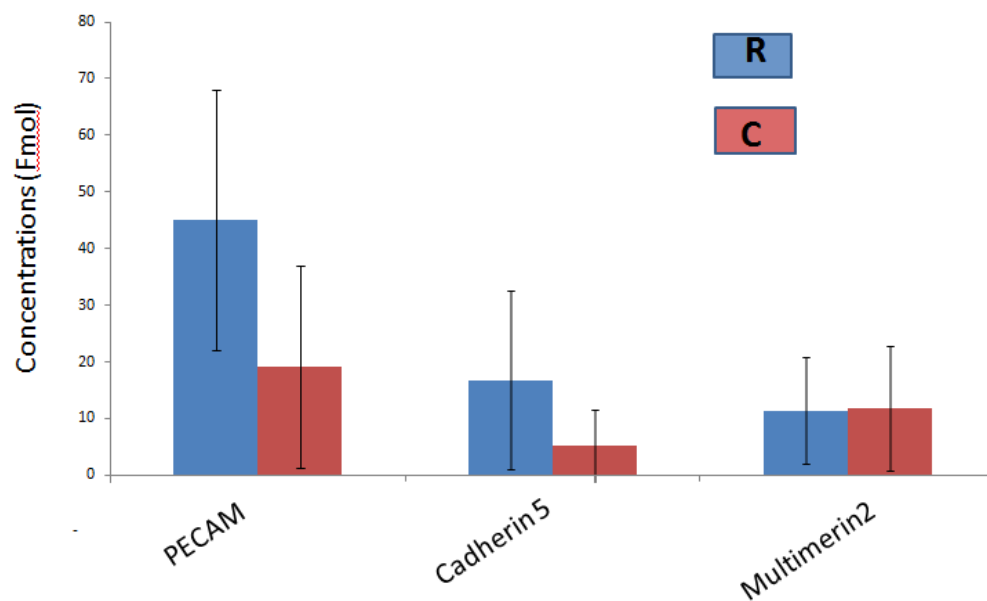


Figure 52. Membrane proteins expression in irradiated (R) and (C) in bEnd3 cells at 48h post irradiation

4.4.4 Discussion

The overall aim of this study was to identify potential protein targets for brain AVMs molecular therapy, and the specific aim was to identify a large number of differentially expressed membrane proteins in the murine endothelial cell cultures in response to irradiation over time. To achieve this specific goal, a relatively new quantitative proteomics method was used, known as MS^E (Jeffery, C. et al 2006), to compare the protein expression in irradiated cell cultures at 6h, 24h and 48h post irradiation to the controls. Although endothelial cell response to irradiation has been reported in previous studies, however, their expression pattern differs from one cell line or tissue to another and it is dose dependent (Rosen and Goldberg 1988; Rubin D 1997).

The total number of proteins identified in irradiated cells was higher than control cells at 24h post irradiation, compared to 6h and 48h (Table 25), this may due to higher cell death in the cultured flasks at 48h of irradiation, as morphological changes in irradiated cells were also

observed at 48h of irradiation (Figure 40 and 41), additional replicates may need to be performed to confirm the data. The most extensive membrane protein upregulations in the irradiated samples were observed at 24 hours. Those membrane proteins were: PECAM-1, cadherin 5, integrin beta 1, endothelial protein C receptor (EPCR), and multimerin 2. These protein expressions increased significantly in irradiated cells at 24 h by 3.8 fold, 5.7 fold, 14.2 fold, 17.7 fold and 3.2 fold respectively. However at 48 h, only PECAM-1 showed significant upregulation in irradiated cells, (2.3) fold. These results are in agreement with iTRAQ data on bEnd3 cells described in chapter 3, section 3.4.1 and with the immunocytochemistry data that validated the expression levels of PECAM-1 and cadherin 5 at these time points, (Chapter 3, sections 3.4.2.1 and 3.4.2.2).

PECAM (or CD31) is a vascular endothelial cell adhesion molecule and makes up the majority of endothelial cell intercellular junctions (Varon D et al 1998). It is also expressed in platelets, macrophages, lymphocytes, megakaryocytes, and neutrophils, and plays important roles in angiogenesis, regulation of integrin-mediated cell adhesion, cell migration, and thrombosis (Newman PJ et al. 1990).

PECAM-1 is a membrane protein; in fact it's used as a membrane protein marker in many immunostaining protocols and to demonstrate the presence of endothelial cells in histological tissues (Vecchi A, et al 1994; Vanzulli S, et al 1997). PECAM-1 is also expressed in certain tumors, which may imply a rapidly growing tumour because of its involvement in angiogenesis. For this reason, PEACM-1 has been investigated and used as an angiogenic inhibitor in cancer targeting therapies (DeLisser H et al 1997; Ouyang JS et al 2014).

Previous *in vitro* studies in human and animal cell cultures showed that when endothelial cells were exposed to irradiation doses from 10 – 20 Gy, the expression levels of PECAM-1 increased (Guagler MH et al, 2004). Adhesion of platelets to endothelial cells has been reported to contribute to vascular occlusion and thrombosis post irradiation (Haemost JT, et al 2004).

The experiments here showed significant upregulation of PECAM-1 at 24 h and 48 h post irradiation, therefore future study will investigate PECAM-1 as a target for AVM molecular therapy with the use of ligands such as $\alpha_v\beta_3$ integrin, CD38, CD51 and CD61 that have been proposed for PECAM-1 (Huss WJ et al 2001; Vecchi A, et al 1994).

Cadherin-5 or (CD144) is another vascular endothelial cell adhesion molecule, belonging to the family of cadherins. Cadherins are calcium-dependent cell adhesion glycoproteins. They control the cohesion and organization of the intercellular junctions. Previous studies on cadherin-5 response to irradiation showed similar expression to that of PECAM-1 (Akimoto et al 1998). The results here indicated that cadherin 5 was significantly upregulated in irradiated cells, at 24 h post irradiation.

Integrin beta-1 (or CD29) is a membrane receptor belonging to the family of integrins, and is involved in cell adhesion and recognition in a variety of biological processes including embryogenesis, haemostasis, and metastatic diffusion of tumour cells (Radford J et al 1996). The subfamily alpha2-beta1 ($\alpha_2\beta_1$) integrin serves as a receptor for collagens, laminin, and many other ligands, and it has been extensively studied as a collagen receptor on platelets (Santoro A et al 1995; Sixma J et al 1997). Many studies suggested that $\alpha_2\beta_1$ is a crucial mediator of platelet adhesion to collagen in the vessel wall after vascular injury, and that this interaction is required for proper haemostasis and thrombosis (Santoro A et al 1995).

In 2002 a study by Cordes N et al, showed that integrin beta-1 was upregulated post irradiation in human lung tumour cells *in vitro* (Cordes N et al. 2002). The proteomics results here showed significant upregulation of integrin beta-1 at 24 h post irradiation ($p = 0.004927$). The role of integrin beta-1 receptor in thrombosis makes it a potential protein target for investigation for the AVM molecular therapy post radiosurgery, by delivering thrombotic agents such as tissue factors or thrombin, through $\alpha_2\beta_1$ and its ligand to induce thrombosis in AVM vessels.

Endothelial protein C receptor (EPCR) or (CD201) is another membrane protein that was upregulated significantly in the irradiated cell cultures at 24 h. This protein is a receptor for activated protein C (APC), which is a serine protease involved in the blood coagulation pathway (Fukudome K et al 1994). Protein C, also known as autoprothrombin IIA and blood coagulation factor XIV, is an inactive form of protein that plays important role in regulating thrombosis (Hall A et al 1999). Protein C is activated by binding to thrombin and protein C's activation is stimulated by the presence of thrombomodulin and EPCR, therefore activated protein C is mainly found in endothelial cells of blood vessel walls (Fukudome K et al 1994; Rothbarth K et al 1999). Due to EPCR's role in regulating thrombosis it makes this protein a worthy candidate for investigation in AVM molecular therapy, perhaps adding APC resistance factors after radiosurgery may induce thrombosis readily in AVM vessels.

Multimerin 2 is a basement membrane glycoprotein secreted into the extracellular matrix that inhibits endothelial cell motility and negatively regulates angiogenesis (Lorenzon E et al 2012; Christian S et al 2001). Some *in vitro* and *in vivo* studies suggested that multimerin 2 may reduce tumour angiogenesis and growth by interfering with the vascular endothelial growth factor (VEGF –A/VEGFR2) pathway thus making it a potential candidate in developing cancer treatment (Lorenzon E et al 2012; Huang W et al 2012). While Multimerin-1 in platelets plays a role in thrombosis (Hayward P et al 1991), multimerin 2 doesn't, and there is no previous evidence of multimerin 2 response to irradiation.

The MS^E proteomics data of bEnd3 cell cultures were in agreement with the iTRAQ-MS data in regards to most protein expression patterns, and the immunostaining data supported the proteomics findings. This suggests that both methods were successful in identifying proteins on the surface of endothelial cells in response to irradiation. These proteins will be investigated as potential targets for the ligand-based molecular therapy for brain AVMs.

The effect of irradiation on endothelial cell surface molecules was further studied by conducting proteomics and irradiation experiments on the rat model of AVM, which is a dynamic model, to compare the data obtained from the latter with those obtained from MS^E and iTRAQ-MS, and to further identify potential protein targets. The following chapters will first describe the optimizations of the *in vivo* biotinylation perfusion method on the rat model of AVM, followed by the irradiation experiments and proteomics MS^E analysis of the rat model.

Chapter 5. *In vivo* biotinylation optimization of the rat model of AVM

5.1. Introduction

Successful development of the *in vivo* biotinylation perfusion protocol was necessary to study the response of AVM endothelium to irradiation in an animal model of AVM.

Six weeks after fistula creation, *in vivo* biotinylation perfusion was performed, model AVM tissues were excised, membrane proteins were extracted and captured on streptavidin resin then digested overnight with trypsin and analysed by nano LC/MS and MS^E.

5.2. First *in vivo* biotinylation perfusion trial

5.2.1. Material sand Methods

5.2.1.1 Rat model

An arteriovenous fistula (AVF) was created in a *Sprague-Dawley* male rat weighting 370 g, according to the Yassari R et al 2004 protocol. After the operation the rat was returned to the animal care facility located on Macquarie University campus and monitored daily for the first week then weekly for five weeks allowing the fistula to reach maturity.

5.2.1.2 In vivo biotinylation perfusion

The rat was narcotized with a subcutaneous injection of combined anaesthesia (ketamine 100 mg/mL, xylazine 20 mg/mL and acepromazine 10 mg/mL). Using blunt scissors, the skin was cut from the abdomen to the thorax, and then dissected to open the peritoneum. The chest was opened through a median sternotomy. The heart was turned around quickly by holding it with forceps at the apex, and an injection needle was inserted into the left ventricle and then to the aorta. A small cut in the right atrium was made with scissors to allow the blood and perfusion solutions to flow out. Using the Gilson Minipuls 3 perfusion pump attached to a tube and needle, the rat was perfused with 200 mL of saline (NaCl) to wash away the blood, immediately followed by 100 mL of freshly prepared biotinylation solution [1 mg/mL of

Sulfo-NHS-LC-Biotin in pre warmed PBS at 37°C + 10% Dextran 40] by pressing the syringe plug with a flow rate of 30 mL/min while monitoring the pressure and keeping it constant at ~100 mm Hg. After 5 min of perfusing the biotinylation solution, the rat was injected with 100 mL of (50 mM Tris-HCl in PBS + 10% Dextran 40) with a flow rate of 30 mL/min to wash out excessive biotinylation reagent, then perfused with 200 mL saline at 30mL/min to wash away Dextran. The fistula tissue then was excised and the surrounding fat and muscle tissue was removed. The vascular tissue was placed in a 1 mL Eppendorf tube and transferred to a -80° C freezer immediately. This protocol was modified from (Roesli, C et al. 2006).

5.2.1.3 Membrane protein extraction

The vascular tissue sample was pulverized in liquid nitrogen and resuspended in 1mL of lysis buffer (20 mM HEPES, 150 mM NaCl, 10 mM NaF, 1 mM Na-EDTA, 1 mM Na-EGTA, pH 7.5, pH adjusted with NaOH) + protease inhibitor (4 µL per mL of HEPES buffer, Sigma P-2714). Each sample was probe sonicated for 15 s, three times in ice with a Branson Sonifier 450 (John Morris Scientific) and centrifuged in a pre-cooled rotor at $1,500 \times g$ for 15 min (4°C). The supernatant was collected and the pellet re-lysed with 0.5 mL of HEPES buffer (same as above steps). The supernatant was collected and pooled with the previous supernatant; the final volume of supernatant was ~1.5 mL. Sodium Bicarbonate solution (0.1 M, pH 11) was added to pooled supernatant (up to 5 mL) and incubated for 1 h at 4°C on a rocking platform. After incubation, the sample was centrifuged at $120,000 \times g$ for 1h (4°C) using a S80-AT3 rotor. The pellet was dissolved with 200 µL of 100 mM Amonium Bicarbonate containing 10 mM DTT (freshly prepared) in water bath sonication (Transsonic 700/H, John Morris Scientific) for 20 min and then incubated for 1h at 37°C to reduce the sample. To alkalize the sample, 5 µL of 1 M idoacetamide stock was added to make a final concentration of 20 mM idoacetamide, and the sample was incubated in the dark at room temperature for 30 min. The sample volume was then brought up to 5 mL with 100 mM Amonium Bicarbonate and centrifuged at $120,000 \times g$ for 1 h (4°C). The pellet was dissolved

with 400 μ L of 100 mM Ammonium Bicarbonate in water bath sonication then 600 μ L of methanol was added.

5.2.1.4 Capture of biotinylated proteins

Biotinylated proteins were captured on streptavidin sepharose (GE health care, Australia). Five hundred microlitres of streptavidin sepharose were washed three times with buffer A (containing 1% w/v NP40, 0.5% w/v SDS in PBS) before adding to cell lysates. Samples then were incubated with washed streptavidin sepharose for 2 h at room temperature. Streptavidin sepharose was pelleted by centrifugation at 1600 \times g for 5 min. Unbound proteins were removed by washing three times with buffer A, once with buffer B (0.1% w/v NP40, 0.5 M NaCl in PBS) and once with digestion buffer (0.25 mM AMB).

5.2.1.5 Tryptic digestion of biotinylated proteins and Nano-LC-MS/MS

Streptavidin sepharose was re-suspended in 200 μ L of digestion buffer. Twenty microlitres of trypsin were then added and the solution incubated overnight at 37°C. The samples were centrifuged at 14,100 \times g for 2 min at room temperature. The supernatant was recovered and dried. Samples were then fractionated by strong cation exchange liquid chromatography (SCX) and the cleaned sample was collected and dried. The cleaned SCX fraction was desalted as described in section 3.2.7 and LC MS/MS was performed as the protocol described in section 3.2.7.

5.2.2. Data analysis

The nanoLC-MS/MS data were submitted to Mascot for protein identification using the SwissProt database containing *Rattus* protein entries. Biotinylated lysine and amino terminus were considered as static modifications. Peptide ion scores above 35 were reported giving a probability of correct identification ($P < 0.05$)

Figure 53 is a schematic representation of the *in vivo* biotinylation steps in the rat model of AVM.

5.2.3. Results

Mass spectrometry detected a total of 135 proteins; 30 were annotated as membrane proteins. Table 32 presents selected membrane proteins, their scores and number of matched peptides using the Mascot search engine and presents all membrane proteins identified by LC-MS.

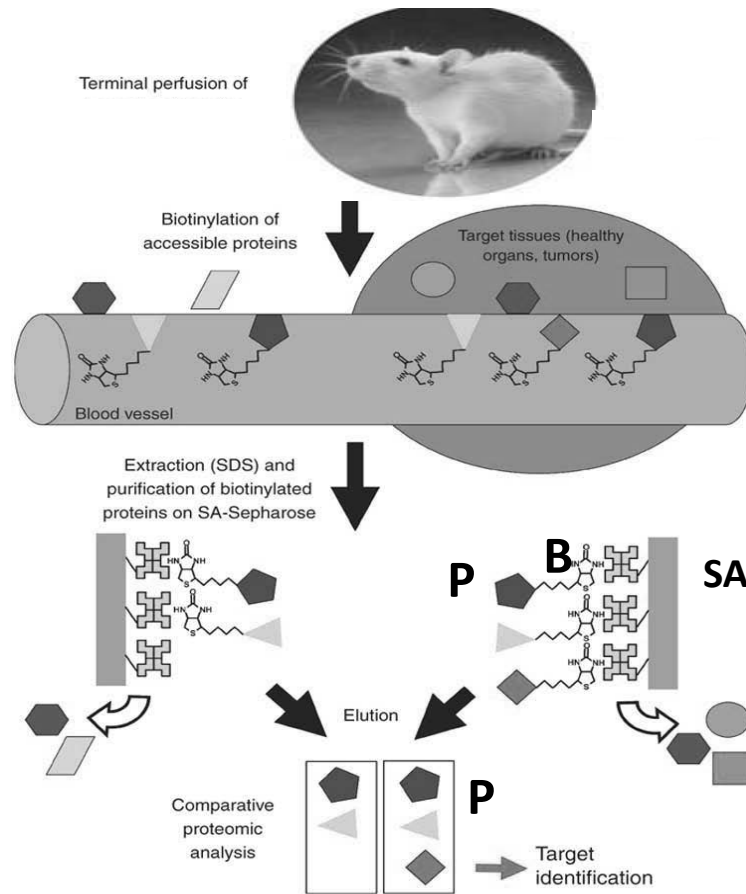


Figure 53. *In vivo* biotinylation perfusion steps in the rat model of AVM. The rat is perfused with biotin (proteins on the luminal surface will be biotinylated), AVF tissue is excised, membrane proteins are captured on streptavidin sepharose, proteomics analysing is then performed to identify the proteins. Un-bound proteins are washed away. P= protein; B= biotin; SA= streptavidin sepharose. (Modified from Ryback J et al 2005)

Table 32. Selected membrane proteins for the AVM rat model identified by LC-MS analysis using the Mascot search engine, their scores and number of matched peptides.

Protein name	Mascot Protein ion	Number of matched peptides
Epithelial cell adhesion molecule	68	2
Cadherin 13	76	1
Platelet glycoprotein	17	1
V-set domain-containing T-cell activation inhibitor	48	3
Complement C3	166	6
Sodium/potassium-transporting ATPase subunit alpha-	68	1
Serine protease inhibitor A3K	70	2
Angiotensin-converting enzyme	42	2
Lumican	55	1
Complement C4	238	7
Membrane primary amine oxidase	131	3
Integrin alpha 6	96	1
Mast cell protease	84	3
Biglycan	71	1
Integrin beta-1	87	5
Integrin alpha-1	40	2
Alpha-1-antiproteinase	156	3
Sodium/potassium-transporting ATPase	44	1
Serine protease inhibitor	137	3
Integrin beta-4	74	1
Lactadherin	65	1

Table 33. All membrane proteins in the rat model of AVM identified by LC-MS

Cell adhesion protein	Integrin beta-4	Platelet glycoprotein	Lactadherin
Cadherin-13	Epithelia cell adhesion molecule	Integrin alpha -1	Fibrinogen gamma chain
Glycerol-3-phosphate acyltransferase	Proton-coupled amino acid transporter 3	Sodium/potassium-transporting ATPase	Integrin beta-1
Sodium/potassium-transporting ATPase	Receptor-type tyrosine-protein phosphatase	Angiotensin-converting enzyme	Phosphoglycerate mutase 1
IGHM	Complement 3	Complement 4	KCF6
Integrin alpha-6	lumican	PCPT1	vetronectin
Potassium voltage-gated channel subfamily S-member	Vitamin D-binding protein	Membrane primary amine oxidase	Matrix-associated zinc metalloprotease Protein Postn

These data demonstrate the viability of derivatizing endothelial cell surface membrane proteins in the rat model of AVM, recovering them and determining their identity using mass spectrometry (Simonian M et al 2012; 2014).

Few haemoglobins and serum albumins were detected in the mass spec data above, this indicates that, rat's blood wasn't washed away completely with saline prior to perfusion with biotin (Figure 54). To obtain better results, further *in vivo* biotinylation perfusion optimization was performed on another eight rats, using different biotin concentrations, different perfusion time/rate, with increased amounts of saline.

(MATRIX) Mascot Search Results

```

User       : margaret
Email      :
Search title :
MS data file : margaret.mgf
Database    : SwissProt 2010x (519348 sequences; 183273162 residues)
Taxonomy    : Rattus (7552 sequences)
Timestamp   : 23 Dec 2010 at 00:50:16 GMT
Protein hits : PYC_RAT Pyruvate carboxylase, mitochondrial OS=Rattus norvegicus GN=
A1M_RAT Alpha-1-macroglobulin OS=Rattus norvegicus GN=A1m PE=1 SV=1
MUG1_RAT Murinoglobulin-1 OS=Rattus norvegicus GN=Mug1 PE=2 SV=1
ALBU_RAT Serum albumin OS=Rattus norvegicus GN=Alb PE=1 SV=2
ALI3_RAT Alpha-1-inhibitor 3 OS=Rattus norvegicus GN=Ali3 PE=1 SV=1
MCCA_RAT Methylcrotonoyl-CoA carboxylase subunit alpha, mitochondria
PCCA_RAT Propionyl-CoA carboxylase alpha chain, mitochondrial (Fragm
MUG2_RAT Murinoglobulin-2 OS=Rattus norvegicus GN=Mug2 PE=1 SV=1
PCCB_RAT Propionyl-CoA carboxylase beta chain, mitochondrial OS=Ratt
MYH4_RAT Myosin-4 OS=Rattus norvegicus GN=Myh4 PE=2 SV=1
CO3_RAT Complement C3 OS=Rattus norvegicus GN=C3 PE=1 SV=3
CO4_RAT Complement C4 OS=Rattus norvegicus GN=C4 PE=1 SV=3
COL1A1_RAT Collagen alpha-1(I) chain OS=Rattus norvegicus GN=Col1a1 PE
HBB1_RAT Hemoglobin subunit beta-1 OS=Rattus norvegicus GN=Hbb PE=1
A1AT_RAT Alpha-1-antiproteinase OS=Rattus norvegicus GN=Serpinal PE=
CBPA3_RAT Mast cell carboxypeptidase A (Fragment) OS=Rattus norvegicu
ITB1_RAT Integrin beta-1 OS=Rattus norvegicus GN=Itgb1 PE=2 SV=1
SPA3L_RAT Serine protease inhibitor A3L OS=Rattus norvegicus GN=Serp
AOC3_RAT Membrane primary amine oxidase OS=Rattus norvegicus GN=Aoc3
HBA_RAT Hemoglobin subunit alpha-1/2 OS=Rattus norvegicus GN=Hba1 P
CERU_RAT Ceruloplasmin OS=Rattus norvegicus GN=Cp PE=2 SV=3
MCCB_RAT Methylcrotonoyl-CoA carboxylase beta chain, mitochondrial O
HEMO_RAT Hemopexin OS=Rattus norvegicus GN=Hpx PE=1 SV=3
FIBB_RAT Fibrinogen beta chain OS=Rattus norvegicus GN=Fgb PE=1 SV=4
FETUA_RAT Alpha-2-HS-glycoprotein OS=Rattus norvegicus GN=Ahsg PE=1 S
IGG2A_RAT Ig gamma-2A chain C region OS=Rattus norvegicus GN=Ig-g2a P
GUAD_RAT Guanine deaminase OS=Rattus norvegicus GN=Gda PE=1 SV=1
TRFE_RAT Serotransferrin OS=Rattus norvegicus GN=Tf PE=1 SV=3
ACTA_RAT Actin, aortic smooth muscle OS=Rattus norvegicus GN=Acta2 P

```

Figure 54. Screen shot of Mascot search results of the rat model of AVM showing identified serum albumins and haemoglobins

5.3. Second *in vivo* biotinylation perfusion trial

Further optimization was carried out on the protocol described above to examine different parameters such as perfusion time/rate and biotin concentration. Mass spectrometry expression (MS^E) was then used for proteomics analysis for better membrane proteins identification

5.3.1. Materials and methods

5.3.1.1 Rats

Eight *Sprague-Dawley* male rats weighing from 310 – 493 g, were used for the second optimization trial. All rats were returned to the animal care facility post AVF creation and monitored as described earlier.

5.3.1.2 *In vivo* biotinylation perfusion

Six weeks after creating the AVF, the eight rats were perfused using the protocol described above with four different modifications (A, B, C and D) of biotin concentration and perfusion time/rates as shown in Table 34. All eight rats were perfused with 1 L of saline (NaCl) instead of 200 mL (used in the first *in vivo* biotinylation trial) to wash away blood, then every two rats were perfused with biotin using each of the 4 modifications A, B, C and D.

Table 34. The four modifications used for the second *in vivo* biotinylation trial in the rat model of AVM

Parameters	Protocols			
	A	B	C	D
Saline to wash away blood before biotin injection	1 L	1 L	1 L	1 L
Biotin concentration	1 mg/mL	2 mg/mL	1.5 mg/mL	1.5 mg/mL
Biotin solution injection flow rate	15 mL/min	30 mL/min	15 mL/min	30 mL/min
Waiting period after perfusing biotin solution	10 min	5 min	5 min	5 min
Tris-Hcl solution injection flow rate	15 mL/min	30 mL/min	15 mL/min	30 mL/min

5.3.1.3 Membrane protein extraction

A slightly modified protocol was used on the eight rats to fit with MS^E analysis. The vascular tissue samples were homogenized, using a Tissue Grinder (Wheaton) in 1 mL of lysis buffer (20 mM HEPES, 150 mM NaCl, 10 mM NaF, 1 mM Na-EDTA, 1mM Na-EGTA, pH 7.5, pH adjusted with NaOH, 0.1% TritonX v/v) + protease inhibitor (4 μ L per mL of HEPES buffer, Sigma P-2714). Samples were probe sonicated for 15 s, three times in ice with Branson Sonifier 450 (John Morris Scientific) and centrifuged in a pre-cooled rotor at $1,500 \times g$ for 15 min (4°C). Supernatants were collected and pellets were re-lysed with 0.5 mL of HEPES buffer (same as above steps). Supernatants were collected and pooled with previous supernatants. The final volume of supernatant was ~1.5 mL. Sodium Bicarbonate solution (0.1 M, pH 11) was added to pooled supernatants (up to 5 mL) and incubated for 1 h at 4°C on rocking platform. After incubation, samples were centrifuged at $100,000 \times g$ for 45 min (4°C) TLA110 rotor. Pellets were washed with 0.5 mL of 100% cold acetone twice and left to dry. Pellets were then dissolved with 200 μ L of 100 mM Amonium Bicarbonate containing 10 mM DTT (freshly prepared) in water bath sonication (FS30H, Fisher Scientific) for 20 min and then incubated for 1 h at 37°C to reduce the samples. To alkalize the samples, 5 μ L of 1 M idoacetamide stock was added to make a final concentration of 20 mM idoacetamide and

the samples were then incubated in the dark at room temperature for 30 min. Sample volumes were then brought up to 5 mL with 100 mM Ammonium Bicarbonate and centrifuged at $100,000 \times g$ for 1 hour (4°C). Pellets were dissolved with 400 μ L of 100 mM Ammonium Bicarbonate in water bath sonication then 600 μ L of methanol was added.

5.3.1.4 Capture of biotinylated proteins

Biotinylated proteins were captured on streptavidin sepharose (GE health care, USA) after washing of streptavidin sepharose three times with 500 μ L of buffer **A** containing (1% w/v NP40, 0.5% w/v SDS in PBS), then three times with 500 μ L PBS. Samples then were incubated with washed streptavidin sepharose for 2 h at room temperature with gentle rotation. Streptavidin sepharose was pelleted by centrifugation at $1600 \times g$ for 5 min. Unbound proteins were discarded by washing three times with 1 mL of 1% Triton-x (v/v), once with 400 μ L of 1% SDS (w/v) and five times with 1 mL of digestion buffer (0.25 mM ammonium bicarbonate). This is the same protocol used on bEnd.3 cells analysed with MS^E.

5.3.1.5 Tryptic digestion of biotinylated proteins and MS^E analysis

Streptavidin sepharose was re-suspended in 200 μ L of digestion buffer. Twenty microlitres of trypsin were then added and incubated overnight at 37 °C. The samples were centrifuged at $14,100 \times g$ for 2 min at room temperature and the supernatant was collected.

Chromatographic separation was achieved using Waters nanoACQUITY UPLC BEH C18 Column as described in section 4.2.2 and mass spectrometry analysis of tryptic peptide was performed utilizing Waters Xevo quadrupole time of flight (Q-TOF) mass spectrometer coupled directly to Waters nanoACQUITY UPLC system per the protocol described in section 4.2.2.

5.3.2. Data analysis

The LC MS and LC MS/MS data were processed using ProteinLynx Global Server (PLGS) version 2.5 (Waters Corporation). The protein identification was based on MS/MS peak lists that were generated by MS^E data independent collision-induced fragmentation using a *Rattus* database. Protein identification were accepted with greater than three fragment ions per peptide, seven fragment ions per protein and one unique peptide per protein identified. Modification parameters were carbamidomethyl cysteine, oxidized methionine and trypsin.

5.3.3. Results

The MS^E analysis of AVM rat model tissues detected a total of 159 proteins from protocol A, 64 proteins from protocol B, 82 proteins from protocol C and 147 proteins from protocol D. In total, 40 membrane proteins were detected, 25 were from protocol D, the remaining 15 were from protocols A, B and C combined. Table 35 present all membrane proteins identified by MS^E

Table 35. All membrane proteins identified by MS^E analysis in the rat model of AVM

Protein name	Uniprot accession #	Membrane protein classification	Protein name	Uniprot accession #	Membrane protein classification
Annexin A2	P07356	Extracellular matrix	GTPase	P20171	Lipid anchor
Annexin A1	P10107	=	Serine protease inhibitor	P27958	Single pass type 1
			Alpha 1 inhibitor3	P10824	Peripheral
Lumican	P51886	=	Annexin 5	P14668	Extracellular matrix
Collagen alpha 2	P081	=	Vesicle associated memb.prot.3	P63035	Single pass type IV
Collagen alpha 1	P02454	=		P26769	Multi pass
			Adenylyl cyclase associated p.		
Decorin	Q01129	=	Prolargin	Q9EQP5	=
Myelin protein P0	P06907	=	Biglycan	P47853	=
Ig gamma 2A chain	P01865	Single pass	Alpha 1 macroglobulin	P06238	=
ATP synthase subunit alpha	P10719	Peripheral		P57780	=
	Q03114	=	Alpha actinin 4 Band 3 anion transport protein	P23562	Multi pass
CDK5 regulatory subunit Prelamin	P48679	Inner nuclear	Lymphocyte transmembrane adapter	Q8BHB3	Transmembrane
Alpha-internexin	P23565	=	Acyl coenzyme A synthetase	Q6SKG1	Matrix
Cavolin	P41350	Peripheral	Gamma enolase	P07323	Extracellular matrix
Vinculin	P85972	=	IST1	Q568Z6	=
Multivesicular body subunit 12A	Q6P777	=	Creatine kinase B type	P07335	=
RabGDP	P50399	=	RAC gamma serine threonine kinase	P47196	plasma
CD99 antigen like protein	Q8R1R5	Single pass type 1	T complex protein	P42346	Peripheral

Since protocol D identified the largest number of membrane proteins, that protocol was used for the *in vivo* biotinylation and irradiation experiments of the rat model of AVM presented in Chapter 6.

Chapter 6. *In vivo* biotinylation and response of endothelial cells to irradiation in the rat model of AVM

6.1. Introduction

After successful labelling of the membrane proteins in the rat model of AVM with *in vivo* biotinylation methodology, the response of membrane proteins to irradiation in the rat model of AVM was studied. Based on the iTRAQ and MS^E data of the murine cell cultures (bEnd.3), the most extensive membrane changes in response to irradiation were observed at 24 h post irradiation. Therefore the membrane protein changes in the rat model of AVM were studied at 24 h post irradiation utilizing proteomics techniques. In total six rats were used for this experiment, three irradiated and three controls, larger numbers of rats would have been favourable, but these experiments are demanding and require resourcing, nevertheless six rats are sufficient to calculate means and variance and apply statistical tests to identify changed proteins.

6.2. Material and Methods

6.2.1 Rats

An arteriovenous fistula (AVF) was created in six *Sprague-Dawley* male rats weighing from 360 – 411 g, according to the protocol of Yassari R et al 2004. Rats were returned to the animal care facility after the operation and monitored daily for the first week then weekly for another five weeks, allowing the fistula to reach maturity (Figure 55).

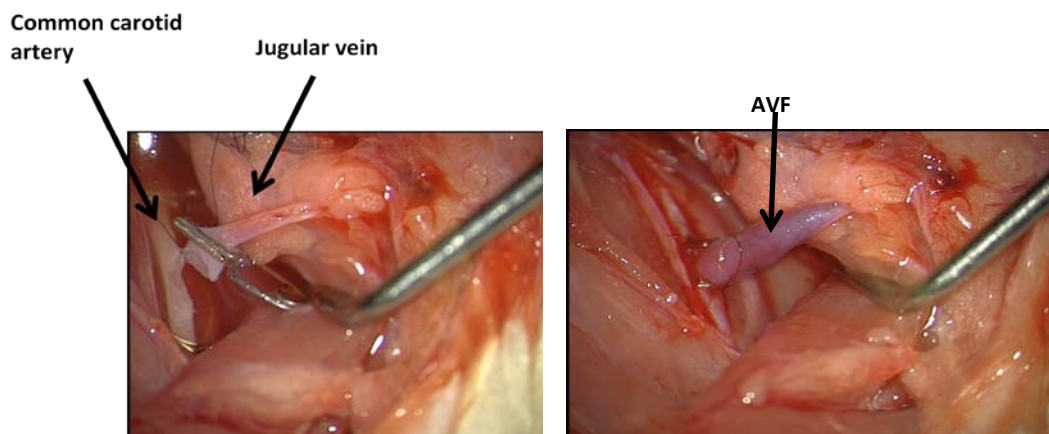


Figure 55. Anastomosis was performed by connecting the Jugular vein to the common carotid artery (Left) to create the arteriovenous fistula (AVF) (Right). The surgeries were performed by members of the neurosurgery department at the Australian School of Advanced Medicine

6.2.2 Gamma knife surgery

After six weeks, three rats were irradiated using the Leksell Gamma Knife Perfexion (Elekta) at Macquarie University Hospital (Sydney, Australia), by delivering 20 Gy to the arteriovenous fistula (AFV) tissues and keeping the dose to the trachea to less than 10 Gy, per the protocol described by Kashba, S et al 2015. Briefly, an axial full-body CT scanning with 3D reconstruction was performed for AVF localization. The skin surface was defined, the nidus was identified, and the model AVM nidus was treated stereotactically with a 20 Gy dose of radiation to the 50% isodose line in a single fraction, ensuring the 10 Gy isodose line did not touch or across the esophagus or trachea (Kashba, S et al 2015). The remaining three non-irradiated rats were used as controls.

6.2.3 In vivo biotinylation perfusion

All six rats were narcotized and prepared for perfusion as described in section 5.2.1. A Gilson Minipuls 3 perfusion pump attached to a tube and needle was used to perfuse the rats with 1 mL of saline (NaCl) with a flow rate of 50 mL/min to wash away the blood, immediately followed by 100 mL of freshly prepared biotinylation solution [1.5 mg/mL of Sulfo-NHS-LC-Biotin in pre-warmed PBS at 37°C + 10% Dextran 40] by pressing the syringe plug with a flow rate of 25 mL/min while monitoring the pressure and keeping it constant at ~100 mm Hg. After 5 min of perfusing the biotinylation solution, the rats were injected with 100 mL of (50 mM Tris-Hcl in PBS + 10% Dextran 40) with a flow rate of 30 mL/min to wash out excessive biotinylation reagent, then were perfused with 200 mL saline at 30 mL/min to wash away the Dextran. The fistula tissues were then excised and the surrounding fat and muscle tissue were removed. The vascular tissues were placed in a 1 mL Eppendorf tube and

transferred to a -80° C freezer immediately. This protocol was modified from (Roesli, C et al 2006 and Simonian M et al 2012), after the *in vivo* biotinylation protocol optimizations described in the previous chapter.

6.2.4 Membrane protein extraction

The vascular tissue samples were homogenized using a tissue grinder with pestle (Wheaton) in 1 mL of lysis buffer (20 mM HEPES, 150 mM NaCl, 10 mM NaF, 1 mM Na-EDTA, 1 mM Na-EGTA, pH 7.5, pH adjusted with NaOH, 0.1% Triton-X v/v) + protease inhibitor (4 μ L per mL of HEPES buffer, Sigma P-2714). Samples were probe sonicated three times for 15 s, using the Branson Sonifier 450 (John Morris Scientific) and centrifuged in a pre-cooled rotor at $1,500 \times g$ for 15 min at 4°C. Supernatants were collected and pellets were re-lysed with 0.5 mL of HEPES buffer (same as above steps). Supernatants were collected and pooled with previous supernatants. The final volume of supernatants was ~1.5 mL. Sodium Bicarbonate solution (0.1 M, pH 11) was added to pooled supernatants (up to 5 mL) and incubated for 1 h at 4°C on a rocking platform. After incubation, samples were centrifuged at $100,000 \times g$ for 45 minutes at 4°C. Pellets were washed with 0.5 mL of 100% cold acetone twice and left to dry. Pellets were then dissolved with 200 μ L of 100 mM Amonium Bicarbonate containing 10 mM DTT (freshly prepared) in water bath sonication (FS30H, Fisher Scientific) for 20 min and then incubated for 1 h at 37°C to reduce the samples. To alkalize the samples, 5 μ L of 1 M idoacetamide stock was added to make a final concentration of 20 mM idoacetamide and the samples were incubated in the dark at room temperature for 30 min. Sample volumes were then brought up to 5 mL with 100 mM Amonium Bicarbonate and centrifuged at $100,000 \times g$ for 1 h at 4°C. Pellets were dissolved with 400 μ L of 100 mM Amonium Bicarbonate in water bath sonication then 600 μ L of methanol was added.

6.2.5 Capture of biotinylated proteins

Biotinylated proteins were captured on streptavidin sepharose (GE health care, USA). Five hundred microlitres of streptavidin sepharose were washed three times with buffer **A** containing (1% w/v NP40, 0.5% w/v SDS in PBS), then three times with 500 μ L PBS. Samples then were incubated with washed streptavidin sepharose for 2 h at room temperature with gentle rotation. Streptavidin sepharose was pelleted by centrifugation at $1600 \times g$ for 5 min. Unbound proteins were eliminated by washing three times with 1mL of 1% Triton-x (v/v), once with 400 μ L of 1% SDS (w/v) and five times with 1mL of digestion buffer 0.25 mM ammonium bicarbonate.

6.2.6 Tryptic digestion of biotinylated proteins and MS^E analysis

Streptavidin sepharose was re-suspended in 200 μ L of digestion buffer. Twenty microlitres of trypsin were then added and incubated overnight at 37 °C. The samples were centrifuged at $14,100 \times g$ for 2 min at room temperature and the supernatant was collected.

Chromatographic separation was achieved using Waters UPLC column as described in section 4.2.2. Mass spectrometry analysis of tryptic peptide was performed utilizing Waters Xevo (Q-TOF) mass spectrometer and Waters nanoACQUITY UPLC system as described in section 4.2.2. All samples were injected into the mass spectrometer in triplicates.

6.3. Data analysis

The LC MS and LC MS/MS data were processed using ProteinLynx Global Server (PLGS) version 2.5 (Waters Corporation). The protein identification was based on MS/MS peak lists that were generated by MS^E data independent collision-induced fragmentation using a *Rattus* database. Protein identification was accepted with greater than three fragment ions per peptide, seven fragment ions per protein and one peptide per protein identified.

Carbamidomethyl cystein was set as a fixed modification while oxidized methionine was set as variable modification.

6.4. Results

Six weeks after creating the fistulae, the model AVM nidus was irradiated with 15 Gy using the Gamma knife. *In vivo* biotinylation perfusion was performed 24 h after irradiation; AVF tissues were excised, membrane proteins were harvested then analysed by mass spectrometry expression (MS^E). To determine the effect of irradiation on AVF endothelium, and to study the upregulated membrane proteins in response to irradiation, 18 mass spectrometry runs were analysed from three irradiated rats and three control rats. Triplicate samples were run for each rat. The proteomics data detected a total of 74 proteins in the irradiated rats, 20 of them were annotated as membrane proteins. A total of 104 proteins were detected in control rats, 37 of them were annotated as membrane proteins.

Twelve membrane proteins shared their presence in both irradiated and control rats (Table 36). Average concentrations (fmol) and average ratios of expression (irradiated: control) were calculated to determine the changes in membrane protein level following irradiation.

Alpha-1 inhibitor protein expression increased in irradiated rats by (2.3) fold, however this increase wasn't significant ($p = 0.164$). Annexin-A2 and lumican proteins showed significant decrease in irradiated rats by (1.0) and (1.5) fold respectively with ($p = 0.025$) and ($p = 0.041$). The remaining 9 membrane proteins didn't show a significant increase or decrease between irradiated and control rats. The other eight membrane proteins presented in Table 37, such as profiling-1, ESAM-1, potassium voltage gated channel, were detected in irradiated rats only and not in control rats; those proteins are of importance, because of their unique detection following irradiation.

Table 36. Membrane proteins shared between irradiated (R) and control (C) rats, their sequence accession number, molecular weight, average concentration on column (fmol) and average concentration ratios (irradiated : control); n=9.

Protein name	Accession #	MW	Ave (fmol) in R	SD	Ave (fmol) in C	SD	Ave (R:C)	(p)
Alpha 1 macroglobulin	Q63041	168494.1	4.2	1.67	5.8	0.29	0.8	0.222
Biglycan	P47853	42105.52	1.5		3.0	0.26	0.5	
Annexin A1	P07150	39171.71	1.4	0.83	2.1	0.13	0.7	0.288
Annexin A2	Q07936	38963.45	5	0.07	6.0	0.60	0.8	0.025
Lumican	P51886	38678.25	2.6	0.30	4.1	0.18	0.6	0.041
GTPase	Q8K3L6	37665.02	5.2		18.9		0.3	
Prolargin	Q9EQP5	43521.63	3.5	0.62	3.9	2.28	0.9	0.727
Serine protease inhibitor	P05544	46448.34	1.1		8.1		0.1	
Alpha1 inhibitor3	P14046	165142.2	6.2	0.32	2.7		2.3	0.164
Collagen alpha 1	P02454	138980.1	7.4	0.40	7.3	0.05	1.0	0.618
Collagen alpha 2	P02466	130077.4	2.1		7.8	0.21	0.3	
Decorin	Q01129	40147.32	1.8	1.15	3.1	0.06	0.6	0.205

The blank cells in SD and *P* columns indicates that corresponding membrane protein was present in only 1 out of the 9 MS runs, hence no values have been calculated.

Table 37. Membrane proteins present in irradiated rats (R) and not in control rats (C), their accession number, molecular weight and average concentration on column (fmol) in irradiated and control rats

Protein name	Accession #	MW	Ave (fmol) R	Ave (fmol) C
Profilin 1	P62963	15128.34	0.6	ND
Endothelial cell specific molecule-1	P97682	21101.27	0.6	ND
Bone morphogenetic protein 3	P49002	53416.56	7.9	ND
Potassium voltage gated channel subfamily A member 5	P19024	67237.32	3.4	ND
Myelin protein	P06907	27741.78	7.4	ND
Chloride intracellular channel protein 2	Q5M883	28446.33	0.6	ND
Vomeromodulin	Q63751	10890.35	7.2	ND
Prothyroliberin	P01150	29454.97	5.3	ND

ND = not detected

A list of all membrane proteins that were present in irradiated rats are presented in (Table38), and the membrane proteins that were present in the control rats are presented in (Table 39).

Table 38. Membrane proteins identified by LC-MS/MS in irradiated rats.

Protein name	Uniprot accession #	Membrane protein classification
Profilin-1	P62962	Cytoskeleton
Annexin A2	P07356	Extracellular matrix
Decorin	Q01129	=
Lumican	P51886	=
Biglycan	P47853	=
Annexin A1	P10107	=
Collagen alpha 1	P02454	=
Prolargin	Q9EQP5	=
Collagen alpha 2	P08123	=
Alpha 1 macroglobulin	P06238	=
Prothyroliberin	P01150	=
GTPase	P20171	Lipid anchor
Alpha 1 inhibitor 3	P04585	=
Mylein	P02688	Peripheral
Potassium voltage gated channel	P15387	Multi pass
Serine protease inhibitor	P27958	Single pass type 1
Endothelial cell specific molecule 1	P35918	=
Chloride intracellular channel protein 2	O35433	Multi pass
Vomeromodulin	Q63751	Extracellular matrix
Bone morphogenetic protein 3	Q06826	=

Table 39. Membrane proteins identified by LCMS/MS in control rats.

Protein name	Uniprot accession #	Membrane protein classification	Protein name	Uniprot accession #	Membrane protein classification
Annexin A2	P07356	Extracellular matrix	GTPase	P20171	Lipid anchor
Annexin A1	P10107	=	Serine protease inhibitor	P27958	Single pass type 1
Collagen alpha 1	P02454	=	Alpha 1 inhibitor3	P10824	Peripheral
Lumican	P51886	=	Annexin 5	P14668	Extracellular matrix
Collagen alpha 2	P08123	=	Vesicle associated memb.prot.3	P63035	Single pass type IV
Neuromodulin	Q63751	=	Fibroblast growth factor 16	P13109	Extracellular matrix
Decorin	Q01129	=	Prolargin	Q9EQP5	=
Regulating synaptic membrane exocytosis protein	Q9JIR4	Peripheral	Biglycan	P47853	=
Ig gamma 2A chain	P01865	Single pass	Alpha 1 macroglobulin	P06238	=
ATP synthase subunit alpha	P10719	Peripheral	Alpha actinin 4	P57780	=
Serotransferrin	P12346	Basement	Jouberin	Q6DTM3	=
Heat shock 75	P48721	Extracellular	Beta defensin 15	Q322H6	=
PKHD domain containing transmembrane protein C1	Q6T3A5	Transmembrane	Plasma kallikrein	P14272	=

Non membrane protein expression also differed between irradiated and control rats. Actins, myosin and tubulin were highly expressed in irradiated rats; while vimentin and fibroblast growth factor 16 expression were detected in control rats only (Supplementary Table 3 and 4).

6.5. Discussion

This study aimed to identify membrane proteins in a rat model of AVM subjected to irradiation as these proteins could have utility for molecular targeting. Previous studies have shown different expression patterns of endothelial proteins in response to irradiation. This may be due to the fact that endothelial cells respond differently to irradiation at different doses; in low doses they mainly decrease expression (Rubin D 1997), which may be due to the DNA double strand breakage (Rombouts C et al 2013). The total number of proteins detected by mass spectrometry analysis in the control rats was higher than in irradiated rats. This was expected since irradiation at doses 15 – 20 Gy may cause some cell death while doses higher than 100 Gy cause cell hypertrophy (Rosen and Goldberg 1988). Smooth muscle proteins (actin and myosin) as well as tubulin expression increased in irradiated rats. This observation is in accordance with previous data obtained from human cerebral endothelial cultures where it was suggested that radiosurgery by Gamma knife induces transformation of fibroblasts into contractile cells containing actin and myosin in AVMs similar to myofibroblasts that may contribute to the obliteration of AVMs after radiosurgery (Major, O et al 2002; Szeifert T et al 2001). In this study fibroblast growth factor 16 was detected in control rats and not in irradiated tissue; this finding supports the theory of transformation of fibroblasts into contractile cells in irradiated rats. Furthermore, in a study by Sekis I et al, 2009, irradiation did not up-regulate the vascular endothelial growth factor in mastocytoma cell lines. All of these observations are in agreement with the *in vitro* study of murine endothelial cultures post irradiation as described in chapter 4, except that the total number of membrane proteins detected in irradiated samples *in vitro* was higher than in the *in vivo* experiment. This may be due to the fact that endothelial cells are more resistant to irradiation *in vivo* than *in vitro* because of the protection provided by the matrix surrounding vessels (Rubin D, 1997). Table 36 indicates 12 membrane proteins that were present in irradiated and control rats. Alpha-1 inhibitor protein expression increased in irradiated rats by (2.3) fold, however this

increase wasn't significant ($p = 0.164$). The remaining proteins didn't show a significant increase. On the contrary, two of them, annexin-A2 and lumican showed significant decreases. The eight membrane proteins that were present mainly in irradiated rats (Table 37) are of importance in this study due to their significant upregulation. Profilin-1 is actin binding protein; hence its increased expression is expected due to increased expression of actin in irradiated rats. Profilin-1 belongs to the profilin family, increases the ADP-to-ATP exchange on G-actin, and prevents the polymerization of actin at high concentrations, whereas at low concentrations it enhances it (Kwiatkowski, J. et al, 1988; Das T et al 2010). Profilin-1 has been regarded as a tumour-suppressor molecule for breast cancer, upregulation of profilin-1 after irradiation facilitated apoptosis in pancreatic cancer cells (Das T et al 2010; Cheng H et al 2013).

Potassium voltage gated channel protein is another membrane protein that was upregulated significantly in irradiated rats'. This protein is an ion channel transport protein and membrane potential that facilitates the flow of potassium ions down an electrochemical gradient (Zhang Y et al, 2003). In the brain the greatest density occurs in the cerebral cortex. Previous studies showed increased expression of this protein in response to irradiation (Zhang Y et al, 2003; De Costa et al, 2002; Purdo and Stuhmer, 2014).

Potassium channels are commonly expressed in tumour cells and have been a target for many drugs. Different agents have been used to target potassium channels in animal tumour models and in clinical trials; they have also been used for the treatment of other diseases such as type 2 diabetes and hypertension, with minimal side effects (Gomez-Varela D. et al 2007; Pillozzi S. et al. 2011; Leanza L et al. 2012). The interference with potassium channels offered a new therapeutic opportunity for cancer treatment because this channel is sometimes expressed in tumour cells and sometimes the abnormally expressed form is different from the physiological one, making it possible to minimise the potential side effects of the drug by channel targeting in ordinary tissues (Chantome A. et al 2013; Purdo and Stuhmer, 2014).

Future work in the laboratory will focus on studying the differential expression of potassium voltage gated channels in AVM vessels and normal vessels. The fact that this protein is extracellularly accessible may simplify targeting and drug design. This protein will be investigated as a potential target for ligand directed therapy for brain AVMs.

Chloride intracellular channel protein 2 is another voltage gated ion channel transmembrane protein. Chloride channel proteins have also been used as molecular targets for cancer therapy (Kwang, S et al 20015). Previous studies on human lung cancer cells and laryngeal cancer cells have shown increased expression of chloride intracellular channel proteins 4 and 1 in response to irradiation, suggesting these proteins as important and novel targets for anti-cancer therapy and radiotherapy for cancer cells (Roboz J, 2001; Kim S et al, 2010).

Therefore, future work will include extensive study of chloride intracellular channel protein 2 as a potential target for molecular therapy for brain AVMs.

Endothelial cell specific molecule -1 (ESM-1) is another upregulated membrane protein expressed in the irradiated rats. ESM-1 is endothelial cell adhesion molecule that is also expressed on platelets. In 2009, Stalker J et al, showed that after platelet activation, ESM-1 was localized to the junctions between adjacent platelets, suggesting a role for this protein in thrombus formation. Exposed tissue factor that was found in some irradiated blood vessels lacking the endothelial lining suggested one mechanism in which thrombosis may occur post radiosurgery, however no significant differences in expression have been shown after irradiation (Storer et al 2007; Tu J et al 2005; Karunanayaka et al 2008). Further investigation of the ESM-1 role in thrombosis in AVM vessels may provide a potential molecular target for vascular therapy.

Chapter 7. General Discussion

7. General discussion

Current treatment methods for brain AVMs are effective and safe for small AVMs, yet one third of large AVMs cannot be effectively treated without high risk. Therefore, a new, safe treatment is needed to target high grade AVMs. Introducing new methods in radiosurgery such as biologically enhancing the thrombotic response to radiosurgery has the potential to improve treatment for large and small AVMs. Endothelial cell molecules on the vascular lumen offer a promising target for this intervention because of their ease of accessibility. They may also meet the criteria of vascular targeting agents, meaning, having a high affinity to AVM vessels and a low affinity to normal vessels.

The aim of this thesis research was to identify irradiation-induced protein targets in AVM endothelium that discriminate these vessels from normal vessels. Identifying those proteins would be a step towards developing a ligand-directed vascular therapy that promotes rapid thrombosis in AVM vessels after radiosurgery. Therefore, capturing and identifying the membrane proteins that are expressed on the surface of endothelial cells post irradiation was a crucial element of the research. This thesis study was the first to employ proteomics techniques to identify and quantify the proteins expressed on AVM endothelium compared to normal vessels; hence *in vitro* and *in vivo* biotinylation methods were developed to label and capture membrane proteins in the murine endothelial cell cultures (bEnd3) and the animal model of AVM (Simonian, M et al 2012; 2014). After the successful development of protein labelling, irradiation experiments were performed on both bEnd3 cell cultures and the rat model of AVM to examine the differentially expressed membrane proteins between irradiated and control samples. Proteins were then identified by various mass spectrometry techniques including iTRAQ-MS and MS^E, and membrane protein expressions were validated with immunocytochemistry. The proteins that were upregulated in both the cell cultures and the rat model post irradiation compare to the controls will be investigated as potential targets for the AVM ligand directed molecular therapy, because those are the discriminating proteins that are

available abundantly on the surface of endothelial cells of the irradiated AVM vessels, and are accessible for targeting via ligands to create thrombosis in those vessels.

The proteomics investigation of bEnd3 cell cultures revealed a large number of membrane proteins that were differentially expressed between irradiated and non-irradiated cells. Many of those were upregulated in the irradiated cells especially at 24 hours. The most significant were PECAM-1, cadherin 5, PDI, integrin alpha5, integrin alpha6, integrin beta1, CD109, EPCR and multimerin2. The proteomics data of the rat model of AVM, again revealed a large number of differentially expressed membrane proteins and, again mostly at 24 hours post irradiation, such as profilin1, potassium voltage gated channel protein, chloride intracellular channel protein 2 and ESAM-1. Most of the membrane proteins identified post irradiation in the cell cultures and the rat model of AVM play an important part in thrombosis, or mediate thrombosis, specifically PECAM-1, ESAM-1, PDI, cadherin5 and integrins. These findings of an increased presence of pro-thrombotic molecules, post irradiation, could potentially enhance the thrombosis process in AVM vessels. Further investigation of the role of these molecules in thrombosis is needed to promote a better understanding of the mechanism of AVM occlusion post radiosurgery, with the promise of identifying new targets for vascular therapy.

The proteomics data also revealed a small number of non-membrane proteins that were upregulated in irradiated samples, such as myosin, plectin, vimentin, lamin, actin cytoplasmic 2 and filamin B. The presences of these cytoplasmic proteins on the surface of irradiated samples are intriguing. Although they do not normally play a direct role in thrombosis, they could potentially be targeted with thrombotic agents, via ligands, to induce thrombosis in AVM vessels. Plectin and filamin B proteins are high in molecular weight; they connect the cytoskeleton to the cell membrane (Svitkina, M 1996; Doherty, J 2008). Actin and myosin are very abundant cytoplasmic proteins, play a role in platelet aggregation (Lefebvre, P et al 1993; Cohen, I et al 1976).

In addition, a 2007 study by Dorota G et al, showed that irradiation of endothelial cells induced rapid actin stress fiber formation and reconstruction of cadherin-5 in microvascular. The increased expression of all of these cytoplasmic proteins on the surface may be the result of induced irradiation, or may be due to the fact that abundant and high molecular weight proteins are readily captured and identified by routine mass spectrometry techniques. Regardless, they could potentially be targeted with thrombotic agents for vascular therapies.

The uses of animal models were necessary to better understand the hemodynamic, molecular biology and physiology of AVM vessels *in vivo*. While there are differences in endothelial cell morphology and protein expression between the *in vitro* cell cultures and *in vivo* animal model experiments, mutually expressed proteins exist, especially mutually expressed membrane proteins, presented in (Table 40). This consistency is important, and will be considered, along with the membrane proteins obtained from *in vitro* future studies of human brain AVM tissues resected during patient surgeries, in candidate selection for the culminating clinical trials.

Not only is it difficult to obtain primary cell cultures from human brain AVM tissues for analysis and comparison with the animal model and the cell cultures, but the actual differences between human brain AVMs and the animal model of AVM could potentially affect the protein expression between the two. The feeding vessel in the animal model is the external jugular vein, while in human AVM the feeding vessels are intracranial arteries; also, the human AVM nidus is located within the brain parenchyma, while the animal model nidus is located in the neck soft tissues (Tu, J et al 2010; Crawford, M et al 1986). The AVM tissue in the animal model is harvested after six weeks of creating the fistula, while human brain AVM tissues are probably present for decades. This may be considered an obstacle in identifying mutually expressed proteins. Still, employing quantitative proteomic analysis on human tissue/cell cultures post irradiation and comparing the data with those obtained from

bEnd3 cells and the animal model of AVM may further provide target proteins for the ligand directed vascular treatment for brain AVMs.

The chosen dose for the irradiation experiments in this research was 20 Gy and 25 Gy, because the current dose used for most AVM radiosurgery is between 20 – 25 Gy. Doses lower than 23 Gy have been shown to be less effective in radiosurgery, and higher than 25Gy causes more complications associated with irradiation (Flickinger, C et al 2013; Friedman, A et al 2003). Future work will investigate the effect of lower irradiation doses on membrane protein expression over time, to determine the lowest effective dose that can be used for radiosurgery, since lower doses reduce complications related to irradiation exposure and ultimately are safer.

In overall, the total number of proteins detected by mass spectrometry analysis in the control samples in both cell cultures and rats' was higher than in irradiated samples. This is expected since previous studies indicated that irradiation of endothelial cells at doses 15 – 20 Gy may cause some cell death while doses higher than 100 Gy cause cell hypertrophy (Rosen and Goldberg 1986). The number of membrane proteins detected in irradiated samples *in vitro* was also higher than in the *in vivo* experiments; this may be due to the fact that endothelial cells are more resistant to irradiation *in vivo* than *in vitro* because of the protection from irradiation that is provided by the matrix surrounding the vessels (Rubin, D. 1997).

The major challenge of this research was sample preparation for mass spectrometry. Sample preparation is the key to any successful proteomics analysis. However, isolating membrane proteins for proteomics analysis is a difficult and challenging task because of their association with the lipid bilayer and their low abundances. They typically represent 10 % of the total protein in the cell. Biotinylation reagents were used to label membrane proteins because they are water soluble and they do not penetrate the cell membrane as long as the cell remains intact (Barat, B et al 2007; Zhang L et al 1999). Numerous *in vitro* and *in vivo* biotinylation optimizations were performed to determine the optimal biotin concentration and incubation

time needed for successful labelling of the membrane proteins in the cell cultures and the animal model of AVM. The current optimal *in vitro* and *in vivo* biotinylation conditions for AVM systems are described at sections 4.4.1.4 and 6.2.3 respectively. This may be further improved by using a magnetic streptavidin beads from ThermoFisher to capture biotinylated proteins, instead of the gel based beads that was used in this research (Hewett PW 2016), or by the use of biotinylated concanavalin A (ConA) with streptavidine magnetic beads. ConA is a lectin used for binding glycosylated membrane proteins, they bind to a specific sequence of sugar functional group and can be used to affinity purify plasma membrane proteins that contain those specific sugar functional groups from cell lysates (Lee YC et al 2008).

Enzymatic biotinylation with *E. coli* biotin ligase (BirA) with the AviTag technology is an alternative method that can be used in the future to label membrane proteins *in vitro* or *in vivo*. BirA is extremely specific in covalently attaching biotin to the 15 amino acid of the recombinant protein bearing the AviTag peptide or (Acceptor Peptide, AP), giving a high yield homogenous product. AviTag are added genetically at the N-terminus, C-terminus or at the exposed loops of target protein (Fairhead, M et al 2015; Howarth, M et al 2005).

BioID for proximity-dependent biotin identification is another labelling method that has been developed in 2012 by Roux KJ et al, to screen protein interactions in living mammalian cells. The *E. coli* biotin enzyme ligase is fused to target protein in cells, where it biotinylates proximal endogenous proteins. Biotinylated proteins are then captured and analysed by mass spectrometry (Roux KJ et al 2012; Kyle J et al 2013). Although this technique would be useful for capturing intracellular proteins, but not specifically surface proteins, as biotin ligase enzyme would need to be in proximity to the target cell surface proteins to tag the specific protein, and to express biotin ligase itself on the surface is not likely based on current literature. Therefore this method may not be beneficial for this thesis project in the future since our proteins of interest are membrane proteins.

The research reported here is the first to use a combination of labelled and label-free quantitative mass spectrometric techniques, such as iTRAQ-MS and MS^E, to identify and quantify potential protein targets for the AVM molecular therapy. Both these labelled and label-free methods combine protein identification and quantitation in one step. However, each method has its advantages and limitations. For experiments that require the comparison of numerous samples, iTRAQ multiplex analysis allows up to eight samples to be quantitatively compared within an experiment. Combining multiple samples in one run reduces instrument time for analysis. The iTRAQ reagents react with primary amines of amino-termini or lysine residues and hence label most peptides and proteins in the cells. During collision induced dissociation (CID), the relative intensities of iTRAQ reporter ions are used for protein quantitation (Trinh H et al 2013). However there is a continuing discussion about the accuracy of the deduced protein quantitations, especially when sample mixtures are highly complex (Chong, K et al 2006). iTRAQ normally reveal fold changes of less than two orders of magnitude compared to other methods, such as microarrays, which can be utilized for expression profiling over three orders of magnitude. This may be recognized as a limitation of the iTRAQ labelling method for quantitative proteomics (Trinh, H et al 2013; Ow, Y et al 2009).

MS^E is a relatively new method for absolute quantification and identification of proteins from MS data of tryptic peptides without requiring the use of any labelling methods (Jeffery, C et al 2006). The MS^E instruments abandon the selection of a precursor ion for individual fragmentation and fragment everything; as a result the exact mass precursor and fragment ion spectra for every detectable component in the samples are identified and quantified in a single analysis (Waters Corporation). The advantages of this technique are: improved sequence and proteome coverage, quantitative accuracy, and lower false positive rates. These advantages are most dramatic for low abundant proteins such as membrane proteins. However, deconvoluting the MS^E data to yield protein identifications and quantification data could be

complicated for very complex mixture (such as cell lysates and tissues) compared to iTRAQ. It has also been discussed that the ProteinLynx Global Server (PLGS) software, provided by Waters Corporation for their MS^E data analysis, overestimates the precision of its ratios in the calculation of the probability of up regulation. (Prieto, G et al 2012).

Although both these proteomics techniques, (iTAQ-MS and MS^E) proved to be effective in identifying protein targets in response to irradiation, a new mass spectrometry based proteomics technique has recently been developed that quantifies almost all peptides and proteins in a sample from a single analysis. This technique is called SWATH; it was developed in the Ruedi Abersold laboratory in 2012 in collaboration with AB SCIEX (life science analytical technology). SWATH uses a data-independent MS-MS acquisition to produce high specificity fragment ion maps to identify and quantify proteins of interest using a targeted data analysis system (Gillet, LC et al 2012). This method provides the speed, quantitative accuracy, specificity, sensitivity and high reproducibility to generate quantitative proteome data (AB SCIEX; Gillet, LC et al 2012). It will be interesting to use this technology in the future to identify further protein targets in response to irradiation.

Another quantitative labelling method that may be interesting to apply in the future is the dimethyl multiplex peptide stable isotope labelling method that was developed in 2009 by Boersema, P et al. In this method, all primary amines (the N terminus and the side chain of lysine residues) in a peptide mixture are converted to dimethylamines. The labelled samples are then mixed and analyzed by LC/MS. The mass difference of the dimethyl labels is used to compare the peptide quantity across all samples. The advantages of this labelling method over others, besides allowing the comparison of multiple samples in a single experiment, is that it uses inexpensive reagents and is applicable to almost any sample (Boersema, P et al 2009).

In conclusion, cell surface protein biotinylation and (iTAQ-MS and MS^E) successfully identified membrane proteins from endothelial cell cultures and rats' model of AVM in response to irradiation. The upregulated membrane proteins identified from this thesis novel

research are currently being investigated as potential targets for the ligand-directed molecular targeting trials in the rat model of AVM. Future study will further include irradiation-induced changes in human primary endothelial cell cultures from resected AVM tissues, using proteomic analysis. Candidate proteins from the animal and human studies will then be investigated for use in ligand-directed human vascular targeting trials to promote rapid thrombosis in AVM vessels after radiosurgery. This is especially important for patients who currently have to wait up to three years after undergoing radiosurgery, for their AVM to be occluded completely, while they remain at risk of haemorrhage.

The Successful development of a radiosurgery-vascular targeting therapy could further have application for treatment of other brain lesions such as tumors and cavernomas.

Table 40. Membrane proteins shared their presence between murine endothelial cell cultures and the rat model of AVM

Annexin A2	Alpha enolase	Vesicle associated membrane protein	Lumican
Fibroblast growth factor 16	Gamma enolase	Prelamin	Decorin
Transmembrane protein	Creatine kinase B type	ATP synthases subunit beta	Profilin 1
ATP synthase subunit beta	Rab GDP dissociation inhibitor	Caveolin 1	Myelin
Biglycan	Heat shock cognate 71	Annexin A1	Serine protease inhibitor
Prolargin	PDI	GTPase IMAP family member 5	Heat shock protein 75

References

- Akimoto T, Mitsuhashi N, Saito Y, Ebara T, Niibe H. (1998). Effect of radiation on the expression of E-cadherin and α -catenin and invasive capacity in human lung cancer cell line *in vitro*. *International Journal of Radiation Oncology, Biology, Physics*. 41 (5) :1171–1176.
- Altin, J.G. (1995). A One-Step Procedure for Biotinylation and Chemical Cross-linking of Lymphocyte Surface and Intracellular Membrane Associated Molecules. *Anal Biochem* 224:382–9.
- Arnold T, Linke D. (2008). The use of detergents to purify membrane proteins. *Current protocol Protein Sci*. Chapter 4: Unit 4.8.1-4.8.30.
- Ball H, Roulhac L, Alzate O. (2010). Multidimensional Techniques in Protein Separations for Neuroproteomics. *Neuroproteomics*. Boca Raton (FL). Chapter 3.
- Barat, B and Wu, AM (2007). Metabolic biotinylation of recombinant antibody by biotin ligase retained in the endoplasmic reticulum. *Biomol Eng*. 24(3): 283–291.
- Baxevanis, A D., and Ouellette Francis BF.(eds) (2005). *Bioinformatics: A Practical Guide to the Analysis of Genes and Proteins*. 3rd edn., John Wiley, Hoboken, NJ.
- Becker RC. (1992). Seminars in thrombosis, thrombolysis, and vascular biology. 6. Procoagulant states. *Ardiology* 80(1):51-64.
- Bevilacqua MP, Pober JS, Majeau GR (1984) Interleukin 1 (IL-1) induces biosynthesis and cell surface expression of procoagulant activity in human vascular endothelial cells. *J Exp Med*. 160:618.
- Bevilacqua MP, Pober JS, Majeau GR (1986). Recombinant tumor necrosis factor induces procoagulant activity in cultured human vascular endothelium: characterization and comparison with the actions of interleukin 1. *Proc Natl Acad Sci*. 83:4533.
- Bodzon-Kulakowska A., Bierzynska-Krzysik A., Dylag T. (2007). Methods for samples preparation in proteomic research. *Journal of Chromatography B-Analytical Technologies in the Biomedical and Life Sciences*. 849:1–31.
- Boer E, Rodriguez P, Bonte E, Krijgsveld J, Katsantoni E, Heck A, Grosveld F, and Strouboulis J. (2003). Efficient biotinylation and single-step purification of tagged transcription factors in mammalian cells and transgenic mice. *Proc Natl Acad Sci* 24; 100(13): 7480–7485.
- Boersema P, Raijmakers, Lemeer S, Shabaz Mohammed S and Heck A (2009). Multiplex peptide stable isotope dimethyl labeling for quantitative proteomics. *Nat. Protocl*. 4 (4):484-94
- Brown RD, Jr., Wiebers DO, Forbes G, O'Fallon WM, Piepgras DG, Marsh WR, Maciunas RJ. (1988). The natural history of unruptured intracranial arteriovenous malformations. *J Neurosurgery*. 68(3):352-357.

- Butcher J (2007). Neuroproteomics comes of age. *Lancet Neurol.* 6:850
- Carlas B., Pineiro C., Calvo E., Lopez-Ferrer D., Gallardo J. (2007). Trends in sample preparation for classical and second generation proteomics. *Journal of Chromatography* 153:235–58.
- Cheng D., Hoogenraad C., Rush J. (2006). Relative and absolute quantification of postsynaptic density proteome isolated from rat forebrain and cerebellum. *Mol Cell Proteomics.* 5:1158–70.
- Chantôme A, Potier-Cartreau M, Clarysse L, Fromont G, Marionneau-Lambot S, Guéguinou M, Pagès JC, Collin C, Oullier T, Girault A, Arbion F, Haelters JP, Jaffrès PA, Pinault M, Besson P, Joulin V, Bournoux P, Vandier C (2013). Pivotal role of the lipid Raft SK3-Orai1 complex in human cancer cell migration and bone metastases. *Cancer Res.* 1;73 (15):4852-61
- Cheng H, Li J, Liu C, Yao W, Xu Y, Frank TS, Cai X, Shi S, Lu Y, Qin Y, Liu L, Xu J, Long J, Ni QX, Li M, Yu XJ (2013). Profilin1 sensitizes pancreatic cancer cells to irradiation by inducing apoptosis and reducing autophagy. *Curr Mol Med.* 13(8):1368-75.
- Chong PK, Gan CS, Pham TK, and Wright PC (2006). Isobaric tags for relative and absolute quantitation (iTRAQ) reproducibility: implication of multiple injections. *Journal of Proteome Research.* 5(5): 1232–1240
- Choudhary J., Grant S. (2004). Proteomics in postgenomic neuroscience: The end of the beginning. *Nature Neuroscience.* 7: 440–45.
- Chowdhury S. K. (1990). Electrospray ionization mass spectrometric peptide mapping: A rapid, sensitive technique for protein structure analysis. *Biochem Biophys Res Commun.* 167, 686–92.
- Christian S., Ahorn H., Novatchkova M., Garin-Chesa P., Park J.E., Weber G., Eisenhaber F., Rettig W.J., Lenter M.C. (2001). Molecular cloning and characterization of EndoGlyx-1, an EMILIN-like multisubunit glycoprotein of vascular endothelium. *J Biol Chem* 276: 48588–48595.
- Chun W, Johnson V. (2007). The role of tau phosphorylation and cleavage in neuronal cell death. *Front Biosci.* 12:733–56.
- Cines DB, Pollak ES, Buck CA, Loscalzo J, Zimmerman GA, McEver RP, Pober JS, Wick TM, Konkle BA, Schwartz BS, Barnathan ES, McCrae KR, Hug BA, Schmidt AM, Stern DM. (1998). Endothelial cells in physiology and in the pathophysiology of vascular disorders. *Blood.* 15;91(10) :3527–61.
- Cohen I, Kaminski E, Glaser T (1976). Actin and myosin from blood platelets or muscle are potent aggregating agents. *J Thrombosis Research,* 8 (3): 383–392
- Corada M, Zanetta L, Orsenigo F, Breviario F, Lampugnani MG, Bernasconi S, Liao F, Hicklin DJ, Bohlen P, Dejana E (2002). A monoclonal antibody to vascular endothelial-cadherin inhibits tumor angiogenesis without side effects on endothelial permeability. *Blood* 100 (3): 905–11

- Cordes N, Blaese MA, Meineke V, Van Beuningen D. (2002). Ionizing radiation induces up-regulation of functional beta1-integrin in human lung tumour cell lines in vitro. *Int J Radiat Biol.* 78 (5): 347-57
- Crosby V, Fleming A, Argraves S, Corada M, Zanetta L, Dejana E, Drake J (2005). VE-cadherin is not required for the formation of nascent blood vessels but acts to prevent their disassembly. *Blood* 105 (7): 2771–6.
- da Costa JG, de Moura MA, Consoni L, Nogueira RA. (2002). *Cell Mol Biol (Noisy-le-grand)*. Can electromagnetic radiations induce changes in the kinetics of voltage-dependent ion channels? 48(5):577-83.
- Das T, Yong Ho Bae, Alan Wells, and Roy P (2010). Loss of Profilin-1 Expression Enhances Breast Cancer Cell Motility by Ena/VASP Proteins *J Cell Physiol.* 219(2): 354–364
- DeLisser HM, Christofidou-Solomidou M, Strieter RM, Burdick MD, Robinson CS, Wexler RS, Kerr JS, Garlanda C, Merwin JR, Madri JA, and Albelda SM. (1997) . Involvement of endothelial PECAM-1/CD31 in angiogenesis. *Am J Pathol.* 151(3): 671–677
- Doherty GJ, McMahon HT (2008). Mediation, modulation, and consequences of membrane-cytoskeleton interactions. *Annu Rev Biophys* 37(1): 65–95.
- Eijkelkamp N, Linley JE, Baker MD, Minett MS, Cregg R, Werdehausen R, Rugiero F, and Wood JN. (2012). Neurological perspectives on voltage-gated sodium channels. *Brain*; 135(9): 2585–2612.
- Esmon CT (2004). Coagulation and inflammation. *J. Endotoxin Res.* 9 (3): 192–8.
- Essex W, K. Chen, M. Swiatkowska (1995). Localization of protein disulfide isomerase to the external surface of the platelet plasma membrane. *Blood*, 86: 2168–2173
- F.G. Giancotti, E. Ruoslahti (1999). *Science*, 285:1028–1032
- Falk E. (1985). Unstable angina with fatal outcome: dynamic coronary thrombosis leading to infarction and/or sudden death. Autopsy evidence of recurrent mural thrombosis with peripheral embolization culminating in total vascular occlusion. *J Circulation.* 71:699.
- Fairhead M and Howarth M (2015). Site-specific biotinylation of purified proteins using BirA. *Methods Mol Biol.* 1266: 171–184.
- Ferch RD, Morgan MK. (2002). High-grade arteriovenous malformations and their management. *J. Clin Neurosci.* 9(1):37-40
- Filmore D (November 2004). It's a GPCR world. *Modern Drug Discovery* . American Chemical Society; 24–28.
- Fishman AP. (1982). Endothelium: A distributed organ of diverse capabilities. *Annals NY Academy of Science*, 401:1-8.
- Friedlander RM (2007) Arteriovenous Malformations of the Brain. *N Engl J Med* 356: 2704-2712.

- Friedman WA, Bova FJ, Bollampally S, Bradshaw P. (2003). Analysis of factors predictive of success or complications in arteriovenous malformation radiosurgery. *Neurosurgery*. 52(2):296–307.
- Fukudome K, Esmon C. (1994). Identification, cloning, and regulation of a novel endothelial cell protein C/activated protein C receptor. *J Biol Chem* 269 (42): 26486–91.
- Furman MI, Benoit SE, Barnard MR, Valeri CR, Borbone ML, Becker RC, Hechtman HB, Michelson AD (1998). Increased platelet reactivity and circulating monocyte-platelet aggregates in patients with stable coronary artery disease. *J Am Coll Cardiol*.;31(2):352.
- GabryS D, Olga Greco O, Patel G, Prise K, Tozer G (2007). Radiation effects on the cytoskeleton of endothelial cells and endothelial monolayer permeability. *J Radiat Oncol Biol Phys*. 69 (5):1553-1562
- Ganz P, Hsue P Y. (2013). Endothelial dysfunction in coronary heart disease is more than a systemic process. *European Heart Journal*. V34 Issue (27): 2025-2027.
- Garlanda C, Dejana E. (1997). Heterogeneity of endothelial cells. Specific markers. *Arterioscler Thromb Vasc Biol*. 17(7):1193-202.
- Gaugler MH, Vereycken-Holler V, Squiban C, Aigueperse J. *Thromb Haemost*. (2004). PECAM-1 (CD31) is required for interactions of platelets with endothelial cells after irradiation. 2 (11) : 2020–6
- Gerald Karp (2009). *Cell and Molecular Biology: Concepts and Experiments*. John Wiley and Sons. 7TH edn. PP128
- Giancotti FG, Ruoslahti E (1999). Integrin signaling, 13;285(5430):1028-32.
- Gillet, LC., P. Navarro, S. Tate, H. Röst, N. Selevsek, L. Reiter, R. Bonner, and Aebersold R (2012). Targeted data extraction of the MS/MS spectra generated by data-independent acquisition: A new concept for consistent and accurate proteome analysis. *Molecular & cellular proteomics*. 11(6).
- Gimbrone MA, Cotran RS, Folkman J (1974). Human vascular endothelial cells in culture. Growth and DNA synthesis. *J Cell Biology*, 60:673
- Gómez-Varela, D. et al. (2007). Monoclonal antibody blockade of the human Eag1 potassium channel function exerts antitumor activity. *Cancer Res*. 67: 7343–7349.
- Grant G, Blackstock P (2001). Proteomics in neuroscience: from protein to network. *J Neurosci*. 1;21 (21) :8315–8.
- Gross PL, Aird WC. (2000). The endothelium and thrombosis. *Semin Thromb Hemost* 26(5):463-78.
- Gygi SP, Rist B, and Aebersold R. (2000). Measuring gene expression by quantitative proteome analysis. *Current Opinion in Biotechnology*. (11); 396–401

- Halim AX, Johnston SC, Singh V (2004). Longitudinal risk of intracranial hemorrhage in patients with arteriovenous malformation of the brain within a defined population. *Stroke*. 35(7):1697–1702.
- Hall J., Morton I. (1999). Concise dictionary of pharmacological agents: properties and synonyms. Kluwer Academic. 255 (12): 5521–4.
- Han PP, Ponce FA, Spetzler RF (2003). Intention-to-treat analysis of Spetzler-Martin grades IV and V arteriovenous malformations: natural history and treatment paradigm. *J Neurosurg*. 98(1):3–7.
- Harris, EMcintyre T, Prescott S and Zimmerman G (2000). The leukocyte integrins. *J Biol Chem* 275 (31) :23409–23412.
- Hashimoto T, Lam T, Boudreau NJ, Bollen AW, Lawton MT, et al. (2001). Abnormal balance in the angiopoietin-tie2 system in human brain arteriovenous malformations. *Circ Res* 89(2): 111-113.
- Hatton MW, Moar SL, Richardson M. (1989). Deendothelialization in vivo thrombogenic reaction at the rabbit aorta surface. Correlation of uptake of fibrinogen and antithrombin III with thrombin generation by the exposed subendothelium. *Am J Pathol*. 135:499.
- Hayward CP, Warkentin TE, Horsewood P, Kelton JG (1991). Multimerin: a series of large disulfide-linked multimeric proteins within platelets. *Blood*; 77(12):2556-60.
- Helenius, A. and Simons, K. (1975) Solubilization of Membranes by Detergents. *Biochim. Biophys. Acta* 415, 29–79.
- Hewett PW (2016). Isolation and Culture of Human Endothelial Cells from Micro- and Macro-vessels. *Methods Mol Biol*. 1430:61-76
- Howarth M, Takao K, Hayashi Y, Ting AY. (2005). Targeting quantum dots to surface proteins in living cells with biotin ligase. *Proc Natl Acad Sci*. 102:7583–7588.
- Huang SW, Lien JC, Kuo SC, Huang TF (2012). Antiangiogenic mechanisms of PJ-8, a novel inhibitor of vascular endothelial growth factor receptor signaling. *Carcinogenesis*. 33(5):1022-30.
- Humphries M. (2000). Integrin structure. *Biochem. Soc. Trans*. 28 (4) :311–339.
- Huss WJ, et al (2001). Angiogenesis and prostate cancer: Identification of a molecular progression switch. *Cancer Res*. 61:2736-2743.
- Hwa C, Sebastian A, Aird WC. (2005). Endothelium. *Endothelial biomedicine: its status as an interdisciplinary field, its progress as a basic science, and its translational bench-to-bedside gap*. 12 (3):139–51.
- Jaffe EA, Nachman RL, Becker CG, Minick CR. Culture of human endothelial cells derived from umbilical veins: Identification by morphologic criteria. *J Clin Invest* 1973;52:2745.
- Jayaramana M, Cloft HJ (2009). Embolization of Brain Arteriovenous Malformations for Cure: Because We Could or Because We Should? *J Neuroradiol*. 30: 107–108

- Jeffrey R, Stodley MA (2009). Postnatal Development of Arteriovenous Malformations. *Pediatr Neurosurg*;45:296–304
- John C, Flickingera, B, Hideyuki, K. Niranjana A, Kondziolka, Lunsforda–c D, Niranjana A, Kano H, Lunsford LD (2013). Dose Selection in Stereotactic Radiosurgery : Gamma Knife Radiosurgery for Brain Vascular Malformations. *Prog Neurol Surg*. 27: 49–57
- Kashba SR, Patel NJ, Grace M, Lee VS, Raoufi-Rad N, Raj JV, Duong TT, Stoodley M. (2015). Angiographic, hemodynamic, and histological changes in an animal model of brain arteriovenous malformations treated with Gamma Knife radiosurgery. *J Thromb Haemost*. 7(11):1886-96.
- Kim JS, Chang JW, Yun HS, Yang KM, Hong EH, Kim DH, Um HD, Lee KH, Lee SJ, Hwang SG (2010). Chloride intracellular channel 1 identified using proteomic analysis plays an important role in the radiosensitivity of HEP-2 cells via reactive oxygen species production. *Proteomics*. 10(14):2589–604.
- Kramer G, Woolerton Y, van Straalen JP, Vissers JPC, Dekker N, Langridge JI, (2015). Accuracy and Reproducibility in Quantification of Plasma Protein Concentrations by Mass Spectrometry without the Use of Isotopic Standards. *PLoS ONE* 10(10): 1–22
- Kuster B, Schire M, mallick P, Aebersold R. (2005). Scoring proteome with proteotypic peptides probes. *Nat Rev Mol Cell Biol*. 6, 577–83
- Kwang S S, Mutoh M, Gerdes M, and Stuart H. (2005). CLIC4, an Intracellular Chloride Channel Protein, Is a Novel Molecular Target for Cancer Therapy. *Yuspa Invest Dermatol Symp Proc* 10: 105–109.
- Kwiatkowski DJ, Bruns GA (1988). Human profilin. Molecular cloning, sequence comparison, and chromosomal analysis. *J Biol Chem*. 263 (12): 5910–5.
- Kyle J. Roux KJ, Kim DI, Burke B (2013). BioID: A Screen for Protein-Protein Interactions. *Curr. Protoc. Protein Sci*. 74:19.23.1-19.23.14
- Lawrence FB (2003). Thrombin and Platelet Activation. *Chest* 124(3): 18–25
- Leanza, L. (2012). Inhibitors of mitochondrial Kv1.3 channels induce Bax/Bak-independent death of cancer cells. *EMBO Mol. Med*. (4): 577–593.
- Lee AG (2005). How lipids and proteins interact in a membrane: a molecular approach. *Mol Biosyst*. 1(3) :203–12
- Lee EC, Lotz MM, Steele GD Jr, Mercurio AM (1992). The integrin alpha 6 beta 4 is a laminin receptor. *J Cell Biol*. 117(3):671–8.
- Lee YC, Block G, Chen H, Folch-Puy ER, et al (2008). One-step isolation of plasma membrane proteins using magnetic beads with immobilized concanavalin . *Protein Expr Purif* 62(2): 223–229.
- Lefebvre P¹, White JG, Krumwiede MD, Cohen I (1993). Role of actin in platelet function. *Eur J Cell Biol*. 62 (2):194–204.

- Lin H, Guidotti G. (2009). Purification of membrane proteins. *Methods Enzymol.* 463:619–29.
- López E, Madero L, López-Pascual J, Latterich M. (2012). Clinical proteomics and OMICS: Clues useful in translational medicine research. *Proteome Science* 10:35
- Lorenzon E, Colladel R, Andreuzzi E, Marastoni S, Todaro F, Schiappacassi M, Ligresti G, Colombatti A, Mongiat M. (2012). MULTIMERIN2 impairs tumor angiogenesis and growth by interfering with VEGF-A/VEGFR2 pathway. *Oncogene.* 31(26):3136–47
- Luis A. Pardo & Walter Stühmer (2014). The roles of K⁺ channels in cancer. *Nature Reviews Cancer* , 14; 39-48.
- Lunsford LD, Niranjan A, Kondziolka D, Sirin S, and Flickinger JC (2008). Arteriovenous Malformation Radiosurgery: A Twenty Year Perspective. *Clinical Neurosurgery*, 55: 108–19
- Marcus K., Schmidt O., Schaefer H. (2004). Proteomics Application to the Brain. *International Review of Neurobiology.* 61:285–311.
- Major O, Szeifert GT, Fazekas I, Vitanovics D, Csonka E, Kocsis B, Bori Z, Kemeny AA, Nagy Z (2002). Effect of a single high-dose gamma irradiation on cultured cells in human cerebral arteriovenous malformation. *J Neurosurg.* (5): 459-63.
- Maruyama K, Kawahara N, Shin M (2005) The risk of hemorrhage after radiosurgery for cerebral arteriovenous malformations. *N Engl J Med* 352: 146-153.
- McCormick WF (1966). The pathology of vascular (“arteriovenous”) malformations. *J Neurosurg.* 24:807–816.
- Millar RP, Newton CL (2010). The year in G protein-coupled receptor research. *Mol. Endocrinol.* 24 (1): 261–74.
- Montesano R, (1990). Increased proteolytic activity is responsible for the aberrant morphogenetic behavior of endothelial cells expressing the middle T oncogene. *Cell* 62: 435-445, 1990.
- Münzel T, Sinning C, Post F, Warnholtz A, Schulz E. (2008). Pathophysiology, diagnosis and prognostic implications of endothelial dysfunction. *Ann Med.* 40 (3):180–96.
- Neugebauer, J.M. (1990). Detergents: An Overview. *Methods Enzymol.* 182, 239–252.
- Newman J, Berndt C, Gorski C, White I, Lyman S, C Paddock, Muller A. (1990). PECAM-1 (CD31) cloning and relation to adhesion molecules of the immunoglobulin gene superfamily. *Science* 247: 1219–1222
- Newman PJ, Berndt MC, Gorski J, White GC, Lyman S, Paddock C, Muller WA (1990). PECAM-1 (CD31) cloning and relation to adhesion molecules of the immunoglobulin gene superfamily. *Science* 247 (4947): 1219–22.
- Ondra SL, Troupp H, George ED, Schwab K. (1990). The natural history of symptomatic arteriovenous malformations of the brain: a 24-year follow-up assessment. *J Neurosurg.* 73(3):387–391.

- Ouyang JS, Li YP, Chen CS, Chen JJ, Chen TK, Cai C and Yang L (2014). Inhibition of lung tumour growth in nude mice by siRNACD31 targeting PECAM-1. *Oncology Letters* 8: 33-40.
- Ow Y, M. Noirel S, Evans C, Rehman I, and Wright P (2009). iTRAQ underestimation in simple and complex mixtures: 'the good, the bad and the ugly'. *Journal of Proteome Research*, 8 (11): 5347–5355.
- Owman C, Hardbeo JE. (1988). Functional heterogeneity of cerebrovascular endothelium. *Brain Behav Evol.* 32:65.
- Pardo LA, Stühmer W. 2014 The roles of K(+) channels in cancer. *Nat Rev Cancer.* 14 (1):39-48.
- Patel VJ, Thalassinou K, Slade S, Connolly JB, Crombie A, et al (2009). A comparison of labelling and label-free mass spectrometry based proteomics approaches. *J Proteome Research.* 8 (7): 3752–3759
- Petricoin E, Zoon C, Kohn C, Barrett C, Liotta A. (2002). Clinical proteomics: translating benchside promise into bedside reality. *Nat Rev Drug Discovery* 1(9):683–95
- Pfendner E, Rouan F, Uitto J (2005). Progress in epidermolysis bullosa: the phenotypic spectrum of plectin mutations. *Exp. Dermatol.* 14 (4): 241–9.
- Phillips M, Stelzer KJ, Griffen TW (1994). Stereotactic radiosurgery: a review and comparison of methods. *J Clinical Oncology*, 12; 1985-1999
- Pierot L, Januel AC, Herbreteau D (2005). Endovascular treatment of brain arteriovenous malformations using Onyx: preliminary results of a prospective multicenter **study**. *Interventional Neuroradiology.* 11:159–64
- Pillozzi, S. (2011). Chemotherapy resistance in acute lymphoblastic leukemia requires hERG1 channels and is overcome by hERG1 blockers. *Blood.* 117: 902–914.
- Popielarski M, Ponamarczuk H, Sobierajska K, Świątkowska M. (2014). Role of protein disulfide isomerase in activation of integrins. *Postępy Hig Med Dosw* 68(0):66-83.
- Prieto G, Aloria K, Osinalde N, Fullaondo A, Arizmendi JM, Matthiesen R. (2012). PAnalyzer: a software tool for protein inference in shotgun proteomics. *BMC Bioinformatics.* 13:288.
- Radford K J, Thorne R F, Hersey P. (1996). "CD63 associates with transmembrane 4 superfamily members, CD9 and CD81, and with beta 1 integrins in human melanoma". *Biochem. Biophys. Res. Commun.* 222 (1): 13–8.
- Roboz J (2001). *Mass Spectrometry in Cancer Research.* p 407
- Rombouts C, Aerts A, Beck M, De Vos WH, Van Oostveldt P, Benotmane MA, Baatout S (2013). Differential response to acute low dose radiation in primary and immortalized endothelial cells. *Int J Radiat Biol.* 89(10):841-50.

- Rosen EM, Goldberg ID, Myrick KV, Halpin PA, Levenson SE (1986). Survival and repair of potentially lethal radiation damage in confluent vascular smooth muscle cell cultures. *Radiother Oncol.* 5(2):159-63.
- Rothbarth K, Dabaghian AR, Stammer H, Werner D (1999). One single mRNA encodes the centrosomal protein CCD41 and the endothelial cell protein C receptor (EPCR). 458 (1): 77–80
- Roux KJ, Kim DI, Raida M, Burke B (2012). A promiscuous biotin ligase fusion protein identifies proximal and interacting proteins in mammalian cells. *J Cell Biol.* 19;196(6):801-10
- Rubenstein, Lester A. and Lanzara, Richard G. (1998). Activation of G protein-coupled receptors entails cysteine modulation of agonist binding. *Journal of Molecular Structure (Theochem)* 430: 57–71.
- Rybak JN, Trachsel E, Scheuermann J, Neri D. Ligand-based vascular targeting of disease. *ChemMedChem.* 2007;2:22-40.
- Satelli A, Li S (2011). Vimentin in cancer and its potential as a molecular target for cancer therapy. *Cell Mol Life Sci.*;68(18):3033-46.
- Sauer FG, Fütterer K, Pinkner JS, Dodson KW, Hultgren SJ, Waksman G (1999). Structural basis of chaperone function and pilus biogenesis. *Science* 285 (5430): 1058–61.
- Sekis I, Gerner W, Willmann M, Rebuzzi L, Tichy A, Patzl M, Thalhammer JG, Saalmüller A, Kleiter MM (2009). Effect of radiation on vascular endothelial growth factor expression in the C2 canine mastocytoma cell line. *Am J Vet Res.*70 (9):1141-50
- Shmuel Shaltiel, J. Lahav, N. Gofer-Dadosh, J. Luboshitz O. Hess, M. Shaklai (2000). Protein disulfide isomerase mediates integrin-dependent adhesion. 475(2): 89–92
- Sikorski EE (1993). The Peyer's patch high endothelial receptor for lymphocytes, the mucosal vascular addressin, is induced on a murine endothelial cell line by tumor necrosis factor-alpha and IL-1. *J. Immunol.* 151: 5239-5250
- Silva J, Gorenstein M, Li Guo-Zhong , Vissers J and Geromanos S. (2006). Absolute Quantification of Proteins by LCMS^EA Virtue of Parallel ms Acquisition. *Molecular and cellular proteomics.* 4:144-156
- Simonian M, Molloy MP and Stoodley MA (2012). *In vitro* and *in vivo* biotinylation of endothelial cell surface proteins in the pursuit of targets for vascular therapies for brain AVMs. *Metabolomics Journal*, (1); 007
- Simonian M, Ogorzalek Loo RR, Loo JA, Stoodley MA and Molloy MP. (2014). Proteomics Detection of Endothelial Cell Surface Proteins Following Irradiation as Potential Targets for Brain Arteriovenous Malformations Molecular Therapy. *J Proteomics & Bioinformatics.* 1: (1)
- Simonian M, Ogorzalek Loo RR, Rannulu N, Loo JA, Molloy MP and Stoodley MA. (2015). Identification of protein targets for brain arteriovenous malformations (AVMs) molecular therapies. Submitted, August 31. *J Proteome Research*

- Singer SJ, Nicolson GL (1972). The fluid mosaic model of the structure of cell membranes. *Science*, 175(4023):720-31.
- Song BW, Vinters HV, Wu D, Pardridge WM. (2002). Enhanced neuroprotective effects of basic fibroblast growth factor in regional brain ischemia after conjugation to a blood-brain barrier delivery vector. *J Pharmacol Exp Ther.* ;301:605–610.
- Spetzler RF, Hargraves RW, McCormick PW, Zabramski JM, Flom RA (1992). Relationship of perfusion pressure and size to risk of hemorrhage from arteriovenous malformations. *J Neurosurg* 76: 918-923.
- Spetzler RF, Martin NA (1986). A proposed grading system for arteriovenous malformations. *J Neurosurg* 65: 476-483.
- Stabenfeldt S E, Gossett J J, Barker T H. (2010). Building better fibrin knob mimics: an investigation of synthetic fibrin knob peptide structures in solution and their dynamic binding with fibrinogen/fibrin holes. *Blood*. 116: 1352.
- Stalker TJ, Wu J, Morgans A, Traxler EA, Wang L, Chatterjee MS, Lee D, Quertermous T, Hall RA, Hammer DA, Diamond SL, Brass LF, Haemost T. (2009). Endothelial cell specific adhesion molecule (ESAM) localizes to platelet-platelet contacts and regulates thrombus formation in vivo. *J Thromb Haemost* ;7(11):1886-96. 2009
- Stefanini MO, Wu FT, Mac Gabhann F, Popel AS. (2009). The presence of VEGF receptors on the luminal surface of endothelial cells affects VEGF distribution and VEGF signalling. *LoS Comput Biol*. 5(12)
- Stein CM, Brown N, Vaughan DE, Lang CC, Wood AJ. (1998). Regulation of local tissue-type plasminogen activator release by endothelium-dependent and endothelium-independent agonists in human vasculature. *J Am Coll Cardiol*. 32(1):117.
- Stern DM, Bank I, Nawroth PP, et al. Self-regulation of procoagulant events on the endothelial cell surface. *J Exp Med* 1985; 162:1223.
- Storer K, Tu J, Karunanayaka A, (2007). Coadministration of low-dose lipopolysaccharide and soluble tissue factor induces thrombosis after radiosurgery in an animal arteriovenous malformation model. *Neurosurgery*. 61(3):604-610.
- Storer KP, Tu J, Karunanayaka A, Morgan MK, Stoodley MA. (2007). Thrombotic molecule expression in cerebral vascular malformations. *J Clin Neurosci*. 14(10):975-980.
- Storer KP, Tu J, Stoodley MA, Smee RI (2010). Expression of endothelial adhesion molecules after radiosurgery in an animal model of arteriovenous malformation. *Neurosurgery* 67: 976-983.
- Sunyer B., Diao W., Lubec G. (2008). The role of post-translational modifications for learning and memory formation. *Electrophoresis*. 29:2593–2602.
- Suzuki S, Sano K, Tanihara H (1991). Diversity of the cadherin family: evidence for eight new cadherins in nervous tissue. *Cell Regulation*. 2 (4): 261–70.

- Suzuki S, Sano K, Tanihara H. (1991). Diversity of the cadherin family: evidence for eight new cadherins in nervous tissue". *Cell Regulation*. 2 (4): 261–70.
- Svitkina TM, Verkhovsky AB, Borisy GG (Nov 1996). Plectin sidearms mediate interaction of intermediate filaments with microtubules and other components of the cytoskeleton. *The Journal of Cell Biology*. 135 (4): 991–1007.
- Szeifert GT, Major O, Fazekas I, Nagy Z (2001). Effects of radiation on cerebral vasculature: a review. *Neurosurgery*. 48 (2):452-3.
- Tanford, C. and Reynolds, J.A. (1976). Characterization of Membrane Proteins in Detergent Solutions. *Biochim. Biophys. Acta* 457, 133–170.
- Trinh HV, Jonas Grossmann J, Gehrig P, Roschitzki B, Schlapbach R, Greber UF, and Hemmi S. (2013). iTRAQ-based and label-free proteomics approaches for studies of human adenovirus infections. *International Journal of Proteomics*. 1–16
- Tu J, Karunanayaka A, Windsor A, Stoodley M. (2010). Comparison of an arteriovenous malformation (AVM) animal model with human AVM. *J Clin Neurosci*. 17(1):96-102.
- Tu J, Stoodley MA, Morgan MK, (2005). Ultrastructural characteristics of hemorrhagic, nonhemorrhagic, and recurrent cavernous malformations. *J Neurosurg*. 103(5):903-909.
- Tu J, Stoodley MA, Morgan MK, Storer KP. (2006). Responses of arteriovenous malformations to radiosurgery: ultrastructural changes. *Neurosurgery*. 58(4):749-758.
- Vanzulli S, et al (1997). Detection of endothelial cells by MEC 13.3 monoclonal antibody in mice mammary tumors. *Biocell* 21:39-46.
- Varon D, Jackson DE, Shenkman B, Dardik R, Tamarin I, Savion N, Newman J. (1998) Blood. Platelet/endothelial cell adhesion molecule-1 serves as a costimulatory agonist receptor that modulates integrin-dependent adhesion and aggregation of human platelets. *15;91 (2) :500–7*.
- Vecchi A, et al (1994). Monoclonal antibodies specific for endothelial cells of mouse blood vessels. Their application in the identification of adult and embryonic endothelium. *Eur. J. Cell Biol*. 63:247-254.
- Verkman AS, Galiotta LJ (February 2009). Chloride channels as drug targets. *Nat Rev Drug Discov*. 8 (2): 153–71.
- Von Heijne, G. (2006). Membrane-protein topology. *Nature Reviews Molecular Cell Biology* 7 (12): 909–918.
- Wilkins MR., Williams K L., Appel RD., and. Hochstrasser DF. (eds). (1997). *Proteome Research: New Frontiers in Functional Genomics (Principles and Practice)* (Kindle Edition) Springer-Verlag, New York.
- Wilkinson B, Gilbert HF (June 2004). "Protein disulfide isomerase". *Biochimica et Biophysica Acta* 1699(1-2): 35–44.

- Williams K., Wu T., Colangelo C., Nairn A. (2004). Recent advances in neuroproteomics and potential application to studies of drug addiction. *Neuropharmacology*. 47:148–66.
- Wombacher R and Cornish V (2011). Applications in live cell fluorescence imaging. *Biophotonics*. 4(6): 391–402
- Wu C, J S Bauer, R L Juliano and J A McDonald (1993). The alpha 5 beta 1 integrin fibronectin receptor, but not the alpha 5 cytoplasmic domain, functions in an early
- Wulfschlegel D, Liotta A, Petricoin F (2003). Early detection: Proteomic applications for the early detection of cancer. *Nat Rev Cancer* 3(4) :267–75.
- Xiong JP, Stehle T, Diefenbach B (2001). Crystal structure of the extracellular segment of integrin alpha Vbeta3. *Science* 294 (5541): 339–45.
- Yassari R, Sayama T, Jahromi BS, Aihara Y, Stoodley M, Macdonald RL. Angiographic, hemodynamic and histological characterization of an arteriovenous fistula in rats. *Acta Neurochir (Wien)*. May 2004;146(5):495-504
- Youngson, Robert M. (2006). Collins Dictionary of Human Biology. Glasgow: HarperCollins. ISBN 0-00-722134-7.
- Zabel-du Bois A, Milker-Zabel S, Huber P, Schlegel W, Debus J. (2007). Risk of hemorrhage and obliteration rates of LINAC-based radiosurgery for cerebral arteriovenous malformations treated after prior partial embolization. *Int J Radiat Oncol Biol Phys*. 15;68(4):999-1003.
- Zhang Y, Song S, Fong CC, Tsang CH, Yang Z, and Yang M (2003). cDNA Microarray analysis of gene expression profiles in human fibroblast cells irradiated with red light. *Journal of Investigative Dermatology*. 120 (5),
- Zhang, L, Song L, Parker EM (1999). Notch from neurodevelopment to neurodegeneration. *J. Biol. Chem*. 274, 8966–8972

Appendix 1:

Margaret Simonian, Mark P Molloy and Marcus A Stoodley (2012). *In vitro* and *in vivo* biotinylation of endothelial cell surface proteins in the pursuit of targets for molecular therapies for brain AVMs. J Metabolomics. SS(1) doi:10.4172/2153-0769.S1-007



Research Article

Open Access

In vitro and *in vivo* biotinylation of endothelial cell surface proteins in the pursuit of targets for molecular therapies for brain AVMs

Margaret Simonian^{1*}, Mark P Molloy² and Marcus A Stoodley¹¹Australian School of Advanced Medicine, Macquarie University, North Ryde, NSW, 2109, Australia²Australian Proteomics Analysis Facility (APAF), Department of Chemistry and Biomolecular Sciences, Macquarie University, North Ryde, NSW, 2109, Australia**Abstract**

Identification of membrane proteins that are expressed on the endothelium after radiosurgery is of fundamental importance in developing a new treatment for brain vascular formations. We optimized then employed *in vitro* and *in vivo* biotinylation methodology to label membrane proteins in a murine cerebral endothelial cell cultures (bEnd.3) and a rat model of arteriovenous malformation (AVM). Membrane proteins were then captured on streptavidin resin and identified using proteomics analysis.

Keywords: Biotinylation; Membrane proteins; Murine cerebral endothelial cells

Introduction

Arteriovenous malformations (AVMs) consist of a tangle of abnormal arteries and veins linked by one or more fistulae [1,2]. AVMs in the brain can occur in any region, and range in size from small (< 3cm) to large (> 6cm). Patients with AVMs present with headaches (migraines), seizures and most commonly haemorrhages. The first haemorrhage is most likely to occur between the ages of 20-40 years [3,4].

Treatment of AVMs depends on their location (eloquent or non-eloquent brain) and size [1,5,6]. Small AVMs located at the surface of the brain are suitable for direct surgery [2]. Large AVMs are usually wedge-shaped and extend deeper into the brain, these are more difficult to treat with surgical removal [2].

Embolization involves occluding the blood flow to an AVM using endovascular catheters and can be effective for rare lesions that are less than 1cm in diameter and fed by a single artery [7,8]. Radiosurgery is a treatment option for lesions < 3cm in diameter and located in eloquent areas where surgery can cause neurological deficits [1]. Compared to other treatments, the immediate risk at the time of the radiosurgery is very low. However, vascular occlusion after radiosurgery can take up to 3 years to complete, and patients remain at risk of haemorrhage during this time [9,10].

Approximately one third of AVMs are unsuitable for current treatment methods. Therefore there is a need for a new treatment, that is safer and more effective than current treatment methods for these large and deep lesions.

In 2007 a study by Storer et al [11], demonstrated induction of thromboses in an animal model of AVM treated with radiosurgery by administering lipopolysaccharide (LPS) and tissue factors which is a non-ligand type of vascular targeting. However this approach wasn't successful in the large vessels and there are safety concerns regarding injecting humans with LPS [11,12].

A ligand-based vascular targeting approach has the potential to overcome these problems, but requires a luminal surface molecule that discriminates AVM vessels from normal vessels. We propose that radiosurgery can stimulate the cell surface expression of discriminating proteins. In this study we aim to identify potential protein targets in AVM endothelium after radiosurgery. These protein candidates could

then be investigated for ligand-directed treatment to promote rapid thrombosis in AVM vessels. To achieve this goal, a successful labelling of cell surface proteins is crucial.

Here we describe the *in vitro* and *in vivo* biotinylation method that we employed to label membrane proteins in the murine endothelial cell culture (bEnd.3) and in an animal model of AVM. Surface biotinylation with biotin derivatives was followed by purification on streptavidin resin. This approach has been shown to be successful in recovering membrane proteins both in *in vitro* and *in vivo* studies [13-15]. Membrane proteins were then identified by ESI-MS/MS analysis.

Materials and Methods***In vitro* biotinylation**

Cell culture: Murine bEnd.3 endothelial cells (American Type Culture Collection, VA, USA) were cultured in Dulbecco's Modified Eagle's Medium (DMEM) with 4.5 g/L D-glucose (Invitrogen Gibco, CA, USA), 4mM L-glutamine, and 0.11 g/L sodium pyruvate containing 10% fetal bovine serum (Invitrogen Gibco), HEPES and streptomycin (Invitrogen Gibco) in a 5% CO₂ atmosphere at 37°C. Cells were seeded in 75 CM² tissue culture flasks until 80% confluent.

Surface biotinylation was performed on the endothelial cell cultures using a modified protocol [13,14].

Each 75 cm² flask containing approximately 1x10⁶ cells was washed four times with PBS pH 7.4. Twenty millilitres of PBS containing 67 μM EZ-link (Sulfo-NHS-LC-Biotin) (Pierce, IL, USA) were added to the flasks and incubated for 5 min at room temperature. The biotinylation reaction was terminated by adding Tris-HCl pH 7.5 to a final concentration of 670 μM. After 5 min incubation the cells

*Corresponding author: Margaret Simonian, Australian School of Advanced Medicine, Macquarie University, Sydney, 2109, Australia. Tel: +61-2-9812 3608; Fax: +61-2-9812 3610; E-mail: Margaret.simonian@mq.edu.au

Received April 17, 2012; Accepted April 28, 2012; Published April 30, 2012

Citation: Simonian M, Molloy MP, Stoodley MA (2012) *In Vitro* and *In Vivo* Biotinylation of Endothelial Cell Surface Proteins in the Pursuit of Targets for Vascular Therapies for Brain AVMs. Metabolomics 8:1007. doi:10.4172/2153-0769.S1-007

Copyright: © 2012 Simonian M, et al. This is an open-access article distributed under the terms of the Creative Commons Attribution License, which permits unrestricted use, distribution, and reproduction in any medium, provided the original author and source are credited.

Appendix 2

Margaret Simonian, Rachel R Ogorzalek Loo, Joseph A Loo, Marcus A Stoodley and Mark P Molloy (2014). Proteomics detection of endothelial cell surface proteins following irradiation as potential targets for brain arteriovenous malformations molecular therapy. *MOJ Proteomics and Bioinformatics*; 1(1): 00002 doi:medcraveonline.com/MOJPB/MOJPB-01-00002.pdf

Proteomics Detection of Endothelial Cell Surface Proteins Following Irradiation as Potential Targets for Brain Arteriovenous Malformations Molecular Therapy

Abstract

Arteriovenous malformations (AVMs) in the brain are vascular neurological lesions consist of abnormal collection of arteries and veins. They are the most common cause of brain haemorrhage in children and young adults. Over 90% of large AVMs (>3 cm) are not curable, or curable with unacceptable risks. Radiosurgery is the treatment option for lesions (< 3cm) in diameter and located in eloquent areas where surgery can cause neurological deficit. However vascular occlusion post radiosurgery can takes up to 3 year to complete while patients remain at risk of haemorrhage. This study aims to develop a molecular therapy for human brain AVMs. Specifically we aim to identify unique protein targets of AVMs that are up-regulated post irradiation. These proteins will then be used to develop a ligand-directed vascular treatment that promotes rapid thrombosis in AVM vessels post radiosurgery.

Proceeding

Volume 1 Issue 1 - 2014

Margaret Simonian^{1,2*}, Rachel R Ogorzalek Loo³, Joseph A Loo³, Marcus A Stoodley¹ and Mark P Molloy³

¹Australian School of Advanced Medicine, Macquarie University, Australia

²David Geffen School of Medicine, Department of Biological Chemistry, University of California Los Angeles (UCLA), USA

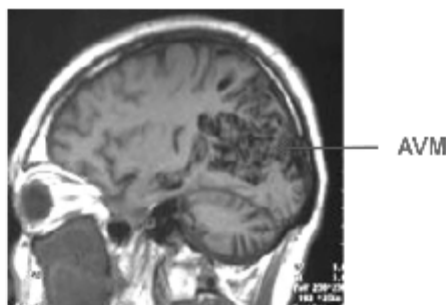
³Department of Chemistry and Biomolecular Sciences, Macquarie University, Australia

*Corresponding author: Margaret Simonian, David Geffen School of Medicine, Department of Biological Chemistry, University of California Los Angeles (UCLA), 611 Charles E. Young Drive East, CA, 90095, USA, Tel: +1-310-794-7308; E-mail: margaret@chem.ucla.edu

Received: April 25, 2014 | Published: April 30, 2014

Introduction

AVMs consist of abnormal collection of arteries and veins. They are the most common cause of haemorrhagic stroke in children and young adults. Radiosurgery is the treatment option recommended for lesions less than 3cm in diameter and located in eloquent areas where surgery can cause neurological deficits. This study aims to identify endothelial protein targets of AVMs that are differentially expressed compared to normal vessels post radiosurgery, to develop a ligand directed vascular treatment that promotes rapid thrombosis in AVM vessels. This is the first time that proteomics approach has been used in AVMs study.



Objectives

- Assess membrane protein changes in the murine endothelial cell culture (bEnd.3) in response to radiation over time using proteomics analysis.
- Determine candidate proteins location with immunocytochemistry.

Appendix 3

Margaret Simonian, Nalaka Rannulu, Rachel R Ogorzalek Loo, Joseph A Loo, Mark P Molloy and Marcus A Stoodley (2015). Identification of protein targets for brain arteriovenous malformations (AVMs) molecular therapies. **J Proteome Research**, submitted Aug. 31.

Margaret Simonian, Dyna Shirasaki, Rachel R Ogorzalek Loo, Joseph Loo, Mark P Molloy and Marcus A Stoodley (2015). Proteomics identification of radiation-induced changes of membrane proteins in the rat model of arteriovenous malformations. Manuscript in preparation

Supplementary Tables

Supp. Table 1. Expression level of the proteins that were significantly up or down regulated in at least one of the three iTRAQ-MS experiments, at different time points

Protein name	C6:S6			C24:S24			C48:S48			S72:C72		
	iTRAQ 1	iTRAQ 2	iTRAQ 3	iTRAQ 1	iTRAQ 2	iTRAQ 3	iTRAQ 1	iTRAQ 2	iTRAQ 3	iTRAQ 1	iTRAQ 2	iTRAQ 3
Plectin	1.06	0.69	1.23	NS	1.5	0.92	0.85	0.81	0.92	1.22	0.75	1.14
Myosin	NS	0.74	1.16	0.85	0.84	NS	NS	0.84	NS	1.38	NS	1.19
Vimentin	0.92	0.59	NS	0.7	1.42	NS	0.45	0.37	0.83	1.12	NS	1.213
Actin, cytoplasmic 1	NS	0.61	NS	NS	1.5	NS	NS	0.57	NS	NS	NS	NS
Actin cytoplasmic 2	0.82	NS	1.27	0.81	NS	NS	0.74	NS	0.88	NS	NS	1.69
Cadherin-5	NS	1.52	NS	NS	0.62	NS	1.32	1.26	NS	NS	NS	0.86
Integrin alpha-6	NS	1.12	NS	NS	0.73	NS	NS	NS	NS	NS	0.77	NS
Intergrin alpha 3	NS	NS	1.33	NS	NS	NS	NS	1.47	NS	NS	0.8	NS
Intergrin beta 1	1.28	NS	NS	NS	NS	NS	NS	1.42	NS	NS	NS	0.83
Integrin alpha-5	NS	NS	0.82	NS	0.708	NS	NS	NS	NS	NS	0.87	NS
Trifunctional enzyme s	NS	0.83	NS	NS	NS	NS	NS	0.82	NS	NS	NS	NS
Peroxiredoxin-1	NS	0.83	NS	NS	NS	NS	NS	NS	NS	NS	NS	NS
Histone H4	NS	0.6	1.56	0.55	2.32	NS	0.52	0.31	1.32	NS	NS	NS
Spectrin alpha chain	NS	0.64	NS	NS	NS	NS	0.75	NS	NS	NS	NS	NS
Spectrin beta chain	NS	NS	NS	NS	NS	NS	0.79	NS	NS	1.15	NS	NS
Filamin-B	NS	0.73	0.92	1.16	NS	NS	NS	NS	0.901	NS	NS	NS
Pyruvate kinase isozyme	NS	0.85	NS	NS	1.32	NS	NS	NS	NS	NS	NS	NS
PDI	NS	0.73	0.705	NS	0.68	1.22	NS	NS	NS	NS	NS	1.2
Histone H1	NS	0.6	NS	0.45	NS	NS	0.51	NS	NS	NS	NS	NS
Endoplasmin	NS	0.74	NS	NS	NS	NS	NS	NS	NS	NS	NS	NS
Histone H2B	NS	0.5	NS	0.42	NS	NS	NS	NS	NS	NS	NS	NS
Pletelet endothelial cell	1.29	NS	NS	NS	0.68	NS	NS	1.24	NS	1.17	NS	NS
Elongation factor 1 alpha	NS	NS	1.18	NS	1.55	NS	NS	1.32	NS	NS	0.7	NS
ADP/ATP translocase	NS	NS	NS	NS	0.56	NS	NS	NS	NS	NS	NS	NS
HSP 90-beta	NS	NS	NS	NS	1.18	NS	NS	NS	NS	NS	NS	NS
Tubulin alpha	NS	NS	NS	NS	1.57	NS	NS	NS	NS	NS	NS	NS
peptidyl-prolyl cis trans	NS	NS	NS	NS	0.63	NS	NS	0.48	NS	NS	NS	NS
Voltage dependent anion	NS	NS	0.76	NS	0.609	1.2	NS	NS	NS	NS	NS	NS
keratin type 1	NS	NS	NS	NS	2.407	NS	NS	1.7	0.58	NS	0.455	1.92
Lamin	0.81	NS	NS	0.67	NS	NS	0.65	0.42	NS	1.08	NS	NS
CD109	1.18	NS	0.782	1.11	NS	NS	1.18	1.867	NS	NS	NS	NS
Histone H2A	NS	NS	NS	0.53	NS	NS	0.52	0.23	NS	NS	NS	NS
Malate dehydrogenase	NS	NS	NS	NS	NS	NS	NS	0.068	NS	NS	NS	NS
Annexin A2	NS	NS	NS	NS	NS	NS	NS	1.49	NS	NS	NS	NS
Streese 70 protein	NS	NS	NS	NS	NS	NS	NS	NS	NS	NS	1.34	NS
plasmalemma vesicle associated p.	NS	NS	NS	NS	NS	NS	NS	NS	NS	NS	0.59	NS
Heterogenous nuclear ribonucleo	0.74	NS	NS	NS	NS	NS	0.53	NS	NS	NS	NS	NS
Myosin light polypeptide	NS	NS	NS	0.66	NS	NS	NS	NS	NS	NS	NS	NS
Myosin 10	NS	NS	NS	NS	NS	NS	1.17	NS	NS	NS	NS	NS
Histon H3.2	NS	NS	NS	0.57	NS	NS	NS	NS	NS	NS	NS	NS

Filamin A	NS	NS	0.85	NS	NS	1.17	NS	NS	NS	NS	NS	NS
Pyruvate carboxylase	NS	NS	0.724	NS	NS	NS	NS	NS	NS	NS	NS	NS
Myoferlin	NS	ND	NS	NS	ND	NS	NS	ND	0.88	NS	ND	NS

NS= not significant, ND= not detected

Supp. Table 2. Membrane proteins of bEn3 cells identified at 6h time point, in irradiated (R) and control (C) samples from two MSE^E analyses, but were not shared between them.

Accession #	Protein name	Ave protein masses	Ave fmol (R6)	Protein replication	Ave Protein score	Ave protein matched peptides	Ave Prot. Seq cover (%)	Ave fmol (C6)	Protein replication	Ave. Protein score	Ave protein matched peptides	Ave Prot. Seq. cover (%)
O35516	Neurogenic locus notch	279071	985.80	1	54.45	3	0.73					
Q6NVD9	Phakinin	45854	48.33	1	52.66	2	9.38					
Q8BNJ2	A disintegrin	92008.7	21.163	2	7.5	266	4.74					
Q6PFD5	Disks large associated protein	106842.	1.174	1	12	223	7.06					
O35608	Angiopoietin 2	57031.8	2.3738	1	7	266	6.65					
Q6PGF7	Exocyst complex	81719.6						8.288	1	148.25	4	6.98
O35214	Visual pigment like recep.	37722.0						5.456	1	118.14	2	7.72
P35821	Tyrosine prot. Phosp.	50220.7						29.49	1	115.86	1	4.4
P30275	Creatine kinase U	47402.9						14.97	1	170.48	4	16.03
Q8C3X4	Translation factor	72805.0						141.5	1	108.41	3	2.92
Q3UIJ9	GRINL1A complex locus	54068.2						1.850	1	105.08	4	9.44
P97814	Proline serine threonine pho	48103.5						7.834	1	92.476	3	7.47
P27773	Protein disulfide isomerase	57134.6						9.826	1	87.919	4	6.93
Q5Y5T1	Probable palmitoyltransferase	44888.2						3.654	1	82.671	5	2.11
A3KGV1	Outer dense fiber protein	96397.0						8.9486	1	78.351	10	6.39
O35655	Serine threonine prote	75456.9						108.4	1	77.014	3	2.92
P04095	Prolactin 2C2	25766.6						42.35	1	11	656	24.55
P61028	Ras related protein Rab 8B	23774.2						5.231	1	6	459	16.43
P04768	Prolactin 2C3	25711.4								12	457	13.84
P18918	Prolactin 2C4	25737.5								8	395	24.55
P56371	Ras related protein Rab 4A	24223.3								3	309	5.16
Q91XV3	Brain acid soluble protein 1	22086.6						1.205	1	3	309	10.62
F8VQN3	12 (S)-hydroxy 5, 8	36269.6						50.46	1	4	300	22.26

P62814	V type proton ATPase	56893.0						9.915	1	3	234	4.7
Q9QUT0	Ammonium transporter Rh	48122.6						91.95	1	3	301	4.34
Q80UU9	Membrane associated progesteron Rec.	23448.2						1.381	1	7	269	17.51
Q91XD2	LIM and senescent	40970.3						6.551	1	7	269	2.93
P49817	Caveolin-1	20709.7						14.48	1	464.77	1	11.8
Q8BNJ2	A disintegrin and metalloprot e	92008.7	21.163	2	7.5	298	4.74					
Q6PFD5	Disks large associated prot	106842.	1.1744	1	12	223	7.06					
O35608	Angiopoietin 2	57031.8	2.3738	1	7	266	6.65					

Supp. Table 3. Expression of actins, tubulin, myosin, vimentin and fibroblast growth factor-16 in control rats

	Accession #	Protein name	Replication	Ave matched Peptides	Ave (Fmol)	Ave Seq. Coverage	Ave score
Rat 1	P60711	Actin cytoplasmic 1	3	12	10.7651	36.17667	1613.145
	P63269	Actin gamma enteric	1	13	20.148	30.05	1843.409
	P68370	Tubulin alpha 1A	3	5.3	3.1273	11.16	375.8343
	P12847	Myosin 3	1	32	0.4095	1.65	40.9358
Rat 2	P68370	Tubulin alpha 1A	3	5.3	2.540633	10.56667	558.2356
	P60711	Actin cytoplasmic 1	2	12.5	8.93525	32.265	1397.233
	P63269	Actin gamma enteric	3	11	17.24823	28.63333	1762.532
Rat 3	P31000	Vimentin	3	14.33	2.718367	16.23667	147.9262
	P60711	Actin cytoplasmic 1	3	14	8.3632	35.37667	1336.817
	P63269	Actin gamma enteric	2	12.5	18.5424	29.52	1640.717
	P68370	Tubulin alpha 1A	1	7	1.5156	9.31	98.3372
	P04462	myosin 8	2	5	0.42985	7.2	88.84755
	O54769	Fibroblast growth factor 16	1	4	36.24	7.8	85.3561

Supp. Table 4. Expression of actins, tubulin and myosin in irradiated rats

	Accession #	Protein name	Replication	Ave matched Peptides	Ave (Fmol)	Ave Seq. Coverage	Ave score
Rat 1	P60711	Actin cytoplasmic 1	3	7	13.181	20.265	287.2407
	P63269	Actin gamma enteric	2	8.5	25.272	23.935	358.1399
	P62738	Actin aortic smooth muscle	3	9	35.507	31.03	517.838
	P68370	Tubulin alpha 1A	2	5	5.2278	12.195	398.9251
Rat 2	P60711	Actin cytoplasmic 1	3	12	10.7651	36.17667	1613.145
	P62738	Actin aortic smooth	2	10.5	17.905	31.565	1669.235
	P68370	Tubulin alpha 1A	3	5.3	3.1273	11.16	375.8343
	P63269	Actin gamma enteric	3	13	20.148	30.05	1843.409
	P12847	Myosin 3	3	32	0.7095	1.65	40.9358
Rat 3	P62738	Actin aortic smooth muscle	3	9	20.87737	27.49667	1048.403
	P60711	Actin cytoplasmic 1	3	9	8.5851	25.77667	962.6231
	P68370	Tubulin alpha 1A	2	4	7.7532	10.755	221.3986

Appendix 4. Conference presentations, Awards and Research Article Reviews

Conference presentations (oral and poster)

- 7th Annual Californian Pituitary and Endocrine Conference, **Californian/USA** (Jan 2015)
- American Society for Mass Spectrometry (ASMS), **Baltimore/USA** (June 2014)
- Society for Neuroscience Annual Congress and Meeting , **San Diego/ USA** (Nov 2013)
- Molecular Neurodegeneration conference, **Cannes/France** (Sep 2013)
- 11th Armenian Medical World Congress, **Los Angeles/ USA** (July 2013)
- Metabolomics & System Biology, **Chicago/USA** (April 2013) [**Invited Speaker**]
- American Society for Mass Spectrometry (ASMS), **Minneapolis,/USA** (June 2013)
- Metabolomics & System Biology, **San Francisco/USA** (Feb 2012) [**Invited Speaker**]
- David S. Sigman Memorial lecture & Symposium, UCLA Molecular Biology Institute, **LA /USA** (Feb 2012)
- Human Proteome Organization (HUPO) 10th Annual World Congress. **Geneva/ Switzerland** (Sep 2011)
- American Society for Mass Spectrometry (ASMS), **Colorado/USA** (May 2011)
- Macquarie Neurosurgery Conference, **Sydney/ Australia** (Nov 2010)
- Human proteome Organization (HUPO) 9th Annual World Congress, **Sydney/ Australia** (Sep 2010)


Awards

- Skipper Postgraduate Research Award, 2010, Macquarie University (\$6000)
- Australian School of Advanced Medicine Postgraduate Travel Award, 2011, Macquarie University (\$2000)
- Australian School of Advanced Medicine Research Award, 2012, Macquarie University (\$2000)
- Australian Postgraduate (PhD) Award Scholarship, 2010- 2013 (\$25,000) per annum
- Australian School of Advanced Medicine stipend, 2010-2013 (\$10,000) per annum
- Macquarie University Postgraduate Research Fund (PGRF), 2008, Masters of Philosophy (MPhil) (\$4000).
- Macquarie University International Postgraduate Travel Grant, 2008, Masters of Philosophy (MPhil) (\$1000)

Reviewed articles for the following journals

- **Journal of Proteomics**, Jan 2012, Article Ref # JPROT-D-12-00394 and August 2015, Article Ref # JPROT-D-15-00496
- **Journal of Arthritis and Research Therapy**, Jan 2011, Article Ref # 4285741835648349
- **Journal of European Proteomics**, Registered Reviewer as of March 2013.
- **Editorial Board Member**, *Journal of Data Mining in Genomics & Proteomics*
- **Editorial Board Member**, *Science publications*

Appendix 5. Final ethics approval



**MACQUARIE
UNIVERSITY**

ANIMAL RESEARCH AUTHORITY (ARA)

AEC Reference No.: 2010/037 - 4 **Date of Expiry:** 30 June 2013

Full Approval Duration: 1 July 2010 to 30 June 2013 (36 Months)

This ARA remains in force until the Date of Expiry (unless suspended, cancelled or surrendered) and will only be renewed upon receipt of a satisfactory Progress Report before expiry. (See approval email for submission details).

Principal Investigator:
 Prof Marcus Stoodley
 Australian School of Advanced Medicine
 Macquarie University NSW 2109
 0407 896 492
 Marcus@teamneuro.com

Associate Investigators:
 Margaret Seemounian 0400 839 735
 Hong Duong 0404 246 318

Other people participating:
 Andrew Davidson 0416 157 859
 Behdad Eftekhari 0422 290 780
 Leon Lai 0432 772 780
 Johnny Wong 0414 506 621
 Christian Gagnaniello 0435 914 076
 Joe Sia 0433 870 408
 Xin Song 0423 492 959
 Vivienne Lee 0416 250 779
 Jude Amalraj 0435 830 607

In case of emergency, please contact:
 Animal Welfare Officer 9850 7758 / 0439 497 383 ; Central Animal House Manager 9850 7780 / 0428 861 163
 or the Principal Investigator / Associate Investigator named above

The above-named are authorised by MACQUARIE UNIVERSITY ANIMAL ETHICS COMMITTEE to conduct the following research:

Title of the project: Proteomics analysis of AVM endothelial membrane protein changes post radiation

Purpose: 4: Research (Human or Animal Biology)

Aims of project: This project aims to identify protein markers for arteriovenous malformation (AVMs) by analysing the endothelial membrane protein changes in the commercially available mouse brain endothelial cell cultures and in the animal AVM post radiation.

Surgical Procedures category: 3 (Major Surgery With Recovery)

All procedures must be performed as per the AEC-approved protocol, unless stated otherwise by the AEC and/or AWQ.

Maximum numbers approved (for the Full Duration):

Species	Strain	Weight(g)	Age(wks)	Total	Supplier/Source
02: rats	Sprague-Dawley	250-300g	6-12	50	ARC Perth
			Total	50	

Location of research:

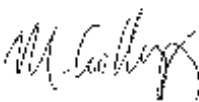
Location	Full street address
Australian School of Advanced Medicine	Level 1, Clinic Building, 2 Technology Place, Macquarie University NSW 2109
Central Animal House Facility	Building F9A, Research Park Drive, Macquarie University NSW 2109

Amendments approved by the AEC since initial approval:

- Addition of Xin Song as other personnel (Approved Oct 2010)
- Addition of Vivienne Lee as other personnel (Approved Feb 2011)
- Addition of Jude Amalraj as other personnel and (Approved March 2011)
- Addition of Hong Duong as associate investigator (Approved March 2011)
- Extension to approval duration (+1 year) (Approved May 2012)

Conditions of Approval: N/A

Being animal research carried out in accordance with the Code of Practice for a recognised research purpose and in connection with animals (other than exempt animals) that have been obtained from the holder of an animal suppliers licence. This authority remains in force until **30 June 2012** unless suspended or surrendered, and will only be renewed upon receipt of a **PROGRESS REPORT** annually.



Prof Michael Gillings (Chair, Animal Ethics Committee)

Approval Date: 19 July 2012

Adapted from Form C (issued under part IV of the Animal Research Act, 1983)